AD

Research and Development Technical Report
ECOM-3421

RADIO POLARIZATION MODULATION

Kurt Ikrath

May 1971

ECOM

UNITED STATES ARMY ELECTRONICS COMMAND · FORT MONMOUTH, N.J.

NOTICES

Disclaimers

The findings in this report are not to be construed as an official Department of the Army position, unless so designated by other authorized documents.

The citation of trade names and names of manufacturers in this report is not to be construed as official Government indorsement or approval of commercial products or services referenced herein.

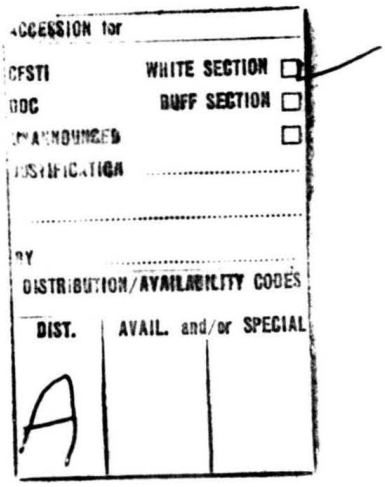

Disposition

Destroy this report when it is no longer needed. Do not return it to the originator.

Security Classification

DOCUMENT CONTROL DATA - R & D

(Security classification of title, body of abstract and indexing annotation must be entered when the overall report is classified)

1. ORIGINATING ACTIVITY *(Corporate author)*
U.S. Army Electronics Command
Fort Monmouth, New Jersey 07703

2a. REPORT SECURITY CLASSIFICATION
Unclassified

2b. GROUP

3. REPORT TITLE
Radio Polarization Modulation

4. DESCRIPTIVE NOTES *(Type of report and inclusive dates)*
Technical Report

5. AUTHOR(S) *(First name, middle initial, last name)*
Kurt Ikrath

6. REPORT DATE
May 1971

7a. TOTAL NO. OF PAGES
115

7b. NO. OF REFS
6

8a. CONTRACT OR GRANT NO.

b. PROJECT NO. ITO 61101A 91A

c. Task No. -09

d. Work Unit No. -601

9a. ORIGINATOR'S REPORT NUMBER(S)
ECOM-3421

9b. OTHER REPORT NO(S) *(Any other numbers that may be assigned this report)*

10. DISTRIBUTION STATEMENT
Approved for public release; distribution unlimited.

11. SUPPLEMENTARY NOTES

12. SPONSORING MILITARY ACTIVITY
U.S. Army Electronics Command
ATTN: AMSEL-NL-R-4
Fort Monmouth, New Jersey 07703

13. ABSTRACT

A theoretical analysis is given of transmission, reflection, and scatter of polarization modulated radio waves. Practical implications for communications and surveillance are discussed.

DD FORM 1 NOV 68 1473 REPLACES DD FORM 1473, 1 JAN 64, WHICH IS OBSOLETE FOR ARMY USE.

Security Classification

14. KEY WORDS	LINK A		LINK B		LINK C	
	ROLE	WT	ROLE	WT	ROLE	WT
Radio						
Polarization						
Reflection						
Scatter						

Reports Control Symbol OSD-1366

TECHNICAL REPORT ECOM-3421

RADIO POLARIZATION MODULATION

by

Kurt Ikrath
Comm/ADP Laboratory

MAY 1971

DA Work Unit No. 1T0 61101A 91A 09 601

Approved for public release;
distribution unlimited

U. S. ARMY ELECTRONICS COMMAND
FORT MONMOUTH, NEW JERSEY 07703

ABSTRACT

A theoretical analysis is given of transmission, reflection, and scatter of polarization modulated radio waves. Practical implications for communications and surveillance are discussed.

CONTENTS

RADIO POLARIZATION MODULATION

INTRODUCTION

In accordance with Radio Engineering terminology polarization is defined as the angle between the electrical field vector and a reference plane such as for example the earth's surface. Radio Polarization Modulation refers to a semaphore type signal transmission mode where information is conveyed by variation of this polarization angle relative to a reference system (Refs. 1 and 2). This system can be defined directly in terms of the geometrical relations and symmetries of the transmitter and receiver antenna configuration or indirectly in relation to their respective environments.

These reference systems need not be static, instead they could be dynamic; but in the dynamic case and for communications, their changes in time and space must be made known to transmitter and receiver. Transmission of both user and or system reference change information via the polarization modulation signal mode is constrained in principle by phenomena intrinsic to the generation of oscillatory rotating electromagnetic fields and by the dynamic range and frequency bandwidth of transmitter and receiver. Practical limitations for communications via the polarization modulated radio signals arise from their great sensitivity to pertubation by tropospheric and ionospheric propagation phenomena (Ref. 2). Similarly variable ground reflectivity and scatter from man made objects do more harm to the polarization modulation mode than to any other transmission mode.

In fact the subsequent theoretical discussion was motivated by the need to find an explanation for the observed influence of automobile traffic density on the Garden State Parkway on the distortion of polarization modulated VHF radio signals which were transmitted via line of sight from Fort Monmouth to Middletown, New Jersey.

DISCUSSION

I. The Ideal Free Space Case

Conforming to the practical experimental implementation of the xmtr antenna, the crossed electrical dipole moments M and N shown in Figure 1 are used as theoretical transmitter model. In the ideal regular polarization modulation case the transmitter antenna is operated in such a way that the moments M and N have equal magnitude A and are 90 degrees out of phase with respect to their radio carrier frequency currents, and in phase with respect to the phase modulation of these RF currents.

This phase modulation is expressed here by the function $\psi(t)$. Using the coordinate and base vector notation of Figure 1

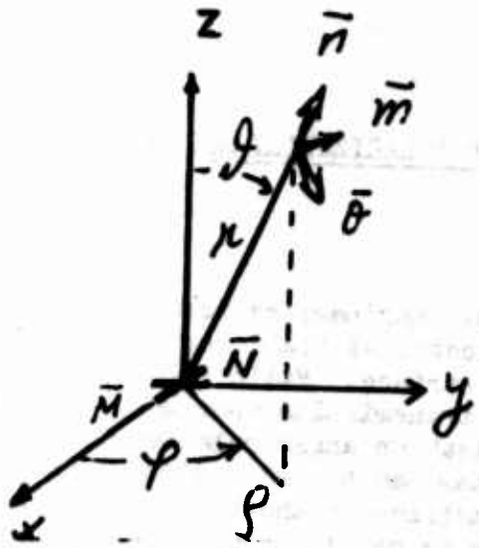

Fig.1. Coordinate and Base Vector Notation

the electrical field equations assume the following format (from app. A equ A.3.5) for equal antenna moments $M_x = M_y = A$:

$$\bar{E}_{ideal} = \sqrt{\frac{\mu}{\varepsilon}} \cdot \frac{A k_s^2}{4\pi \cdot k_s \cdot r} \cdot$$

	$\cdot \cos\alpha(r;t)$	$\cdot \sin\alpha(r;t)$
$\bar{n} \cdot \sin\vartheta$	$+\frac{2}{(k_s r)^2}$	$-\frac{2}{(k_s r)^2} \cdot \left(1 + \frac{\dot{r}}{\omega_s}\right)$
$\bar{m}$	$\frac{1 + \frac{\dot{r}}{\omega_s}}{k_s r} + \frac{\ddot{r}}{\omega_s^2}$	$\frac{1}{(k_s r)^2} - \left(1 + \frac{\dot{r}}{\omega_s}\right)^2$
$\bar{\theta} \cdot \cos\vartheta$	$-\frac{1}{(k_s r)^2} + \left(1 + \frac{\dot{r}}{\omega_s}\right)^2$	$\frac{1 + \frac{\dot{r}}{\omega_s}}{k_s r} + \frac{\ddot{r}}{\omega_s^2}$

where: $$\alpha(r;t) = \omega_s t - k_s r + \varphi + \psi(\tau) \qquad (1)$$

$$\tau = \frac{k_s}{\omega_s} \cdot r - t$$

In this equation one recognizes the appearance of the phase modulation function ψ in the amplitude terms. The superscript dot denotes differentiation with respect to local time t of ψ as function of retarded time τ ; $\omega_s = k_s$ c denotes the steady state carrier frequency in radians per unit time, k_s the propagation factor and c speed of light. The physical meaning of $\frac{\dot{\psi}}{\omega_s}$ and of $\frac{\ddot{\psi}}{\omega_s^2}$ becomes evident by considering for example

$$\psi(t) = \Delta\Phi \cdot \sin\omega_p t = \frac{\Delta\Omega}{\omega_p} \cdot \sin\omega_p t \qquad (2)$$

where ω_p is the polarization modulation frequency; $\Delta\Phi$ and $\Delta\Omega$ denote respectively the maximum phase and frequency deviation. It follows that the

$$\left|\frac{\dot{\psi}}{\omega_s}\right|_{max} = \frac{\Delta\Omega}{\omega_s} = \frac{\omega_p}{\omega_s} \cdot \Delta\Phi \qquad (3)$$

constitutes the FM modulation index and

$$\left|\frac{\ddot{\psi}}{\omega_s^2}\right|_{max} = \frac{\Delta\Omega}{\omega_s} \cdot \frac{\omega_p}{\omega_s} \qquad (4)$$

the product of this FM modulation index with the ratio of modulation to RF carrier frequency. The numerical values involved are very small in practice. For example for $f_p = \frac{\omega_p}{2\pi} = 10$ kHz $\Delta F = \frac{\Delta\Omega}{2\pi} = 100$ kHz and $f_s = \frac{\omega_s}{2\pi} = 100$ MHz the values of $\left|\frac{\dot{\psi}}{\omega_s}\right|_{max}$ and $\left|\frac{\ddot{\psi}}{\omega_s^2}\right|$ are respectively 10^{-3} and 10^{-7}. Though $\dot{\psi}/\omega_s$ and $\ddot{\psi}/\omega_s^2$ are in practice very small compared to one their appearance in the amplitude terms of the electrical field in Equation 1 shows that polarization modulation is accompanied by a small amplitude modulation. The geodesic features of the polarization modulated radiation field $\bar{E}_p$ are seen by writing the transverse field ($\bar{M}$ and $\bar{O}$ components) as a superposition of two fields $\bar{E}_{p1}$ and $\bar{E}_{p2}$ as follows:

$$\bar{E}_p = \mathcal{E}_{p1} \cdot \begin{Bmatrix} -\bar{m} \cdot \sin\alpha(r;t) \\ +\bar{e} \cdot \cos\psi \cdot \cos\alpha(r;t) \end{Bmatrix} \qquad (5)$$

where

$$\mathcal{E}_{p1} = \sqrt{\frac{\mu}{\epsilon}} \cdot \frac{A k_s^2}{4\pi k_s r} \cdot \left(1 + \frac{\ddot{\psi}}{\omega_s}\right)^2 \qquad (5')$$

and

$$\bar{E}_{p2} = \mathcal{E}_{p2} \cdot \begin{cases} +\bar{m} \cdot \cos\alpha(r;t) \\ +\bar{\theta} \cos\vartheta \cdot \sin\alpha(r;t) \end{cases} \qquad (6)$$

where

$$\mathcal{E}_{p2} = \sqrt{\frac{\mu}{\epsilon}} \cdot \frac{A k_s^2}{4\pi k_s r} \cdot \frac{\ddot{\psi}}{\omega_s^2} \qquad (6')$$

An observer located off from the z symmetry axes viewing the transmitter antenna under an angle ϑ would see the $\bar{E}_p$ field vector trace an ellipse with an eccentricity of $\sin\vartheta$. This is illustrated by the normalised $\bar{E}_{p1}/E_{p2}$ and $\bar{E}_{p2}/E_{p2}$ vector diagrams in Figures 2a, 2b.

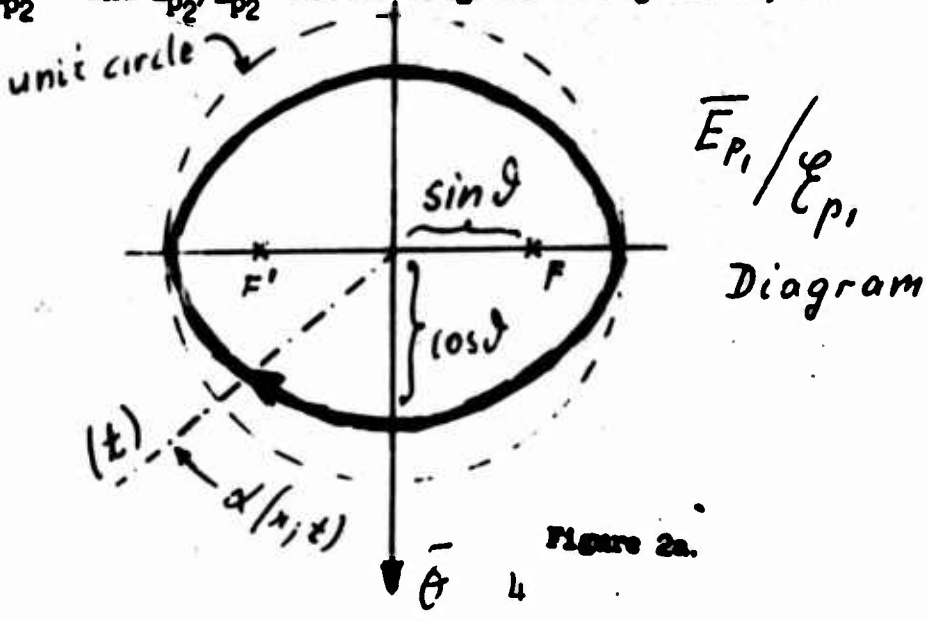

Figure 2a.

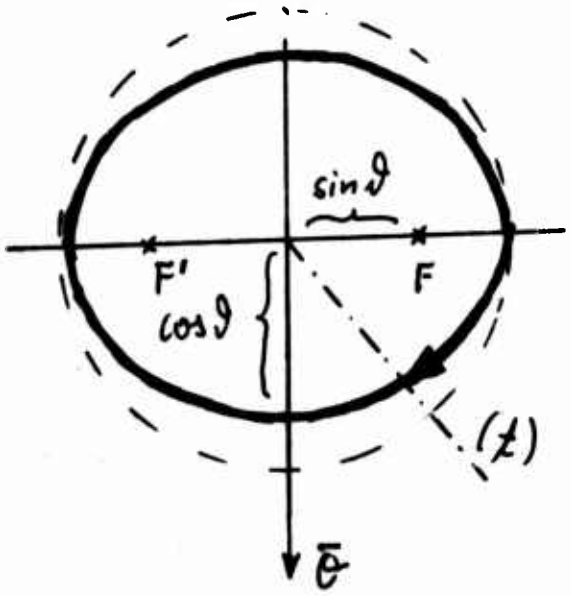

$E_{\rho_2} / \mathcal{E}_{\rho_2}$ Diagram

Figure 2b.

Referring to Equation (6') and the previously mentioned values for one can assume that contributions by $\bar{E}_{p_2}$ to the total field are negligibly small in practice. The observed radiation field $\bar{E}_p$ is therefore described by $\bar{E}_{p_1}$. Using the numerical example the amplitude modulation of $\bar{E}_p$ is found via

with $$\left(1+\frac{\dot{\varkappa}}{\omega_s}\right)^2 \doteq 1+2\,\frac{\dot{\varkappa}}{\omega_s}+\cdots$$

$$2\frac{\dot{\varkappa}}{\omega_s} = 2\,\frac{\Delta\Omega}{\omega_s}\cdot\cos\omega_p t = 2\times 10^{-3}\cdot\cos\omega_p t$$

i.e. negligibly small in this case.

Carrier Suppressed Polarization Modulation

The steady state rotation of the electrical field vector at the carrier frequency ω_s is purely redundant and can be suppressed. The corresponding mathematical expressions are obtained by replacing ω_s with $-\omega_s$ in Equation 1 to yield $\bar{E}$ and by forming: $\frac{1}{2}(E + \bar{E})$. The resultant carrier suppressed $\bar{E}$ (CS) polarization modulated field is described below:

$$\bar{E}^{(CS)} = \sqrt{\frac{\mu}{\epsilon}} \cdot \frac{A k_s^2}{4\pi k_s H} \cdot \qquad (7)$$

	$\cos\psi$		$\sin\psi$	
	$\cos\gamma$	$\sin\gamma$	$\cos\gamma$	$\sin\gamma$
$\bar{n}\sin\vartheta$	$\frac{2}{(k_s H)^2}$	$-\frac{2}{k_s H}\cdot\frac{\dot{\chi}}{\omega_s}$	$-\frac{2}{k_s H}$	0
$\bar{n}1$	$\frac{1}{k_s H}$	$-2\frac{\dot{\chi}}{\omega_s}$	$-\left[1+\left(\frac{\dot{\chi}}{\omega_s}\right)^2\right]-\frac{1}{k_s H}$	$-\frac{\ddot{\chi}}{\omega_s^2}-\frac{1}{k_s H}\cdot\frac{\dot{\chi}}{\omega_s}$
$\bar{\theta}\cdot\cos\vartheta$	$\left[1+\left(\frac{\dot{\chi}}{\omega_s}\right)^2\right]-\frac{1}{(k_s H)^2}$	$\frac{\ddot{\chi}}{\omega_s^2}+\frac{1}{k_s H}\cdot\frac{\dot{\chi}}{\omega_s}$	$\frac{1}{k_s H}$	$-2\frac{\dot{\chi}}{\omega_s}$

where

$$\gamma = \omega_s t - k_s H + \varphi$$

The $\bar{E}^{(CS)}$ field is generated in practice by amplitude modulation of the RF carrier such that there is a 90 degree phase difference between the audio modulation radiated on respectively the M and N dipole carrier. Neglecting the $\frac{\dot{\chi}}{\omega_s}$ and $\frac{\ddot{\chi}}{\omega_s^2}$ terms in Equation (7) the carrier suppressed polarization modulated far field reduced to:

$$\bar{E}^{(s)} \doteq \sqrt{\frac{\mu}{\varepsilon}} \cdot \frac{A \cdot k_s^2}{4\pi k_s x} \cdot \cos\left[\omega_s t - k_s x + \varphi\right] \cdot$$

$$\cdot \left\{ \begin{matrix} -\bar{m} \cdot \sin\gamma \\ +\bar{e} \cdot \cos\vartheta \cdot \cos\gamma \end{matrix} \right\}$$

(8)

A discussion of polarization modulation would not be complete without an investigation of the effects from faulty operating conditions, e.g. wrong phasing of the crossed dipoles. Such an investigation is carried out in the appendix where the field obtained with a 180 degree instead of a 90 degree RF phase difference is derived (Appendix A, Section 4, Equation A.4.5).

In effect faulty phasing conditions and corresponding signal distortions arise also from propagation phenomena such as discussed in the following sections.

II. Automobile Traffic Density Induced Distortion of Polarization Modulated Signal Transmissions.

For the purpose of discussion consider a VHF line of sight radio link and the corresponding theoretical model described by Figure 3.

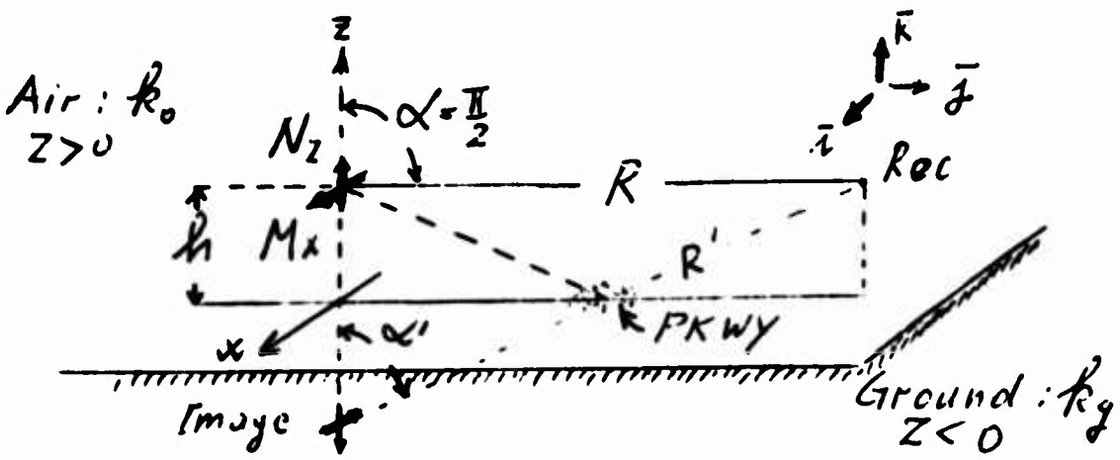

Fig.3. VHF - Line of Sight Radio Link

As before the crossed M_x and N_z dipoles are driven 90 degrees out of phase with respect to the radio carrier frequency. To provide a physical understanding of the well known mathematical solutions for the fields from vertical and horizontal dipoles above various types of ground (Refs. 3 to 6) consider first the electrostatic case. From the static point of view the antenna field distribution is conceived as generated by primary and secondary source charges; in this case the secondary source charges are the imperfect image and the influence charges at the air to ground boundary which balance the primary charges. These primary and secondary charges become in the dynamic case the sources of primary (direct) and secondary waves. Hence the secondary source charges are also referred to as reflected and refracted charges. These give rise to reflected and refracted and boundary surface wave modes. The latter provides the continuity between the wave fronts of the reflected and refracted waves at the boundary of the different media involved.

From the mathematical point of view surface wave modes represent the smooth spatial transient response to the discontinuity in the wave number spectrum associated with these media boundaries i.e. in our case the boundary between air ($k_0 = \omega\sqrt{\varepsilon_0\mu_0}$ and ground ($k_g = \omega\sqrt{\varepsilon_g\mu_0}\cdot\sqrt{1+j\frac{\chi_g}{\omega\varepsilon_g}} = n_g \cdot k_0$).

In this respect surface wave modes are similar to the smooth voltage or current transients in electrical circuits which are caused by jump like changes of lumped circuit parameters. Closed solutions for Fourier Integral representations for these parametric induced circuit transients may not be attainable in practice. In this case one resorts to numerical methods of evaluation using computers or guided by the physical nature of the problem approximations for the integrals involved.

These latter type of approximations are used here for the Hankel Integral representations of the Hertz Vector functions Π_x and Π_z for respectively the horizontal M_x and the vertical N_z dipole moment (Appendix B, Equ. B.2.1 to B.2.8).

In this approximation known as the Saddle Point Method of Integration, the Hankel functions in the Integrand are replaced by their asymptotic values and the integration with respect to ϑ^x, the complex elevation angle, is carried out along an extremal path, i.e. a path for which the integral value changes most rapidly within the shortest path length. This path leads through the extremum of the complex integrand. i.e. the Saddle Point (hence the name "Saddle Point Method").

This extremal path of integration through the Saddle Point intersects the real ϑ^x axes at an angle of 45 degrees (Appendix B, Fig. B.3.4) and yields the first term, the Saddle Point Contribution, that represents the reflected space waves (Appendix B, Equ. B.3.39).

The surface wave modes which arise from singularities in the integrand correspond to higher order terms in the approximations for the Hankel Integrals. Higher order is here synonymous to values of α' which are larger than the critical angle α_c' for striking incidence of rays emanating

from the image source location (Fig. 3 and Appendix B. Equs. B.3.43 to B.5.57). In the long wave-low frequency-case, where the ground medium is in the conductive regime ($\omega < \kappa_g/\varepsilon_g = \omega_g$) and transmitter and receiver heights as well as the surface roughness of the terrain are small compared to the wave length, the series expansion approximation would be dominated by the pole-residue term which is usually referred to as the ground surface wave mode. This mode is characterized by the negative half power of the distance type decay of its field strength.

This mode plays a dominant role in thecomposition of LOW frequency radio signals at distances from the transmitter which are short relative to the dimensions of the earth-ionosphere duct. These ground surface wave contributions become negligibly small at frequencies which exceed the critical ground frequency $\omega_g = \kappa_g/\varepsilon_g$. In the corresponding dielectric ground regime the path through the Saddle Point traps instead of the pole a branch cut singularity as α exceeds the critical angle .

The resultant "branch cut" term dominates the series expansion approximation for transmitter and receiver heights h and h_r which are governed by:

$$0 < k_0 h_x < |n_g| k_0 h < 10 \qquad (9)$$

In practice the roughness of the terrain becomes a SIGNIFICANT factor in the attenuation by diffuse scatter of this kind of ground wave mode which is also referred to as the lateral wave mode (Ref. 6). Applying the field equations obtained by Saddle Point Approximation Method (Appendix B, Equs. B.3.22 to B.3.73) to the problem described by Figure 3 one arrives at the following equation for the received electrical field vector (from Appendix B, Equ. B.5.16).

$$\bar{E}(0;y;h) \doteq \frac{k_0^2}{4\pi}\cdot\sqrt{\frac{\mu_0}{\varepsilon_0}}\cdot\frac{1}{k_0 y}\cdot \qquad (10)$$

$$\left[\left(e^{j[k_0 y - \omega t - \gamma]}\right)\left\{\begin{matrix}(-\bar{\imath})M_x \cdot k_0 h\left(\frac{2h}{y}\right) \\ 0 \\ +\bar{K}\cdot N_z\left[\mp j k_0 h\left(\frac{2h}{y}\right)+(1\mp 1)\right]\end{matrix}\right\}\right.$$

$$\left. -\frac{1}{2}\left(e^{-jn_g k_0 h + jn_g k_0 y}\right)\cdot\left\{\begin{matrix}+\bar{\jmath}\cdot N_z\cdot\left(\frac{2h}{y}\right)\cdot\left[n_g^2+1\right] \\ 0 \\ +\bar{K}\cdot N_z\cdot\left[1+jn_g^2\right]\end{matrix}\right\}\right\}$$

For balanced antenna moments $M_x=N_z=A$ and for the transmitter and receiver height h used in practice the second lateral wave term characterised by exponential decay with height h is negligible, except for possibly the small wave front tilt produced by its y component. The most significant contribution to the total field is for all practical purposes given by the first term in Equation 10. This term represents the superposition of the direct with the reflected wave where the upper minus signs are valid for the dielectric and the lower plus signs for the conductive regime in the local reflecting area half way between transmitter and receiver. (Fig. 3). This local reflecting area is in the experimental system identified as the Red Bank Section of the Garden State Parkway about half way between the Fort Monmouth and Middletown, New Jersey Terminals. This section of the parkway bulges toward north at and around its No. 109 exit-entrance.

Thus, equating the dielectric ground regime with zero and the conductive ground regime with infinite automobile traffic density as limiting cases, explains the observed influence of traffic density on the distortion of the polarization modulated VHF signals.

Inspection of Equation (10) shows that these distortions arise primarily from the changes in the vertical field component E_z. Within the given limits

$$\bar{E}(0;y;h) \approx 2\left(\frac{h}{y}\right)^2 \begin{Bmatrix} -\bar{\imath}M_x \\ 0 \\ -\bar{\kappa}N_z \end{Bmatrix} + \ldots \quad \text{for zero density} \tag{11}$$

$$\bar{E}(0;y;h) \approx +\bar{\kappa}\frac{2N_z}{k_0 y} + \ldots \quad \text{for infinite traffic density} \tag{12}$$

Thus knowledge gained about the traffic density at and around the Parkways No. 109 Red Bank exit-entrance is paid by information lost to the corresponding signal distortions.

Hence, from the traditional engineering point of view, there seems to be no reason why polarization modulation by itself would be a better mode of radio communications. In fact, the depolarization effects associated with propagation through heterogeneous and anisotropic natural radio propagation media and ground reflections do more harm to the polarization modulation mode than to any other conventional radio signal transmission mode as far as preservation of signal information is concerned.

However, the communications capability of the system is not completely sacrificed in applying this sensing sensitivity of polarization modulation radio signal transmission to ground surveillance. In fact, communications and surveillance functions can be combined by control of RF power, corresponding AM modulation index and phase of the modulation functions $\psi_x(t)$ and $\psi_z(t)$ which must be applied to the M_x and N_z transmitter antenna elements respectively so as to compensate for signal distortions produced by target-induced variations of the reflectivity of the local reflecting area which is under surveillance.

By neglecting interference from the ground surface wave (branch cut) terms and terms involving $\frac{\dot{\psi}}{\omega} \ll 1$ and $\frac{\dot{\psi}}{\omega_1} \ll 1$, one could compensate for the bumper-to-bumper parkway traffic density induced signal distortion by changing either the RF or the modulation phase difference between the M_x and the N_z channel by 90 degrees and redistribution of the transmitter power to satisfy the condition:

$$\sqrt{\frac{k_1}{y}} \cdot \sqrt{k_0 h_1} \cdot M_x = \sqrt{\frac{y}{h_1}} \cdot \frac{1}{\sqrt{k_0 h_1}} \cdot N_z \tag{13}$$

Further in constructive partnership with conventional radio signal transmission modes, polarization modulation can provide another dimension to radio communications and surveillance-related functions. As a practical example, let us consider radio communications using polarization and amplitude modulation.

III. Dual Amplitude Modulated and Polarization Modulated Radio Signal Transmission.

Replace in Eq. 1 the dipole moment A (in Amp. meter) by

$$A \cdot (1 + a \cdot \cos \omega_a t) \tag{14}$$

where "a" defines the amplitude modulation index ($0 \leq a \leq 1$) and ω_a defines the corresponding AM-signal frequency (e.g., in the audio frequency range). Consider the relations between the amplitude modulation and the polarization modulation frequencies be specified by:

$$\frac{\omega_a}{\omega_p} \ll 1 < \frac{\Delta\Omega}{\omega_p} = \Delta\Phi \tag{15}$$

such that $\Delta\Phi$ is either constant or varies in proportion with the amplitude of the ω_p signal that is applied to the polarization modulation channel.

In practice, one must therefore consider the spectrum functions of the signals transmitted via polarization modulation and AM respectively over the circular polarized radio carrier (ω_s).

Conventional radio antenna and receivers tuned to ω_s, which are located in the radiation field of the transmitter respond in the following way. The rapidly rotating EM-vector field induces into the conventional linearly-polarized receiver antenna an electromagnetic field vector that is proportional to the cosine of the angle between the fixed direction of polarization of the antenna and the instantaneous direction of polarization of the field.

The resultant antenna output response then involves the cosines and sines of $\psi(\tau)$ and φ_a the angle of orientation of the receiver antenna relative the transmitter coordinate system (Figure 1, Equ. 1). The voltage delivered by the antenna to the receiver input therefore has an FM- and AM- like frequency spectrum conforming to:

$$\mathcal{F} = [1 + a\cos\omega_a t] \sum_{n=-\infty}^{n=+\infty} J_n(\Delta\Phi)\cdot\cos[(\omega_s + n\omega_p)t] \qquad (16)$$

where $J_n(\Delta\Phi)$ are Bessel functions of the order n = 0, $\pm$ 1, 2, etc, and of argument $\Delta\Phi$. In practice, this spectrum is bandwidth limited, such that components of order (n) larger than (n) max vanish. For example, a conventional AM receiver would resolve (in the case specified by (1.2.4) only the very small portion of the spectrum restricted to essentially the n=0 spectrum component.

Thus, a conventional AM receiver yields an output that corresponds to the cross modulation product of the AM signal with the fundamental spectrum component $J_0(\Delta\Phi)$ evidently for constant $\Delta\Phi$, a conventional AM radio-receiver receives the AM channel signal undistorted; conversely a conventional (amplitude limited) FM receiver connected to the same antenna the polarization modulation channel signal. The FM receiver output will conform closely to the polarization modulation function $\psi(t)$ if the overall bandwidth of the antenna and receiver circuitry are wide to include spectrum components $J_n(\Delta\Phi)$ of order n, at least up to values n which are approximately equal to the FM modulation index $\frac{\Delta\Omega}{\omega_p} = \Delta\Phi$.

Hence, if the polarization modulation phase deviation, $\Delta\Phi$, and the resultant received FM modulated index, $\Delta\Omega/\omega_p$, are kept constant, the dual polarization modulation and AM signal transmissions on one and the same radio-carrier frequency, ω_s, can be received separately by connecting an AM and an FM receiver to a conventional linearly polarized receiver antenna. The dual channel polarization modulation and AM signal transmission capability of a single radio carrier frequency, ω_s, can also be utilized for protection of radio communications against noise interference and unauthorized interception of radio messages. For these purposes, polarization modulated and

AM signals may be correlated relative to a third standard of coherence signal or reference code.

Practical implementations of polarization modulation VHF radio transceiver systems involving forward and return signal transmissions can thus be exploited for interrelated functions: communications, ground surveillance, and system control to adapt the communications circuit to reflectivity changes of the local ground environment under surveillance.

These functions may be carried out by using a deterministic sequence of alternate periods of communications, sensing, and feedback control signal transmissions or by a statistical distribution of communications, sensing and control signalling periods. The moments of this distribution would then be used for adaptive control of the communications and surveillance performance characteristics of the system.

In addition to these protective measures for communications; the geodesic features of polarization modulated radio signals in correlation with AM-signals are applicable to aircraft radio navigations. For these applications, bearing and timing information can be readily derived from the AM pulse signals; and the wave shape distortion of the received polarization modulated signals as function of deviation angles ϑ from the transmitters antenna z-symmetry axis (Figures 2a and b). This is in effect similar to "VOR" (VHF omnidirectional range) navigation, but for only one single radio carrier frequency, ω_s. Evidently, dual channel systems using conventional and polarization modulation radio signal transmission modes on a single radio frequency carrier are able to perform a large variety of tasks.

However, in the assignment of specific roles to the respective signal transmission modes, the sensitivity of polarization modulated radio signals to secondary propagation effects, (reflection, refraction, and scatter) must be considered and properly exploited. Proper exploitation of this sensitivity results in dual channel systems with the ability to sense and compare, as required for surveillance related applications. The theoretical aspects of these applications are explored further in the subsequent section.

IV. Side Scatter of Polarization Modulated Radio Waves by Strip-Shaped Conductors.

Side scatter of polarization modulated radio wave signals has the following implications. Degradation of radio communications on the one hand, and scatter target sensing and tracking on the other hand. The detailed mathematical discussions of Appendix C, side scatter of polarization modulated radio wave signals from strip-shaped conductors are of practical interest in connection with: (1) Parasitic scatter interference from wire lines, fences, poles, and towers outside the transmitter to receiver transmission line and (2) scatter target detection and determination of the dynamic characteristics of target motion.

The mathematical foundations for solution of EM scatter problems are given in Sections C.1 and C.2 of Appendix C. Practical specializations of the resultant integral equations are discussed in Section C.3 of Appendix C.

The problem involved is the following: A conductive strip-shaped scatter body is located in the plane formed by the elements of the crossed dipole antenna of the transmitter. Given the distance from the transmitter, the orientation, and the dimensions of this scatter body, evaluate the effect on the radiation field of the transmitter at a given receiver location. For this purpose, required explicit field solutions are derived for an infinite conductive scatter strip at a distance x_s from the transmitter, such that the transmitters y-dipole radiator and thelength "l" of the strip are parallel, whereas the transmitter's x-dipole radiator is perpendicular to the "b-wide" surface of the strip. In conformance with practical conditions, the receiver locations are chosen on or close to the transmitter's symmetry z-axis of the transmitter-antenna, at distances z_p, x_s, as shown in Figure 4.

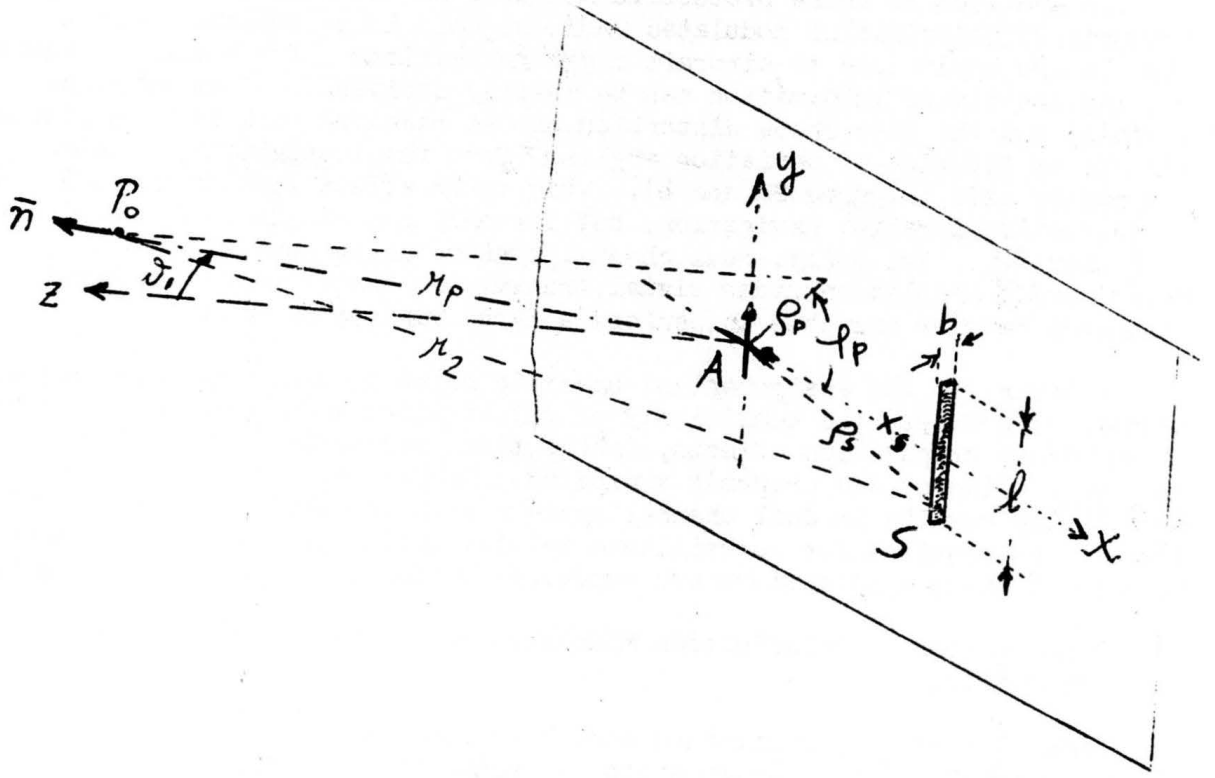

Fig. 4. Geometry of the Scatter Problem

These geometrical specifications of the problem permit the introduction of simplifying approximations for the integral equations that relate incident and scattered fields (Appendix C, Equation C.2.14). Resultant approximate solutions for the scattered field in the regular polarization modulation case are derived in Appendix C, Section 3 and given by Equations C.3.20 to 20''' in terms of the Carthesian System in Figure 4. By transformation to the spherical coordinates originating from the transmitter location one gets for receiver locations P_0 close to the z-axes (Fig. 4) approximately:

$$\mathcal{E}_{\vartheta}^{(M)'} \doteq \mathcal{E}_{x}^{(M)'} \cdot \cos\varphi_p ; \quad \mathcal{E}_{\varphi}^{(M)'} \doteq -\mathcal{E}_{x}^{(M)'} \cdot \sin\varphi_p ; \quad \mathcal{E}_{x}^{(M)'} = \mathcal{E}_{z}^{(M)'} \qquad \text{(17)}$$

In this format, the scatter field and the direct field (Appendix A, Equation A.3.5) are superimposed at the point of observation P_0 ($r_p \doteq z_p ; \varphi_p ; \vartheta_p \approx \frac{\rho_p}{z_p} \ll 1$) to yield the resultant field.

Neglecting the $\dot{\omega}/\omega_0$ and $\frac{\ddot{\omega}}{\omega_0^2}$ amplitude terms in both the direct (p) and the scattered (s) field the equations for the components of the resultant field are obtained as follows:

$$\mathcal{E}_{x} \doteq j\sqrt{\frac{\mu_0}{\varepsilon_0}} \cdot \frac{A k_0^2 h l}{(4\pi z_p)^2} \cdot e^{-j[k_0(z_p + x_s) - \omega_0 t - \gamma_s]} \qquad \text{(18)}$$

$$\mathcal{E}_{\varphi} \doteq j\sqrt{\frac{\mu_0}{\varepsilon_0}} \cdot \frac{A k_0^2}{4\pi k_0 z_p} \cdot e^{-j[k_0 z_p - \omega_0 t - \gamma_p - \gamma_p - \frac{\pi}{2}]} \cdot \left[1 + \frac{k_0^2 h l}{4\pi k_0 x_s} \cdot e^{-j[k_0 x_s + \varphi_p + \frac{\pi}{2} + (\gamma_p - \gamma_s)]}\right] \qquad \text{(19)}$$

$$\mathcal{E}_{\vartheta} \doteq j\sqrt{\frac{\mu_0}{\varepsilon_0}} \cdot \frac{A k_0^2}{4\pi k_0 z_p} \cdot e^{-j[k_0 z_p - \omega_0 t - \varphi_p - \gamma_p]} \cdot \left[1 - \frac{k_0^2 h l}{4\pi k_0 x_s} \cdot \cos\varphi_p \cdot e^{-j[k_0 x_s + \varphi_p + (\gamma_p - \gamma_s)]}\right] \qquad \text{(20)}$$

The absolute magnitude $|\mathcal{E}_T|$ of the "Transverse Field" as determined by from the $\mathcal{E}_\varphi$ and $\mathcal{E}_\vartheta$ components with

$$|\mathcal{E}_T| \doteq \sqrt{2\frac{\mu_0}{\varepsilon_0}}\cdot\frac{A k_0^2}{4\pi k_0 z_p}\cdot\sqrt{1-\frac{k_0^2 b\ell}{4\pi k_0 x_s}\cdot\cos\left[2\psi_p + k_0 x_s + (\gamma_p - \gamma_s)\right]} \tag{21}$$

reveals the influence of side scatter interference on the transmission of polarization modulated radio signals. Inspection of Eq. 21 shows that side scatter interference induces a spurious amplitude modulation which is characterized by a modulation index

$$\alpha_s \doteq \frac{1}{2}\frac{k_0^2 b\ell}{4\pi k_0 x_s} = \frac{1}{4}\cdot\frac{b\ell}{\lambda_0 x_s} \tag{22}$$

and a spurious frequency modulation conforming to the difference of the modulation functions

$$\gamma_{sp} = \gamma_p(\tau_p) - \gamma_s(\tau_s) \tag{23}$$

In terms of the signal propagation times from the transmitter to the scatter strip T_s and to the receiver location T_p, assumes for the sinusoidal type modulation (Equ. 2) at a Frequency ω_p the format

$$\gamma_{ps} = 2\frac{\Delta\Omega}{\omega_p}\cdot\sin\omega_p\frac{T_p - T_s}{2}\cdot\sin\left[\omega_p\left(\frac{T_p + T_s}{2} - t\right)\right] \tag{24}$$

For the purpose of discussion of these equations assume that the receiver knows all the parameter values except his own range z_p. Then, provided he has the ability to extract a_s (Equ. 22) from the wave shape of the received signals, he could derive his range value z_p; or knowing z_p he could find x_s instead.

Thus in principle side scatter induced wave shape distortions of the received polarization modulated signals could be used for the extraction of information that is useful for surveillance and navigation. However considering practical numerical values e.g. f_0 60 MHz, i.e. λ_0 = 5 m; x_s = 20 m; l = 2 m; b = 0.1 m which gives $a_s = 5 \times 10^{-4}$, the change to discriminate the side scatter induced modulation from the natural noise modulation is extremely small. Translated into communications this means that side scatter effects from other VHF antennas separated by more than 20 m from the crossed dipole transmitter antenna are negligibly small in practice.

This is obviously not the case when larger scatter objects are involved. Though the accuracy of the formulas for the received electrical field (Eqs. 18 to 20) diminishes in these cases the fundamental relations whereby side scatter induced signal distortion is proportional to the area of the scatter body remain valid. Then, with corresponding larger values of a_s, the dynamic characteristics of the motion of such a larger scatter body are readily extracted (by differentiation) from the receiver output signal. This capability can be further enhanced if the small longitudinal component (Eq. 19) is sensed and correlated with the transverse field, such that the RF-dependent automatic gain control response in conjunction with the low audio output signals of a longitudinal and of a transverse radio receiver yields the z and x movements of the scattery body relative to the transmitter, even in the side scatter case. Obviously, direct back scatter of the main beam is a much simpler case where the polarization modulation function $\psi(t)$ can be easily controlled by the back scatter signals. The resultant target motion tracking capability is particularly useful when long and thin shaped scatter bodies that perform progressive as well as gyrating (tumbling) movements are involved; using carrier suppressed polarization modulated sensing signal transmissions; it becomes relatively easy to discriminate between free gyrations and forced (internally controlled) gyrations of such scatter bodies.

Conclusions

On the basis of experience gained with experimental implementations of Polarization Modulated Radio Systems and from the further theoretical exploration of the performance and applications of such systems, the conclusions can be stated as follows:

Polarization modulation adds new dimensions of time and space to VHF and UHF radio communications and surveillance and in constructive partnership with conventional modulation provides a dual information channel transmission capability on a single RF carrier.

REFERENCES

1. G. Vogt, "An Electronic Method for Steering the Beam and Polarisation of HF Antennas," IEEE Trans on Antenna and Propagation, AP-10, No. 2, pp. 193-200, March 1962.

2. G. Vogt, "Analogue Polarisation Follower for Measuring the Faraday Rotation of Satellite Signals, "The Radio And Electronic Engineer, England, Vol. 28, No. 4, October 1964, pp 269-278.

3. K. A. Norton, "The Physical Reality of Space and Surface Waves in the Radiation Field of Radio Antennas Pt. III Proc. IRE 25 - Nov 9 pp 1192-1202 Sept. 1937.

4. H. Ott, "Reflection and Refraction of Spherical Waves"; Second Order Effects Annalen der Physic 5, Vol. 41 pg 443, 1942.

5. A. Sommerfeld: "Problems In Wireless Telegraphy (Vorlesungen ueber Theoretische Physik) Vol. VI 1947.

6. L. M. Brekhovskikh: Waves in Layered Media pg. 270 Academic Press 1960.

ACKNOWLEDGMENTS

The author wishes to thank Dr. Schwering, Dr. Bennett, Mr. Murphy and Mr. Johnson for their help and support in preparation of this paper.

APPENDIX

A. ANALYSIS OF VARIOUS POLARIZATION MODULATION CASES.

A.1 Derivation of free space field equations from a pair of crossed electrical dipole antennas with moments M and N.

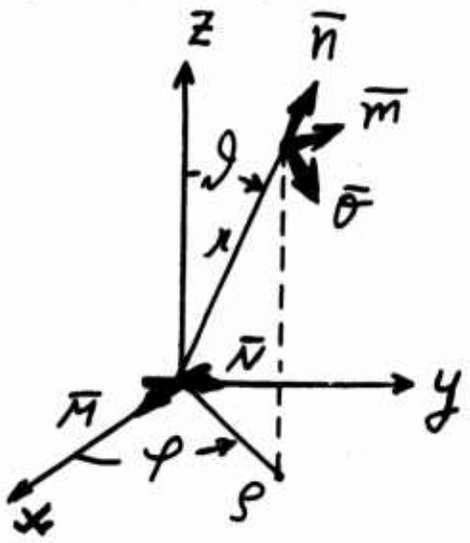

Figure A.1 shows location and orientation of the dipole antennas M and N relative to the x, y, and z coordinates and in the spherical system with the direction unit vectors $\bar{n}$, $\bar{m}$, $\bar{o}$.

The electromagnetic fields are derived from the Hertz-vector functions $\bar{\pi}_1$ and $\bar{\pi}_2$:

$$\bar{\pi}_1 = \sqrt{\frac{\mu}{\varepsilon}} \cdot \frac{\bar{M}}{4\pi k_s r} \cdot \cos\left[k_s r - \omega_s t - \varphi_1\left(\frac{k_s}{\omega_s} r - t\right)\right] \cdot \left\{\bar{n}\cos\varphi \cdot \sin\vartheta - \bar{m} \cdot \sin\varphi + \bar{o} \cdot \cos\varphi \cdot \cos\vartheta\right\} \qquad \text{A.1.1}$$

$$\bar{\bar{\Pi}}_2 = \sqrt{\frac{\mu}{\varepsilon}} \cdot \frac{\bar{N}}{4\pi \cdot k_s \cdot r} \cdot \sin\left[k_s r - \omega_s t - \psi_2\left(\frac{k_s}{\omega_s} r - t\right)\right]$$

A.1.2

$$\cdot \left\{\bar{n} \sin\varphi \cdot \sin\vartheta + \bar{m} \cdot \cos\varphi + \bar{o} \cdot \sin\varphi \cdot \cos\vartheta\right\}$$

As conventionally used in technical applications, the electrical antenna dipole moments M and N are given in amp. meter. Time in connection with the signal carrier -- radiated frequency ω_s in rad/sec is counted negative. $\psi_1(t)$ and $\psi_2(t)$ are phase functions. These functions in connection with the magnitude of M and of N in $\bar{\pi}_1$ and $\bar{\pi}_2$ determine the character of the emanated EM fields. The signal carrier propagation factor is defined by:

$$k_s = \frac{\omega_s}{c} = \frac{2\pi}{\lambda_s} \qquad \text{A.1.3}$$

The characteristic impedance of the propagation medium is:

$$\sqrt{\mu/\varepsilon} = \omega_s \cdot \mu \qquad \text{A.1.4}$$

ε . . . dielectric permitivity ($\frac{10^3}{36\pi} \cdot 10^{-12} \frac{A \cdot S}{V \cdot M}$ for air)

μ . . . magnetic permeability ($0.4\pi \cdot 10^{-6} \frac{AS}{V \cdot M}$ for air)

Magnetic fields H are derived from the Hertz-Vector:

$$\bar{H} = -\frac{1}{\mu c^2} \cdot \nabla \times \dot{\bar{\Pi}} \qquad \text{A.1.5}$$

and the electrical fields by:

$$\bar{E} = \nabla(\nabla \cdot \bar{\Pi}) - \frac{1}{c^2} \ddot{\bar{\Pi}} \qquad \text{A.1.6}$$

where the Del Operator for the spherical system is:

$$\nabla_{\cup} = \left[\bar{n}\frac{\partial}{\partial r} + \frac{\bar{m}}{r\cdot\sin\vartheta}\cdot\frac{\partial}{\partial\varphi} + \frac{\bar{\vartheta}}{r}\cdot\frac{\partial}{\partial\vartheta}\right]_{\cup} \qquad \text{A.1.7}$$

The derivatives of the direction unit vectors are:

$$\frac{\partial\bar{n}}{\partial\vartheta} = \bar{\vartheta} \quad ; \quad \frac{\partial\bar{\vartheta}}{\partial\vartheta} = -\bar{n} \qquad \text{A.1.8}$$

$$\frac{\partial\bar{n}}{\partial\varphi} = \bar{m}\cdot\sin\vartheta \quad ; \quad \frac{\partial\bar{\vartheta}}{\partial\varphi} = \bar{m}\cdot\cos\vartheta \qquad \text{A.1.9}$$

Employing the identity:

$$k_s = \frac{k_s}{c}\cdot\frac{1}{\sqrt{\varepsilon\mu}} = \frac{k_s}{\mu c}\cdot\sqrt{\frac{\mu}{\varepsilon}} \qquad \text{A.1.10}$$

one gets the "magnetic field"

$$\bar{H}_1 = \frac{M\cdot k_s^2}{4\pi(k_s r)}\cdot\left\{\left[\cos\left[k_s r-\omega_s t-\varphi_1\right]\right]\cdot\left(1+\frac{\dot{\varphi}_1}{\omega_s}\right)^2\right.$$

$$\left.-\left[\frac{\ddot{\varphi}_1}{\omega_s^2}+\frac{1+\frac{\dot{\varphi}_1}{\omega_s}}{k_s r}\right]\cdot\sin\left[k_s r-\omega_s t-\varphi_1\right]\right\}\cdot \qquad \text{A.1.11}$$

$$\cdot\begin{Bmatrix}\bar{n}\cdot 0\\ \bar{m}\cdot\cos\varphi\cdot\cos\vartheta\\ \bar{\vartheta}\cdot\sin\varphi\end{Bmatrix}$$

which is radiated from the dipole moment M (Figure 1). By replacing in Equation A.1.11:

$$M \longrightarrow N$$
$$\varphi \longrightarrow \varphi - \pi/2 \qquad \text{A.1.12}$$
$$\gamma_1 \longrightarrow \gamma_2 - \pi/2$$

one gets

$$\bar{H}_2 = \frac{+N \cdot k_s^2}{4\pi \cdot k_s \cdot r} \cdot \left\{ \left[\sin[k_s r - \omega_s t - \gamma_2] \right] \cdot \left(1 + \frac{\dot{x}_2}{\omega_s}\right)^2 \right. \qquad \text{A.1.13}$$

$$\left. + \left[\frac{\ddot{x}_2}{\omega_s^2} + \frac{1 + \frac{\dot{x}_2}{\omega_s}}{k_s r} \right] \cos[k_s r - \omega_s t - \gamma_2] \right\} \cdot$$

$$\cdot \begin{Bmatrix} \bar{n} \cdot 0 \\ \bar{m} \cdot \sin\varphi \cdot \cos\vartheta \\ \bar{\vartheta} \cdot (-\cos\varphi) \end{Bmatrix}$$

Further, for the explicit formulation of E, we need:

$$-\frac{1}{c^2} \ddot{\bar{\Pi}} = -\sqrt{\frac{\mu}{\varepsilon}} \cdot \frac{M \cdot k_s^2}{4\pi \cdot k_s r} \cdot$$

$$\cdot \left\{ -\left(1 + \frac{\dot{x}_1}{\omega_s}\right)^2 \cdot \cos[k_s r - \omega_s t - \gamma_1] + \right. \qquad \text{A.1.14}$$

$$\left. + \frac{\ddot{x}_1}{\omega_s^2} \cdot \sin[k_s r - \omega_s t - \gamma_1] \right\} \cdot$$

$$\cdot \left\{ \bar{n} \cdot \cos\varphi \cdot \sin\vartheta - \bar{m} \cdot \sin\varphi + \bar{\vartheta} \cdot \cos\varphi \cdot \cos\vartheta \right\}$$

$$-\frac{1}{c^2}\ddot{\bar{\Pi}} = +\sqrt{\mu/\varepsilon}\cdot\frac{N\cdot k_s^2}{4\pi\cdot k_s r}\cdot$$

A.1.15

$$\cdot\left\{+\left(1+\frac{\dot{\gamma}_2}{\omega_s}\right)^2\cdot\sin\left[k_s r-\omega_s t-\gamma_2\right]+\right.$$

$$\left.+\frac{\ddot{\gamma}_2}{\omega_s^2}\cdot\cos\left[k_s r-\omega_s t-\gamma_2\right]\right\}\cdot$$

$$\cdot\left\{\bar{n}\cdot\sin\varphi\cdot\sin\vartheta+\bar{m}\cdot\cos\varphi+\bar{\theta}\cdot\sin\varphi\cdot\cos\vartheta\right\}$$

and

$$div\,\bar{\bar{\Pi}}=(\nabla\cdot\bar{\bar{\Pi}})=\frac{1}{r^2}\frac{\partial}{\partial r}(r^2\Pi_r)+$$

$$+\frac{1}{r\cdot\sin\vartheta}\frac{\partial\Pi_\varphi}{\partial\varphi}+\frac{1}{r\sin\vartheta}\cdot\frac{\partial}{\partial\vartheta}(\sin\vartheta\cdot\Pi_\vartheta)=$$

$$=\frac{2}{r}\Pi_r+\frac{\partial}{\partial r}\Pi_r+\frac{1}{r\sin\vartheta}\frac{\partial\Pi_\varphi}{\partial\varphi}+$$

A.1.16

$$+\frac{1}{r}\cdot\frac{\cos\vartheta}{\sin\vartheta}\cdot\Pi_\vartheta+\frac{1}{r}\frac{\partial}{\partial\vartheta}\Pi_\vartheta$$

With Equations A.1.1 to A.1.9, A.1.15 and A.1.16 one gets the follcwing schematic representation for the E_1 components:

$$\bar{E}_1 = \sqrt{\mu/\varepsilon} \cdot \frac{M \cdot k_s^2}{4\pi \cdot k_s r} \cdot$$

A.1.17

$\cos[k_s r - \omega_s t - \psi_i]$	$+\sin[k_s r - \omega_s t - \psi_i]$	
$+\frac{2}{(k_s r)^2}$	$+\frac{2}{k_s r}\left(1+\frac{\dot{\psi}_i}{\omega_s}\right)$	$\bar{n} \cdot \cos\varphi \cdot \sin\vartheta$
$-\left(1+\frac{\dot{\psi}_i}{\omega_s}\right)^2 + \frac{1}{(k_s r)^2}$	$+\frac{\ddot{\psi}_i}{\omega_s^2} + \frac{1+\frac{\dot{\psi}_i}{\omega_s}}{k_s r}$	$\bar{m} \cdot \sin\varphi$
$+\left(1+\frac{\dot{\psi}_i}{\omega_s}\right)^2 - \frac{1}{(k_s r)^2}$	$-\frac{\ddot{\psi}_i}{\omega_s^2} - \frac{1+\frac{\dot{\psi}_i}{\omega_s}}{k_s r}$	$\bar{\vartheta} \cdot \cos\varphi \cdot \cos\vartheta$

By replacing in Equation A.1.17:

$$M \rightarrow N\,; \quad \varphi \rightarrow \varphi - \frac{\pi}{2}\,; \quad \psi_1 \rightarrow \psi_2 - \frac{\pi}{2}$$

one obtains the E_2 components:

$$\bar{E}_2 = \sqrt{\mu/\varepsilon} \cdot \frac{N k_s^2}{4\pi \cdot k_s r} \cdot$$

$\sin[k_s r - \omega_s t - \psi_2]$	$-\cos[k_s r - \omega_s t - \psi_2]$	A.1.18
$+\frac{2}{(k_s r)^2}$	$+\frac{2}{k_s r}\left(1+\frac{\dot{\psi}_2}{\omega_s}\right)$	$\bar{n} \cdot \sin\varphi \cdot \sin\vartheta$
$-\left(1+\frac{\dot{\psi}_2}{\omega_s}\right)^2 + \frac{1}{(k_s r)^2}$	$+\frac{\ddot{\psi}_2}{\omega_s^2} + \frac{1+\frac{\dot{\psi}_2}{\omega_s}}{k_s r}$	$-\bar{m} \cdot \cos\varphi$
$+\left(1+\frac{\dot{\psi}_2}{\omega_s}\right)^2 - \frac{1}{(k_s r)^2}$	$-\frac{\ddot{\psi}_2}{\omega_s^2} - \frac{1+\frac{\dot{\psi}_2}{\omega_s}}{k_s r}$	$\bar{\theta} \cdot \sin\varphi \cdot \cos\vartheta$

For example, the r-component E_r or E_2 is read off from the schematic representation Equation A.1.18 with:

$$E_{2r} = \sqrt{\mu/\varepsilon} \cdot \frac{N \cdot k_s^2}{4\pi \cdot k_s r} \cdot (\sin\varphi \cdot \sin\vartheta) \cdot \qquad \text{A.1.19}$$

$$\left\{ \left[\frac{2}{(k_s r)^2} \right] \cdot \sin(k_s r - \omega_s t - \psi_2) + \right.$$

$$\left. - \left[\left(1 + \frac{\dot{r}_s}{\omega_s}\right) \frac{2}{k_s r} \right] \cdot \cos(k_s r - \omega_s t - \psi_2) \right\}$$

Similarly the φ and ϑ components of $\bar{E}_2$, in the $\bar{n}$ and $\bar{\sigma}$ directions, follow from the terms in the second and third row of the schematic Equation A.1.18.

A.2 DISCUSSION OF THE FIELD EQUATIONS.

We are especially interested in the "combined field"

$$\bar{E} = \bar{E}_1 + \bar{E}_2 \qquad \text{A.2.1}$$

from the M and N dipole antennas. First of all the E_p component of $\bar{E}$ which is perpendicular to the radial direction. This E_p component follows from Equations A.1.17 and A.1.18 by super-position of the m and o components.

To reduce the amount of writing, we abbreviate the following expressions by setting:

$$[k_s r - \omega_s t - \gamma_1] = \beta_1 \qquad \text{A.2.2}$$

$$[k_s r - \omega_s t - \gamma_2] = \beta_2$$

Super-position of the ρ and ϑ components of E_1 and of E_2 yields E_p in the format of Equation A.2.3 as follows:

$$\bar{E}_\rho = \sqrt{\mu/\varepsilon} \cdot \frac{k_3^2}{4\pi \cdot k_3 r} \cdot$$

A.2.3

$$\cdot \left[\bar{m} \cdot \left[\begin{array}{l} M \cdot \sin\varphi \cdot \left\{ \left[\frac{1}{(k_3 r)^2} - \left(1 + \frac{\dot{\psi}_1}{\omega_3}\right)^2 \right] \cdot \cos\beta_1 + \left[\frac{1+\frac{\dot{\psi}_1}{\omega_3}}{k_3 r} + \frac{\ddot{\psi}_1}{\omega_3^2} \right] \cdot \sin\beta_1 \right\} + \\ + N \cos\varphi \cdot \left\{ \left[\frac{1+\frac{\dot{\psi}_2}{\omega_3}}{k_3 r} + \frac{\ddot{\psi}_2}{\omega_3^2} \right] \cdot \cos\beta_2 + \left[\frac{1}{(k_3 r)^2} - \left(1 + \frac{\dot{\psi}_2}{\omega_3}\right)^2 \right] \cdot \sin\beta_2 \right\} \end{array} \right] + \right.$$

$$\left. + \bar{\theta} \cdot \cos\vartheta \cdot \left[\begin{array}{l} -M \cos\varphi \left\{ \left[\frac{1}{(k_3 r)^2} - \left(1 + \frac{\dot{\psi}_1}{\omega_3}\right)^2 \right] \cdot \cos\beta_1 + \left[\frac{1+\frac{\dot{\psi}_1}{\omega_3}}{k_3 r} + \frac{\ddot{\psi}_1}{\omega_3^2} \right] \cdot \sin\beta_1 \right\} + \\ + N \sin\varphi \cdot \left\{ \left[\frac{1+\frac{\dot{\psi}_2}{\omega_3}}{k_3 r} + \frac{\ddot{\psi}_2}{\omega_3^2} \right] \cdot \cos\beta_2 - \left[\frac{1}{(k_3 r)^2} - \left(1 + \frac{\ddot{\psi}_2}{\omega}\right)^2 \cdot \sin\beta_2 \right\} \right] \end{array} \right]$$

and the radical component of $\bar{E}$

$$E_r = \sqrt{\frac{\mu}{\varepsilon}} \cdot \frac{k_1^2}{4\pi \cdot k_1 r} \cdot \sin\vartheta \cdot \qquad \text{A.2.4}$$

$$\cdot \left[\begin{array}{l} M \cdot \cos\varphi \cdot \left\{ \left[\frac{2}{(k_1 r)^2} \right] \cdot \cos\beta_1 + \left[\left(1 + \frac{\dot{r}_1}{\omega_1}\right) \cdot \frac{2}{k_1 r} \right] \cdot \sin\beta_1 \right. \\ \left. + N \cdot \sin\varphi \cdot \left\{ \left[\frac{2}{(k_1 r)^2} \right] \cdot \sin\beta_2 - \left[\left(1 + \frac{\dot{r}_2}{\omega_1}\right) \cdot \frac{2}{k_1 r} \right] \cdot \cos\beta_2 \right. \end{array} \right]$$

The component magnetic field $\bar{H}$:

$$\bar{H} = \bar{H}_1 + \bar{H}_2 \qquad \text{A.2.5}$$

follows from Equations A.1.11 and A.1.13 with

$$\bar{H} = \frac{k_s^2}{4\pi(k_s R)} \cdot$$

A.2.6

$$\cdot \Big\{ \bar{m} \cdot \cos\vartheta \cdot \Big[-M \Big[\Big(1+\frac{\dot{\chi}_1}{\omega_s}\Big)^2 \cdot \cos\beta_1 - \Big(\frac{\ddot{\chi}_1}{\omega_s^2} + \frac{1+\frac{\dot{\chi}_1}{\omega_s}}{k_s R}\Big) \sin\beta_1 \Big] \cdot \cos\varphi$$

$$- N \cdot \Big[\Big(1+\frac{\dot{\chi}_2}{\omega_s}\Big)^2 \cdot \sin\beta_2 + \Big(\frac{\ddot{\chi}_2}{\omega_s^2} + \frac{1+\frac{\dot{\chi}_2}{\omega_s}}{k_s R}\Big) \cos\beta_2 \Big] \cdot \sin\varphi \Big]$$

$$+ \bar{\vartheta} \cdot \Big[-M \Big[\Big(1+\frac{\dot{\chi}_1}{\omega_s}\Big)^2 \cdot \cos\beta_1 - \Big(\frac{\ddot{\chi}_1}{\omega_s^2} + \frac{1+\frac{\dot{\chi}_1}{\omega_s}}{k_s R}\Big) \cdot \sin\beta_1 \Big] \cdot \sin\varphi$$

$$+ N \cdot \Big(1+\frac{\dot{\chi}_2}{\omega_s}\Big) \cdot \sin\beta_2 + \Big(\frac{\ddot{\chi}_2}{\omega_s^2} + \frac{1+\frac{\dot{\chi}_2}{\omega_s}}{k_s R}\Big) \cdot \cos\beta_2 \Big] \cdot \cos\varphi \Big] \Big\}$$

With regard to practical applications the most important specialization of E and H (Equations A.2.3 to A.2.6) involves:

A.3 THE "IDEAL POLARIZATION MODULATION" CASE

Ideal polarization modulation is characterized by:

a. Equal magnitudes of the dipole moments:

$$M = N = A \qquad \text{A.3.1}$$

b. Time phase quadrature, corresponding to:

$$\psi_1(\tau) = \psi_2(\tau) = \psi(\tau) \qquad \text{A.3.2}$$

This gives

$$\beta_1 = \beta_2 = \beta = [k_3 r - \omega_3 t - \psi(\tau)] \qquad \text{A.3.3}$$

and in combination with the spatial angle:

$$[\omega_3 t + \psi(\tau) + \varphi - k_3 r] = \varphi - \beta = \alpha(\tau) \qquad \text{A.3.4}$$

Introducing these specializations into Equations A.2.3 and A.2.4 gives the $\bar{E}$ field components for the ideal polarization modulation case.

$$\underset{(Ideal)}{\bar{E}} = \sqrt{\frac{\mu}{\varepsilon}} \cdot \frac{A k_s^2}{4\pi \cdot k_s r} \cdot \qquad \text{A.3.5}$$

$\cdot$	$+\cos[\alpha(\tau)]$	$+\sin[\alpha(\tau)]$
$\bar{n}.\sin\vartheta$	$+\frac{2}{(k_s r)^2}$	$-\frac{2}{k_s r}\cdot\left(1+\frac{\dot{\alpha}}{\omega_s}\right)$
$\bar{m}$	$+\frac{\ddot{\alpha}}{\omega_s^2}$ $+\frac{1}{k_s r}\cdot\left(1+\frac{\dot{\alpha}}{\omega_s}\right)$	$-\left(1+\frac{\dot{\alpha}}{\omega_s}\right)^2$ $+\frac{1}{(k_s r)^2}$
$\bar{\theta}.\cos\vartheta$	$+\left(1+\frac{\dot{\alpha}}{\omega_s}\right)^2$ $-\frac{1}{(k_s r)^2}$	$+\frac{\ddot{\alpha}}{\omega_s^2}$ $+\frac{1}{k_s r}\left(1+\frac{\dot{\alpha}}{\omega_s}\right)$

and the H field for the ideal polarization modulation case:

$$\overline{H}_{Ideal.} = \frac{A \cdot k_s^2}{4\pi \cdot k_s r} \cdot$$

A.3.6

$$\cdot \left\{ \overline{m} \cdot \cos\vartheta \cdot \left[\left(1 + \frac{\dot{x}}{\omega_s}\right)^2 \cdot \cos\alpha + \left(\frac{1 + \frac{\dot{x}}{\omega_s}}{k_s r} + \frac{\ddot{x}}{\omega_s^2} \right) \cdot \sin\alpha \right] \right.$$

$$\left. + \overline{\vartheta} \cdot \left[\left(1 + \frac{\dot{x}}{\omega_s}\right)^2 \cdot \sin\alpha - \left(\frac{1 + \frac{\dot{x}}{\omega_s}}{k_s r} + \frac{\ddot{x}}{\omega_s^2} \right) \cdot \cos\alpha \right] \right\}$$

The Pointing Vector

$$\overline{P} = \overline{E} \times \overline{H} \qquad \text{A.3.7}$$

in the far-zone, i.e., for

$$k_s r \gg 1 \qquad \text{A.3.8}$$

is obtained from E and H of Equations A.3.5 and A.3.6 by dropping the terms involving negative powers of larger than one. This yields the Pointing Vector (power flow per unit cross section area) in the far-zone radiation field,

$$\overline{P}_{\text{Ideal for } k_s r \gg 1} \doteq \sqrt{\frac{\mu}{\varepsilon}} \cdot \left(\frac{A k_s^2}{4\pi k_s r} \right)^2 \cdot \qquad \text{A.3.9}$$

$+\overline{\Pi}$	$\left(1+\frac{\dot{\varkappa}}{\omega_s}\right)^4 \cdot \left\{1-\cos^2\alpha \cdot \sin^2\vartheta\right\} + \dots$
$-\overline{\Pi\Pi}$	$\frac{\sin\vartheta}{k_s r} \cdot \left\{2\left(1+\frac{\dot{\varkappa}}{\omega_s}\right)^3 \cdot \sin^2\alpha - \frac{\ddot{\varkappa}}{\omega_s^2}\left(1+\frac{\dot{\varkappa}}{\omega_s}\right) \cdot \sin 2\alpha\right\} + \dots$
$+\overline{\Theta}$	$\frac{\sin 2\vartheta}{k_s r} \cdot \left\{\frac{\ddot{\varkappa}}{\omega_s^2} \cdot \left(1+\frac{\dot{\varkappa}}{\omega_s}\right) \cdot \sin^2\alpha + \frac{1}{2}\left(1+\frac{\dot{\varkappa}}{\omega_s}\right) \cdot \sin 2\alpha\right\} + \dots$

For graphical representation, note that $E_{p\ ideal}$ (i.e., the ϑ, φ components (Equation A.3.5)) split INTO:

$$\bar{E}_{p_1} = \mathcal{E}_{p_1} \cdot \begin{cases} -\bar{m} \cdot \sin(\alpha(t)) \\ +\bar{\theta} \cdot \cos\vartheta \cdot \cos(\alpha(t)) \end{cases} \qquad \text{A.3.10}$$

where

$$\mathcal{E}_{p_1} = \sqrt{\frac{\mu}{\varepsilon}} \cdot \frac{A k_s^2}{4\pi k_s r} \cdot \left[\left(1 + \frac{\dot{\nu}}{\omega_s}\right)^2 - \frac{1}{(k_s r)^2} \right] \qquad \text{A.3.10'}$$

and

$$\bar{E}_{p_2} = \mathcal{E}_{p_2} \cdot \begin{cases} \bar{m} \cdot \cos(\alpha(t)) \\ \bar{\theta} \cdot \cos\vartheta \cdot \sin(\alpha(t)) \end{cases} \qquad \text{A.3.11}$$

where

$$\mathcal{E}_{p_2} = \sqrt{\frac{\mu}{\varepsilon}} \frac{A k_s^2}{4\pi k_s r} \cdot \left[\frac{\ddot{\nu}}{\omega_s^2} + \frac{1 + \frac{\dot{\nu}}{\omega_s}}{k_s r} \right] \qquad \text{A.3.11'}$$

Since the sign of $\mathcal{E}_{p1}$ depends on the relative magnitude of $k_s r$; $\bar{E}_{p1}$ in the near-zone ($k_s r \ll 1$) and $\bar{E}_{p1}$ in the far-zone ($1 \ll k_s r$) are 180 degrees out of phase. Equations A.3.10 and A.3.11 correspond to Ellypses. Figures A.3.a and b below show the relations between normalized $\bar{E}_{p1}$ and $\bar{E}_{p2}$ in diagram form.

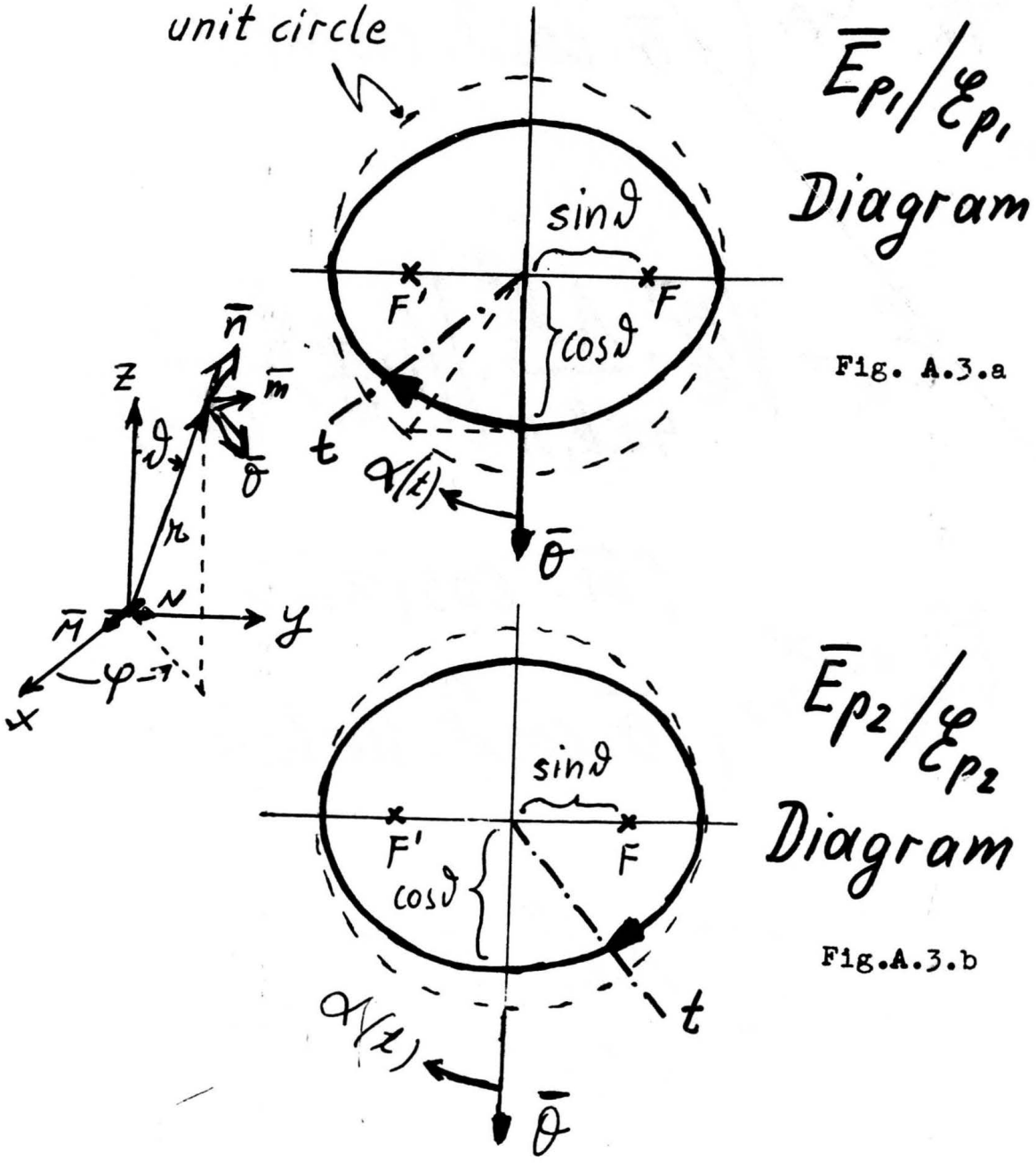

Fig. A.3.a

Fig.A.3.b

The positions of $\bar{E}_{p1}$ and $\bar{E}_{p2}$ shown in the diagrams of Figures A.3.a and A.3.b are given for the same t.

Of significance is the proportionality of E_{p2} with respect to $\ddot{\psi}/\omega_s^2$ (for $k_s r \gg 2$, in the Far-Zone). This ratio $\ddot{\psi}/\omega_s^2$ represents the FM-index $\Delta\Omega/\omega_s$ times the ratio of audio to carrier frequency ω_a/ω_s .

Similarly the $E_{p'}$ component (Equation A.3.10,p-direction) depends on this modulation index in the Far-Zone. Hence, different to the conventional FM signal modulation and transmission techniques, polarization modulated signal transmission involves modulation of the wave by $\dot{\psi}/\omega_s$ and $\ddot{\psi}/\omega_s^2$ in the far-zone of the antenna.

Physically, radiation of power into the $\bar{m}$ and $\bar{o}$ directions ($\sin^2\alpha$... in A.3.9) can be attributed to the accelerated motion of electrical charge in the plane of rotation of the resultant effective dipole moment of the antenna. This plane of rotation is in our case the x-y plane (Figure A.1) and the axes of rotation the z-axes. The modulation function $\psi(t)$, superimposed over the space angle φ controls the rotation of the resultant effective dipole moment and of the radiated field vectors (Equation A.3.4). The dependence on the angle ϑ of the electrical and of the magnetic field (Equations A.3.5 and A.3.6) amounts to a ϑ dependent distortion of the polarization modulated signal transmissions.

A.4 INCORRECT PHASING OF CROSSED DIPOLES.

To evaluate the effects of incorrect phasing conditions we consider the following specializations:

$$M = N = A \qquad \text{A.4.1}$$

as before in section A.3 for the ideal case, but

$$\psi_2(t) = \psi_1(t) + \frac{\pi}{2} \qquad \text{A.4.2}$$

i.e., M and N are 180 degrees out of phase (see Equations A.1.1 and A.1.2). The resultant electrical field components are obtained from Equations A.1.17 and A.1.18 by replacing:

$$\sin\beta_2 \longrightarrow \sin\left(\beta_1 - \frac{\pi}{2}\right) = -\cos\beta_1 = -\cos\beta \qquad \text{A.4.3}$$

$$\cos\beta_2 \longrightarrow \cos\left(\beta_1 - \frac{\pi}{2}\right) = +\sin\beta_1 = +\sin\beta$$

where β_1 and β_2 are given by Equation A.2.2.

This gives the radial component and the perpendicular electrical field component E_r and E_p as follows:

$$(E_\vartheta)_{\Delta=180^\circ} = \sqrt{\mu/\varepsilon}\cdot\frac{A k_s^2}{4\pi k_s r}\cdot \sin\vartheta\cdot(\cos\varphi-\sin\varphi)\cdot$$

A.4.4

$$\cdot\left\{\frac{2}{(k_s r)^2}\cos\beta + \frac{2}{k_s r}\left(1+\frac{\dot{\varkappa}}{\omega_s}\right)\sin\beta\right\}$$

$$(\bar{E}_\rho)_{\Delta=180^\circ} = \sqrt{\mu/\varepsilon}\cdot\frac{A k_s^2}{4\pi k_s r}\cdot$$

A.4.5

$$\cdot\left\{\left[\frac{1}{(k_s r)^2}-\left(1+\frac{\dot{\varkappa}}{\omega_s}\right)^2\right]\cdot\cos\beta+\left[\frac{1+\frac{\dot{\varkappa}}{\omega_s}}{k_s r}+\frac{\ddot{\varkappa}}{\omega_s^2}\right]\sin\beta\right\}\cdot$$

$$\cdot\left\{\begin{array}{l}\bar{m}\cdot(\cos\varphi+\sin\varphi)\\ \bar{\vartheta}\cdot\cos\vartheta\cdot(\sin\varphi-\cos\varphi)\end{array}\right\}$$

---

with:

$$\beta = k_s r-\omega_s t-\varkappa_1 = \beta_1 =$$
$$= k_s r-\omega_s t-\left(\varkappa_2-\frac{\pi}{2}\right) = \beta_2+\frac{\pi}{2}$$

A.4.6

Using the trigometric identity:

$$(\cos\varphi+\sin\varphi)^2+\cos^2\vartheta\cdot(\sin\varphi-\cos\varphi)^2=$$
$$=2\left[1-\frac{1}{2}\sin^2\vartheta\cdot(1-\sin 2\varphi)\right] \qquad \text{A.4.7}$$

one gets the absolute value of E_p and of E_r:

$$|E_p|_{\Delta=180^\circ}=\sqrt{\mu/\varepsilon}\cdot\frac{A k_s^2}{4\pi k_s r}\cdot\sqrt{2}\cdot$$
$$\cdot\sqrt{1-\frac{1}{2}\sin^2\vartheta\cdot(1-\sin 2\varphi)}\cdot \qquad \text{A.4.8}$$
$$\cdot\sqrt{\left[\left(1+\frac{\dot{\varkappa}}{\omega_s}\right)^2-\frac{1}{(k_s r)^2}\right]^2+\left[\frac{\ddot{\psi}}{\omega_s^2}+\frac{1+\dot{\varkappa}/\omega_s}{k_s r}\right]^2}$$

$$|E_r|_{\Delta=180^\circ}=\sqrt{\mu/\varepsilon}\cdot\frac{A k_s^2}{4\pi k_s r}\cdot\sin\vartheta\cdot(\cos\varphi-\sin\varphi)\cdot \qquad \text{A.4.9}$$
$$\cdot\sqrt{\left[\frac{2}{(k_s r)^2}\right]^2+\left[\frac{2}{k_s r}\cdot\left(1+\frac{\dot{\varkappa}}{\omega_s}\right)\right]^2}$$

A.5 CARRIER SUPPRESSED (CS) POLARIZATION MODULATION (Method: G. Vogt and Associates, USAECOM, IER)

In the carrier suppressed polarization modulation case the radiated EM field rotates at audio signal frequencies. The rotation of the (HF, VHF, UHF) signal carrier field is suppressed in accordance with the following equations for the Hertz-Vector Functions:

$$\Pi_x^{(CS)} = \frac{1}{2}\left[\Pi_x + \tilde{\Pi}_x\right] = \frac{1}{2}\cdot\sqrt{\frac{\mu}{\varepsilon}}\cdot\frac{A}{4\pi k_s r}\cdot \qquad \text{A.5.1}$$

$$\cdot\left[\cos(k_s r - \omega_s t - \psi(\tau)) + \cos(k_s r - \omega_s t + \psi(\tau))\right]$$

i.e: $$\Pi_x^{(CS)} = \frac{\sqrt{\frac{\mu}{\varepsilon}}\cdot A}{4\pi k_s r}\cdot\cos\psi(\tau)\cdot\cos(k_s r - \omega_s t) \qquad \text{A.5.2}$$

and $$\Pi_y^{(CS)} = \frac{1}{2}\left[\Pi_y - \tilde{\Pi}_y\right] = \frac{1}{2}\sqrt{\frac{\mu}{\varepsilon}}\cdot\frac{A}{4\pi k_s r}\cdot \qquad \text{A.5.3}$$

$$\cdot\left[\sin(k_s r - \omega_s t - \psi(\tau)) - \sin(k_s r - \omega_s t + \psi(\tau))\right]$$

i.e;

$$\Pi_y^{(CS)} = -\frac{\sqrt{\frac{\mu}{\varepsilon}}A}{4\pi k_s r}\cdot\sin\psi(\tau)\cdot\cos(k_s r - \omega_s t) \qquad \text{A.5.4}$$

In practice $\bar{\Pi}_x^{(cs)}$ and $\bar{\Pi}_y^{(cs)}$ are obtained by amplitude modulation of the carrier. The phase between the audio modulation signals radiated via the M and N dipole is in this case 90 degrees. By replacing in Equation A.3.5

$$\psi \rightarrow -\psi$$
$$\bar{E} \rightarrow \tilde{\bar{E}}$$

and forming $\bar{E}^{(cs)} = \frac{1}{2}[\bar{E} + \tilde{\bar{E}}]$

one gets :

$$\bar{E}^{(cs)} = \sqrt{\mu/\varepsilon} \cdot \frac{A k_s^2}{4\pi k_s r} \cdot$$

	$\cos\psi(t)$		$\sin\psi(t)$	
	$\cos\gamma$	$\sin\gamma$	$\cos\gamma$	$\sin\gamma$
$\bar{n}$ $\sin\vartheta$	$\frac{2}{(k_s r)^2}$	$-\frac{\dot{\psi}}{\omega_s} \cdot \frac{2}{k_s r}$	$-\frac{2}{k_s r}$	0
$\bar{m}$	$\frac{1}{k_s r}$	$-2 \cdot \frac{\dot{\psi}}{\omega_s}$	$-\left[1+\left(\frac{\dot{\psi}}{\omega_s}\right)^2\right]$ $-\frac{1}{(k_s r)^2}$	$-\frac{\ddot{\psi}}{\omega_s^2}$ $-\frac{\dot{\psi}}{\omega_s} \cdot \frac{1}{k_s r}$
$\bar{\vartheta}$ $\cos\vartheta$	$\left[1+\left(\frac{\dot{\psi}}{\omega_s}\right)^2\right]$ $-\frac{1}{(k_s r)^2}$	$\frac{\ddot{\psi}}{\omega_s^2} +$ $+\frac{\dot{\psi}}{\omega_s} \cdot \frac{1}{k_s r}$	$\frac{1}{k_s r}$	$-2\frac{\dot{\psi}}{\omega_s}$

where

$$\gamma = [\omega_s t - k_s r + \varphi]$$

B. THE INFLUENCE OF GROUND PROPERTIES ON TRANSMISSION AND RECEPTION OF POLARIZATION MODULATED SIGNALS VIA CROSSED DIPOLES

B.1 Geometrical Definition of the Problem (Figure B.1):

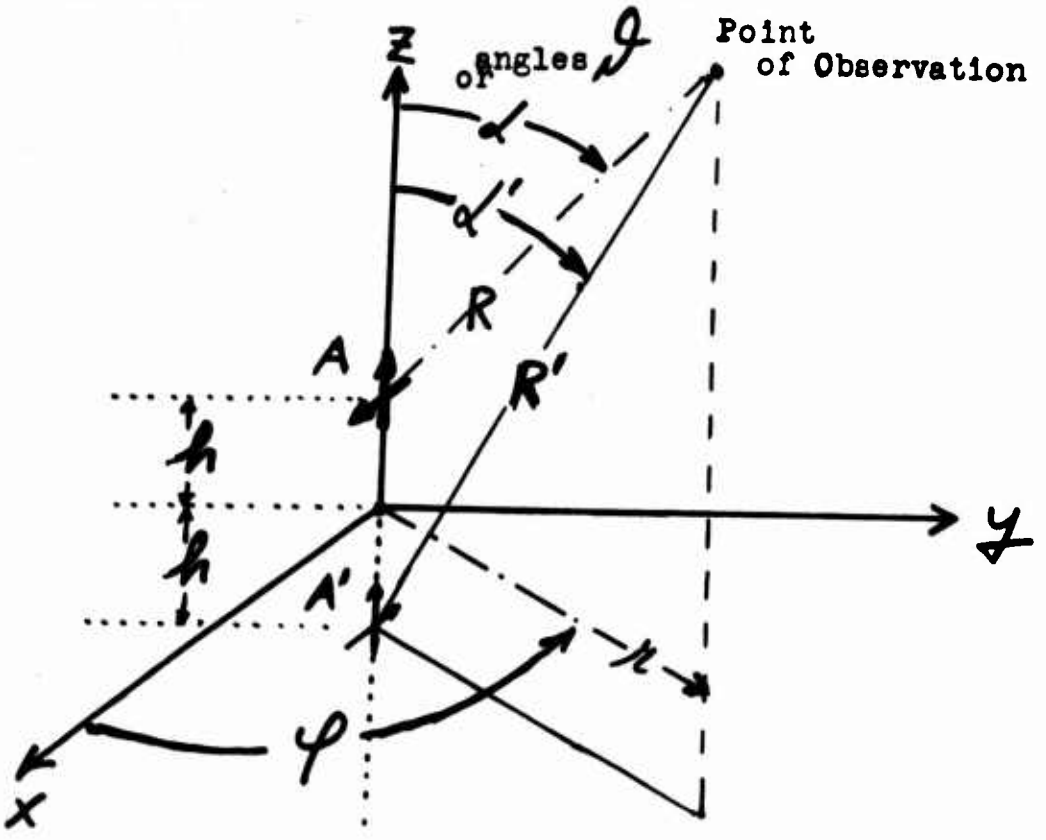

Figure B.1: $z > 0$ = Air, $z < 0$ = Ground, A Primary = antenna at height h above ground; A' image with respect to ground of A.

EM-characteristics: Air $k_0^2 = \omega^2 \varepsilon_0 \mu_0 = \left(\frac{2\pi}{\lambda_0}\right)^2$

Ground $k_g^2 = \omega^2 \varepsilon_g \mu_0 + j\omega \sigma_g \mu_0 = \omega^2 \varepsilon_g \mu_0$

Index of Refraction of ground relative to air: n;

$$n_g^2 = k_g^2 / k_0^2 = \varepsilon_{g\,rel} [1 + j\, \delta_g / \delta] = \varepsilon_{g\,rel}$$

Critical ground frequency: $f_g = \sigma_g / 2\pi \varepsilon_g$

Dielectric Regime: $f \gg f_g$;

Conductive Regime: $\delta \ll \delta_g$

B.2 Hertz-Vector Functions for Air and Ground.

With $\psi/\omega_1 \ll 1$ and ψ slowly variable (i.e. treated const. in the Fourier int.) the Hertz-Vector functions of horizontal and vertical electrical dipoles above flat ground are given in the literature (e.g., reference 1). In our case the Hertz-Vectors of the horizontal dipole element of the antenna (M) are given in the form of a super-position of the "direct", the "reflected" and the "refracted" components as follows:

a. In the air half space $z > 0$:

$$\Pi_x^{(0)} = -\frac{j}{4\pi}\sqrt{\frac{\mu_0}{\varepsilon_0}}\cdot M_x \cdot e^{-j[\omega t+\psi]} \cdot$$

$$\left\{ \frac{e^{-jk_0 R}}{k_0 R} - \frac{e^{-jk_0 R'}}{k_0 R'} + \right. \qquad \text{B.2.1}$$

$$+\frac{j}{2}\cdot \int_{-\frac{\pi}{2}+j\infty}^{+\frac{\pi}{2}-j\infty} d\vartheta_0 \cdot \sin\vartheta_0 \cdot \left[\frac{2\cos\vartheta_0}{\cos\vartheta_0 + \sqrt{n_g^2 - \sin^2\vartheta_0}} \cdot \right.$$

$$\left. \left. \cdot \left[H_0^{(1)}(k_0 r \sin\vartheta_0)\right] e^{-jk_0(z+h)\cos\vartheta_0} \right] \right\}$$

b. In the ground half space $z < 0$:

$$\Pi_x^{(g)} = -\frac{j}{4\pi}\sqrt{\frac{\mu_0}{\varepsilon_0}}\cdot\frac{M_x}{n_g^2}\cdot e^{-j[\omega t+\psi]}\cdot$$

$$\cdot\frac{j}{2}\cdot\int_{-\frac{\pi}{2}+j\infty}^{+\frac{\pi}{2}-j\infty} d\vartheta_0\cdot\sin\vartheta_0\left(\frac{2\cos\vartheta_0}{\cos\vartheta_0+\sqrt{n_g^2-\sin^2\vartheta_0}}\cdot\right.$$

$$\cdot\left[H_0^{(1)}(k_0 r\sin\vartheta_0)\right]\cdot$$

$$\left.\cdot e^{-jk_0 z\cdot\left[\sqrt{n_g^2-\sin^2\vartheta_0}-\frac{h}{z}\cdot\cos\vartheta_0\right]}\right) \qquad \text{B.2.2}$$

Here, the angle ϑ_0 has been introduced from the following relations between angles ϑ_0 in air and ϑ_g in the ground resultant from the air to ground boundary conditions:

Snell's Law

$$\sin\vartheta_0 = n_g\cdot\sin\vartheta_g \qquad \text{B.2.3}$$

and

$$h k_0\cos\vartheta_0 = h_g k_g\cos\vartheta_g \qquad \text{B.2.4}$$

where h_g corresponds to the "height of the refracted dipole charges below the ground surface. These give rise to a z-component:

a. In the Air Half-Space $z > 0$

$$\Pi_z^{(o)} = \sqrt{\frac{\mu_o}{\varepsilon_o}} \cdot \frac{M_x}{4\pi} \cdot e^{-j[\omega t + \psi]} \cdot \cos\varphi \cdot$$

$$\cdot \frac{j}{2} \int_{-\frac{\pi}{2}+j\infty}^{+\frac{\pi}{2}-j\infty} d\vartheta_o \cdot \sin\vartheta_o \left[2\sin\vartheta_o \cdot \cos\vartheta_o \cdot \right.$$

B.2.5

$$\left. \cdot \frac{\cos\vartheta_o - \sqrt{n_g^2 - \sin^2\vartheta_o}}{n_g^2 \cos\vartheta_o + \sqrt{n_g^2 - \sin^2\vartheta_o}} \cdot \left[H_1^{(1)}(k_o x \sin\vartheta_o) \right] \cdot \right.$$

$$\left. \cdot e^{+jk_o(z+h)\cdot\cos\vartheta_o} \right]$$

and fully analogous to $\Pi_x^{(g)}$ for the ground space:

b. In the Ground Half Space $z < 0$

$$\Pi_z^{(g)} = \frac{1}{n_g^2} \cdot \sqrt{\frac{\mu_0}{\varepsilon_0}} \cdot \frac{M_x}{4\pi} \cdot e^{-j[\omega t + \varphi]} \cdot \cos\varphi \cdot$$

$$\cdot \frac{j}{2} \cdot \int_{-\frac{\pi}{2}+j\infty}^{+\frac{\pi}{2}-j\infty} d\vartheta_0 \cdot \sin\vartheta_0 \cdot \Big[2 \cdot \sin\vartheta_0 \cdot \cos\vartheta_0 \cdot$$

B.2.6

$$\cdot \frac{\cos\vartheta_0 - \sqrt{n_g^2 - \sin^2\vartheta_0}}{n_g^2 \cdot \cos\vartheta_0 + \sqrt{n_g^2 - \sin^2\vartheta_0}} \cdot \left[H_1^{(1)}(k_0 \cdot r \cdot \sin\vartheta_0) \right] \cdot$$

$$\cdot e^{-jk_0 z \cdot \left[\sqrt{n_g^2 - \sin^2\vartheta_0} - \frac{h}{z}\cos\vartheta_0 \right]} \Big]$$

Whereas the Hertz-Vector function for M_x, the horizontal dipole, required an x and a z-component, the Hertz-Vector function for M_z, the vertical dipole, requires only a z-component to satisfy the boundary conditions at the ground surface z = 0, for the EM fields.

The Hertz Function for the vertical dipole N_z is:

a. In the Air Half Space $z > 0$

$$\Pi_z^{(0)} = -\frac{j}{4\pi}\sqrt{\frac{\mu_0}{\varepsilon_0}}\cdot N_z \cdot e^{-j\left[\omega t + \varphi - \frac{\pi}{2}\right]} \cdot$$

$$\cdot\left\{\frac{e^{jk_0R}}{k_0R} + \frac{e^{jk_0R'}}{k_0R'}\right.$$

B.2.7

$$\left. -\frac{j}{2}\cdot\int_{-\frac{\pi}{2}+j\infty}^{+\frac{\pi}{2}-j\infty} d\vartheta_0 \cdot \sin\vartheta_0 \cdot \left[\frac{2\cdot\sqrt{n_g^2-\sin^2\vartheta_0}}{n_g^2\cos\vartheta_0+\sqrt{n_g^2-\sin^2\vartheta_0}}\cdot\right.\right.$$

$$\left.\left.\cdot\left[H_0^{(1)}(k_0\cdot r\cdot\sin\vartheta_0)\right]\cdot e^{jk_0\cdot(z+h)\cos\vartheta_0}\right]\right\}$$

and similarly to $\Pi_z^{(g)}$ of Equation B.2.2 follows the Hertz function for N_z in the ground space.

b. In the Ground Half-Space $z < 0$

$$\Pi_z^{(g)} = -\frac{j}{4\pi}\cdot\sqrt{\frac{\mu_0}{\varepsilon_0}}\cdot N_z\cdot e^{-j[\omega t+\varphi-\frac{\pi}{2}]}\cdot$$

$$\cdot\frac{j}{2}\cdot\int_{-\frac{\pi}{2}+j\infty}^{+\frac{\pi}{2}-j\infty} d\vartheta_0\cdot\sin\vartheta_0\cdot\left[\frac{2\cos\vartheta_0}{n_g^2\cdot\cos\vartheta_0+\sqrt{n_g^2-\sin^2\vartheta_0}}\right.\cdot$$

B.2.8

$$\cdot\left[H_0^{(1)}(k_0 r\cdot\sin\vartheta_0)\right]\cdot$$

$$\left.\cdot e^{-jk_0\cdot z\cdot\left[\sqrt{n_g^2-\sin^2\vartheta_0}-\frac{h}{z}\cos\vartheta_0\right]}\right]$$

The functions $H_0^{(1)}$ and $H_1^{(1)}$ of $k_0 r\cdot\sin\vartheta_0$ are Hankel functions of the first kind and of zero and first order respectively. The Hankel-Integral representations for the Hertz-Vector component functions (Equations B.2.1, B.2.2, B.2.5 to B.2.8) are based on the following Fourier-Integral and Hankel-Integral identity:

$$\frac{e^{-jkR}}{kr} \equiv \frac{1}{2\pi} \cdot \iint_{\varphi' \vartheta} d\varphi' \cdot d\vartheta \cdot \sin\vartheta \cdot e^{\mp jk\left[r\sin\vartheta \cdot \cos(\varphi-\varphi') \pm (z-h)\cos\vartheta\right]} \equiv$$

$$\equiv \frac{1}{2} \cdot \int_{-\frac{\pi}{2}+j\infty}^{+\frac{\pi}{2}-j\infty} d\vartheta \cdot \sin\vartheta \cdot \left[H_0^{(1)}(kr \cdot \sin\vartheta)\right] \cdot e^{\pm jk \cdot (z-h)\cdot\cos\vartheta}$$

B.2.9

with: (+) for $z > h$

(−) for $z < h$

In conjunction with:

$$\frac{d}{d\rho} H_0^{(1)}(\rho) = -H_1^{(1)}(\rho) \qquad \text{B.2.10}$$

the resultant Hankel-Integral representations for the Hertz-Vector component functions (Equations B.2.1, B.2.2 and B.2.5 to B.2.8) satisfy the EM boundary conditions at z = 0:

$$\frac{\partial}{\partial z} \cdot \Pi_x^{(0)} = n_\ell^2 \cdot \frac{\partial}{\partial z} \Pi_x^{(\ell)} \qquad \text{B.2.11}$$

$$\frac{\partial}{\partial r} \Pi_z^{(0)} = n_\ell^2 \cdot \frac{\partial}{\partial r} \Pi_z^{(\ell)} \qquad \text{B.2.12}$$

$$\frac{\partial}{\partial r} \Pi\!\Pi_z^{(0)} = n_\ell^2 \cdot \frac{\partial}{\partial r} \Pi\!\Pi_z^{(\ell)} \qquad \text{B.2.13}$$

$$\Pi_x^{(0)} = n_\ell^2 \cdot \Pi_x^{(\ell)} \qquad \text{B.2.14}$$

B.2.15

$$\cos\varphi \cdot \frac{\partial}{\partial r} \Pi_x^{(0)} + \frac{\partial}{\partial z} \Pi_z^{(0)} = \cos\varphi \cdot \frac{\partial}{\partial r} \Pi_x^{(\ell)} + \frac{\partial}{\partial z} \Pi_z^{(\ell)}$$

$$\frac{\partial}{\partial z} \Pi\!\Pi_z^{(0)} = \frac{\partial}{\partial z} \Pi\!\Pi_z^{(\ell)} \qquad \text{B.2.16}$$

The expression in the integrands, involving n_g^2, $\sin \vartheta_o$ and $\cos \vartheta_o$ are (explicitly or inplicitly) reflections and refraction coefficients:

For Π_x :

$$\mathcal{R}_x = \frac{2\cos\vartheta_o}{\cos\vartheta_o + \sqrt{n_g^2 - \sin^2\vartheta_o}} = n_g^2 \cdot \mathcal{G}_x = \qquad \text{B.2.17}$$

$$= \frac{2\cos\vartheta_o}{n_g^2 - 1} \cdot \left[\sqrt{n_g^2 - \sin^2\vartheta_o} - \cos\vartheta_o\right]$$

For Π_z :

$$\mathcal{F}_z = n_g^2 \cdot \mathcal{L}_z = \qquad \text{B.2.18}$$

$$= j \cdot 2 \cdot \sin\vartheta_o \cdot \cos\vartheta_o \cdot \frac{\cos\vartheta_o - \sqrt{n_g^2 - \sin^2\vartheta_o}}{n_g^2 \cos\vartheta_o + \sqrt{n_g^2 - \sin^2\vartheta_o}}$$

For III_z :

$$R_z = \frac{2\cdot\sqrt{n_g^2-\sin^2\vartheta_0}}{n_g^2\cdot\cos\vartheta_0+\sqrt{n_g^2-\sin^2\vartheta_0}} = \text{(via B.2.3)}$$

B.2.19

$$= \frac{2\cdot\sqrt{n_g^2-\sin^2\vartheta_0}}{n_g^4\cdot\left[1-\frac{1}{n_g^2}\right]} \cdot \frac{n_g^2\cos\vartheta_0-\sqrt{n_g^2-\sin^2\vartheta_0}}{1+\left[1+\frac{1}{n_g^2}\right]\cdot\sin^2\vartheta_0}$$

$$q_z = \frac{2\cdot\cos\vartheta_0}{n_g^2\cdot\cos\vartheta_0+\sqrt{n_g^2-\sin^2\vartheta_0}} = \text{(via B.2.3)}$$

B.2.20

$$= \frac{2\cdot\cos\vartheta_0}{n_g^4\left[1-\frac{1}{n_g^2}\right]} \cdot \frac{n_g^2\cos\vartheta_0-\sqrt{n_g^2-\sin^2\vartheta_0}}{1-\left[1+\frac{1}{n_g^2}\right]\cdot\sin^2\vartheta_0}$$

B.3 Evaluation of the Hankel-Integral expressions for the components of Π and $\Pi\!\Pi$.

In conjunction with Equations B.2.9, B.2.10, and B.2.17 to B.2.20, the integral expressions for the components of Π and $\Pi\!\Pi$, Equations B.2.1 and B.2.5 to B.2.8 can be derived from the following common format:

$$J_x = \frac{\pi}{2} \int_{-\frac{\pi}{2}+j\infty}^{+\frac{\pi}{2}-j\infty} d\vartheta \cdot \sin\vartheta \cdot \left[\frac{\cos\vartheta - \sqrt{n_2^2 - \sin^2\vartheta}}{\cos\vartheta + \sqrt{n_2^2 - \sin^2\vartheta}} \cdot \right. \qquad \text{B.3.1}$$

$$\left. \cdot [H_0^{(1)}(k_0 r \sin\vartheta)] \cdot e^{jk_0(z+h)\cos\vartheta} \right]$$

where we replaced ϑ_0 by ϑ as integration variable.

Since we are interested here the "Farfield" configuration in space and time we employ the Assymptotic Approximation for Hankel functions $H_0^{(1)}(\varsigma)$ for $|\varsigma| \gg 1$.

For example, in our case:

$$H_0^{(1)}(k_0 r \sin\vartheta) \rightarrow \sqrt{\frac{2}{\pi}} \cdot \frac{e^{j[k_0 r \sin\vartheta - \frac{\pi}{4}]}}{\sqrt{k_0 r \cdot \sin\vartheta}} \qquad \text{B.3.2}$$

This integral J_x becomes with the image system coordinates of Figure B.3.1:

$$J_x \doteq \frac{\pi}{2} \cdot \int_{-\frac{\pi}{2}+j\infty}^{+\frac{\pi}{2}-j\infty} d\vartheta \left[\sin\vartheta \cdot \sqrt{\frac{2}{\pi}} \cdot e^{-j\frac{\pi}{4}} \cdot \right.$$

B.3.3

$$\cdot \frac{\cos\vartheta - \sqrt{n_2^2 - \sin^2\vartheta}}{\cos\vartheta + \sqrt{n_2^2 - \sin^2\vartheta}} \cdot \frac{1}{\sqrt{k_0 R' \sin\alpha' \cdot \sin\vartheta}} \cdot$$

$$\left. \cdot e^{j k_0 R' [\sin\alpha' \cdot \sin\vartheta + \cos\alpha' \cdot \cos\vartheta]} \right]$$

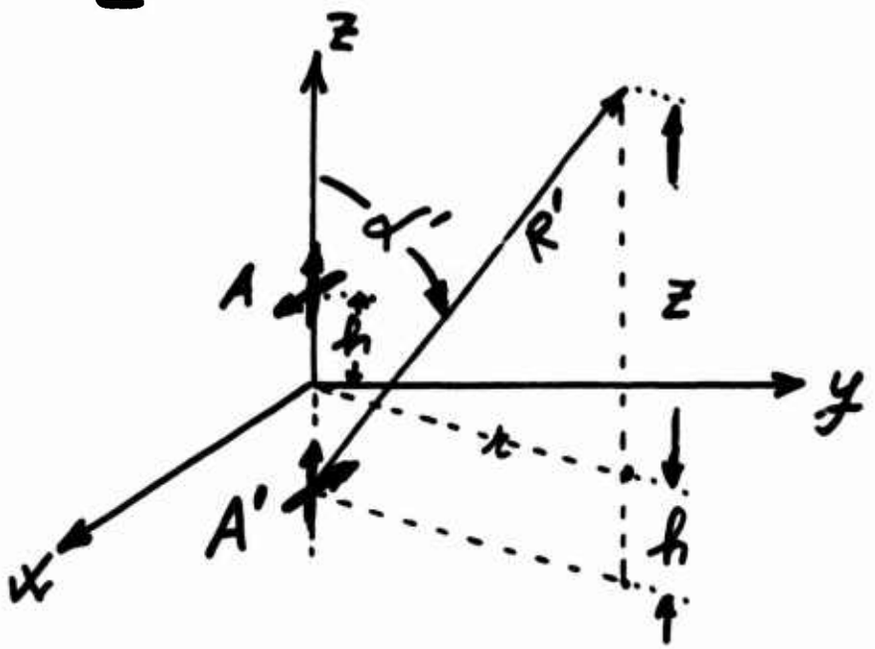

Figure B. 3.1. Image (A') Coordinate System

The "Exponential Term" in the integral

$$e^{jk_0R'[\sin\alpha'\sin\vartheta+\cos\alpha'\cos\vartheta]} = e^{jk_0R'[\cos(\alpha'-\vartheta)]} \qquad \text{B.3.3'}$$

defines the regions of convergence of J_x in the complex ϑ- plane:

$$\vartheta = \vartheta_1 + j\vartheta_2 \qquad \text{B.3.4}$$

as follows:

$$\text{for } \vartheta_2 \geq 0 : \begin{cases} -\sin(\alpha'-\vartheta_1) \leq 0 \\ 0 \leq (\alpha'-\vartheta_1) \leq \pi \\ \alpha'-\pi \leq \vartheta_1 \leq \alpha' \end{cases} \qquad \text{B.3.5}$$

$$\text{for } \vartheta_2 \leq 0 \begin{cases} -\sin(\alpha_1'-\vartheta_1) \geq 0 \\ -\pi \leq (\alpha'-\vartheta_1) \leq 0 \\ \alpha' \leq \vartheta_1 \leq \alpha'+\pi \end{cases} \qquad \text{B.3.6}$$

Simiarly for $\Pi_x^{(\vartheta')}$, $\Pi_z^{(\vartheta')}$ and $\Pi_z^{(\vartheta')}$ (Equations B.2.2, B.2.6 and B.2.8, the e-exponent term must satisfy the condition of convergence, as $z \to -\infty$. This requires that:

$$\text{Imag.}\left[k_0|z|\sqrt{n_2^2-\sin^2\vartheta}+k_0h\cos\vartheta\right] \geq 0 \qquad \text{B.3.7}$$

The resultant subregions of convergence and divergence (of Π_1^{ϑ} Π_2^{ϑ}; Π_1^{ϑ} for $z \to -\infty$) are identified in the complex ϑ domain by respectively the upper and lower sheets of the Riemann Surfaces of the domain.

The branch cuts, which segregate upper and lower sheets, are defined by the equal sign in the expression B.3.7.

Setting in this expression:

$$\sqrt{n_g^2 - \sin^2\vartheta} = w_1 + j w_2 = w \qquad \text{B.3.7'}$$

and

$$\cos\vartheta = \cos\vartheta_1 \cdot \mathrm{Ch}\vartheta_2 - j \sin\vartheta_1 \mathrm{Sh}\vartheta_2 \qquad \text{B.3.8}$$

$$\sin\vartheta = \sin\vartheta_1 \cdot \mathrm{Ch}\vartheta_2 + j \cos\vartheta_1 \mathrm{Sh}\vartheta_2 \qquad \text{B.3.8'}$$

yielding for Equation B.3.7:

$$k_0|z| \cdot w_2 - k_0 h \cdot \sin\vartheta_1 \mathrm{Sh}\vartheta_2 \geq 0$$

one finds that the following conditions must be met:

I.E.

$$w_2 \geq \frac{h \cdot \sin\vartheta_1 \cdot \mathrm{Sh}\vartheta_2}{|z|} \to 0 \qquad \text{B.3.9}$$

$$(z \to -\infty)$$

in the upper Riemann sheet.

Introducing the equivalence:

$$\sin^2\vartheta = \frac{1}{2}(1 - \cos 2\vartheta) \qquad \text{B.3.10}$$

we get via Equation B.3.7 to B.3.20 for:

(a) The dielectric regime ($f_{sig} \gg f_g$, n_g = real)

$$w_1^2 - w_2^2 = n_g^2 - \frac{1}{2}\cdot[1 - \cos 2\vartheta_1 \cdot \mathrm{ch}\, 2\vartheta_2]$$

B.3.11

$$2 w_1 \cdot w_2 = -\frac{1}{2}\cdot \sin 2\vartheta_1 \cdot \mathrm{Sh}\, 2\vartheta_2$$

(b) The critical regime ($f_{sig} \approx f_g$; n_g = complex)

$$n_g = |n_g| \cdot (\cos\nu + j\cdot \sin\nu) \qquad \text{B.3.12}$$

$$w_1^2 - w_2^2 = |n_g^2| \cdot \cos 2\nu - \frac{1}{2}(1 - \cos 2\vartheta_1 \cdot \mathrm{ch}\, 2\vartheta_2)$$

B.3.13

$$2 w_1 \cdot w_2 = |n_g^2| \cdot \sin 2\nu - \frac{1}{2} \sin 2\vartheta_1 \, \mathrm{Sh}\, 2\vartheta_2$$

The two branches of $w = 0$, $w_1 = 0$ and $w_2 = 0$ follow from:

$$0 = n_g^2 \cdot \sin 2\nu + \frac{1}{2} \sin 2\vartheta_1 \cdot \mathrm{Sh}\cdot 2\vartheta_2 \qquad \text{B.3.14}$$

Their common branch point is given by:

$$\sin \vartheta_B = n_g = |n_g| \cdot [\cos\nu + j \sin\nu] \qquad \text{B.3.15}$$

For small values $\nu \ll 1$ where approximately

$$n_g \doteq |n_g| \cdot (1 + j\nu) \qquad \text{B.3.16}$$

one gets from B.3.13 for $|n_g| = 0$

$$Sh\vartheta_2 \doteq \frac{4 \cdot |n_g^2| \cdot \nu}{\sin 2\vartheta_1} \qquad \text{B.3.17}$$

and for the branch point

$$\sin\vartheta_{1B} \cdot Ch\,\vartheta_{2B} \doteq n_g$$
$$\cos\vartheta_{1B} \cdot Sh \cdot \vartheta_{2B} \longrightarrow 0 \qquad \text{B.3.18}$$

(with $\nu \ll 1$)

Since $|n_g| > 1$, the only possible solutions of Equations B.3.17 and B.3.18 are:

$$\vartheta_{1B} \doteq \frac{\pi}{2} \quad ; \quad \vartheta_{2B} \doteq Ar\,Ch\,n_g \qquad \text{B.3.19}$$

The branch $w_2 = 0$ (Equation B.3.17) is identified by setting into Equation B.3.13. This gives in the vicinity of the branch point:

$$w_1^2 - w_2^2 \doteq n_g^2 - \frac{1}{2} Ch 2\vartheta_2 =$$
$$= n_g^2 - \frac{1}{2} - (1 + 2\,Sh^2\vartheta_2) = \qquad \text{B.3.20}$$
$$= n_g^2 - 3/2 - 2\,Sh^2\vartheta_2$$

the correspondence

$$-w_2^2 \longleftrightarrow -2\,Sh^2\vartheta_2 \qquad \text{B.3.21}$$

identifies then the branch cut $w_2 = 0$ as this part of Equation B.3.13 where $\vartheta_2 \rightarrow 0$ i.e., for $\vartheta_2 \geq 0$ beneath the branch points.

The following diagram shows the complex ϑ-plane, and the branch cuts $w_2 = 0$ by solid lines. Sub-regions of convergence of the integrals in Equations B.2.1 to B.2.8 are labelled $w_2 > 0$ (upper Riehmann sheet) and regions of divergence are labelled $w_2 < 0$ (lower Riehmann sheet). Regions of convergence for the Hankel integrals and resultant prototype integral J_x (Equation B.3.3) are shown shaded in Figure B.3.2 below.

Associated poles P_l and P_u on the lower and upper sheet in the vicinity of $\vartheta_1 = \pi/2$ are shown separately in Figure B.3.3.

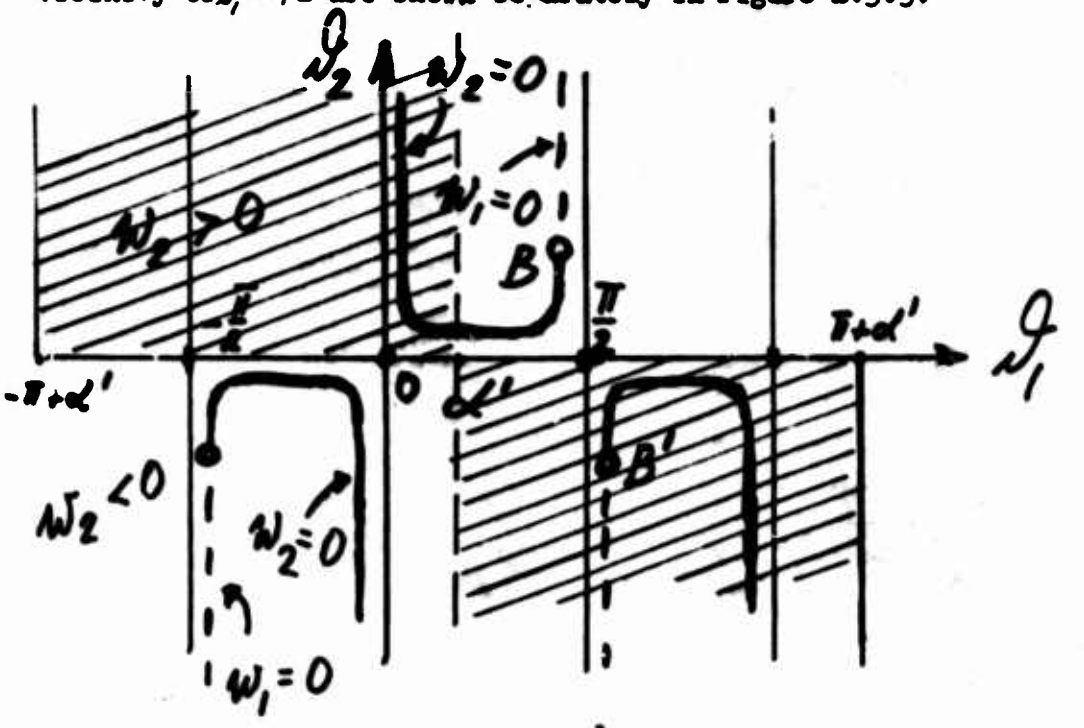

Figure B.3.2. Complex ϑ Domain

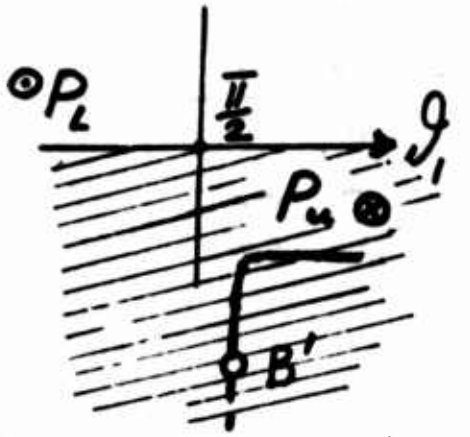

Part of ϑ-Domain enlarged ; Poles P_l and P_u for $1 < |n_g| \leq 10$ and $f > f_g$

Fig.B.3.3.

Inspection of this diagram for the complex ϑ domain in conjunction with the integration path for J_x (Equation B.3.3) shows that the integration path must cross at $\vartheta = \alpha'$ from the first to the second region of convergence (shaded). This path is determined by essentially the exponent function in Equation B.3.3'. Thus, we analyze the path described by:

$$s = j \cos(\vartheta^* - \alpha') \qquad \text{B.3.22}$$

in terms of:

$$\vartheta^* = \vartheta_1 - j|\vartheta_2|$$

(i.e., in the lower half space of ϑ, and corresponding replacement of the integration variable ϑ by ϑ^*.

The extreme of s follows from:

$$\frac{ds}{d\vartheta} = -j \sin(\vartheta^* - \alpha') = 0 \qquad \text{B.3.23}$$

with

$\vartheta^* = \alpha'$; $\vartheta_1 = \alpha'$; $\vartheta_2 = 0$. This identifies the point $\vartheta^* = \alpha'$ as saddle point through which all paths of integration must cross from $\vartheta_2 > 0$ to $\vartheta_2 < 0$.

In the vicinity of this saddle point one can express s by the expansion:

$$[s]_{\vartheta^* = \alpha'} = j \cos(\vartheta^* - \alpha') \doteq j\left[1 - \frac{(\vartheta^* - \alpha')^2}{2} + \ldots\right] \qquad \text{B.3.24}$$

employing:

$$\vartheta^x - \alpha' = |\vartheta^x - \alpha'| \cdot e^{-j\delta} \qquad \text{B.3.25}$$

in the vicinity $\vartheta^* \approx \alpha'$

one gets:

$$s_1 = \frac{1}{2} \cdot |\vartheta^x - \alpha'|^2 \cdot \sin 2\gamma \qquad \text{B.3.26}$$

$$s_2 = 1 - \frac{1}{2} \cdot |\vartheta^x - \alpha'|^2 \cdot \cos 2\gamma \qquad \text{B.3.27}$$

The path of steepest ascendence and of descendence through the saddle (given by the imaginary part of s) is:

$$s_2 = \text{const} = 1 - \frac{1}{2} \cdot |\vartheta^x - \alpha'|^2 \cdot \cos 2\gamma \qquad \text{B.3.28}$$

Hence, the most rapid change of the integral (Equation B.3.3) over the shortest path length occurs along this path through the saddle point. In connection with the exponent functions (Equations B.3.3' and B.3.7) this path permits estimation of the integral values. For this purpose, the slowly varying terms are taken out from under the integral, and the rapidly varying terms (i.e., the exponentials) are left under the integral.

The value of the constant s_2 obtained by substitution in Equation B.3.22 of $\vartheta^x = \alpha'$, follows with unity.

Consequently,

$$1 = 1 - \frac{1}{2} |\vartheta^x - \alpha'|^2 \cdot \cos 2\gamma \qquad \text{B.3.29}$$

and

$$\gamma = \frac{(+)}{-} \cdot \frac{\pi}{4} \qquad \text{B.3.30}$$

The (-) sign is valid here, because s is expressed in terms of the conjugate complex values ϑ^* of ϑ. As the path through the saddle crosses under -45° the real axes, one can set this path in the vicinity of α':

$$\vartheta^x - \alpha' = l \cdot e^{-j\frac{\pi}{4}} \qquad \text{B.3.31}$$

and

$$d\vartheta^x = e^{-j\frac{\pi}{4}} \cdot dl \qquad \text{B.3.32}$$

where l is a real variable. The integration path

$$s = j - \frac{l^2}{2} \qquad \text{B.3.33}$$

is bounded by

$$-\varepsilon \leq l \leq +\varepsilon \qquad \text{B.3.34}$$

The saddle point contribution to the integral J_x (Equation B.3.3) along the path of steepest ascendence and descendence (B.3.33) becomes then:

$$J_x^{(saddle;\alpha')} \doteq \frac{j}{2}\sqrt{\frac{2}{\pi}} \cdot e^{-j\frac{\pi}{4}} \cdot \frac{\sin\alpha'}{\sqrt{k_0 R' \cdot \sin\alpha'}} \cdot \qquad \text{B.3.35}$$

$$\cdot \frac{\cos\alpha' - \sqrt{n_g^2 - \sin^2\alpha'}}{\cos\alpha' + \sqrt{n_g^2 - \sin^2\alpha'}} \cdot \int_{-\varepsilon}^{+\varepsilon} dl \cdot e^{-j\frac{\pi}{4}} \cdot e^{k_0 R' [j - l^2/2]}$$

The paths of integration beyond the critical angle α_c' must be detoured around the lower branch cut to prevent the path from dropping to the divergent Riehmann sheet $w_2 > 0$ and from terminating on this sheet at infinity. Thus for $\alpha' > \alpha_c'$ one must add to the saddle point contribution the branch cut detour contributions to the integral J_x.

The detour, defined by the integration variable ϑ_B, in

$$w_{2B'} = \mathrm{Imag}\sqrt{n_g^2 - \sin^2\vartheta_{B'}} = 0 \qquad \text{B.3.36}$$

is equivalent to:

$$w_{1B'} = \pm\sqrt{n_g^2 - \sin^2\vartheta_{B'}} = \text{real} \qquad \text{B.3.37}$$

Since the outer and inner banks of the branch cuts involve respectively $w_2 < 0$ and $w_2 > 0$ one can map via

$$w = \sqrt{n_g^2 - \sin^2\vartheta} \qquad \text{B.3.38}$$

the branch cuts from the ϑ domain (Figure B.3.4) onto the real axes of the w domain. The results of this mapping,

$$\sin\vartheta \cdot d\vartheta = -\frac{w \cdot dw}{\sqrt{1-(n_g^2-w^2)}} \qquad \text{B.3.39}$$

and the corresponding w diagram is shown in Figure B.3.5.

The solution:

$$J_x^{(\text{Saddle})} \underset{\alpha' < \alpha_c'}{\doteq} \frac{\cos\alpha' - \sqrt{n_g^2 - \sin^2\alpha'}}{\cos\alpha' + \sqrt{n_g^2 - \sin^2\alpha'}} \cdot \frac{e^{jk_0R'}}{k_0R'} \qquad \text{B.3.39'}$$

is restricted to angles α less or equal to a critical angle:

$$\alpha \leq \alpha_c \qquad \text{B.3.39''}$$

As demonstrated by the diagram below (Figure B.3.4), for angles α' that exceed α_c, the path ($\gamma = -\pi/4$) of integration becomes trapped into a detour around the lower branch cut.

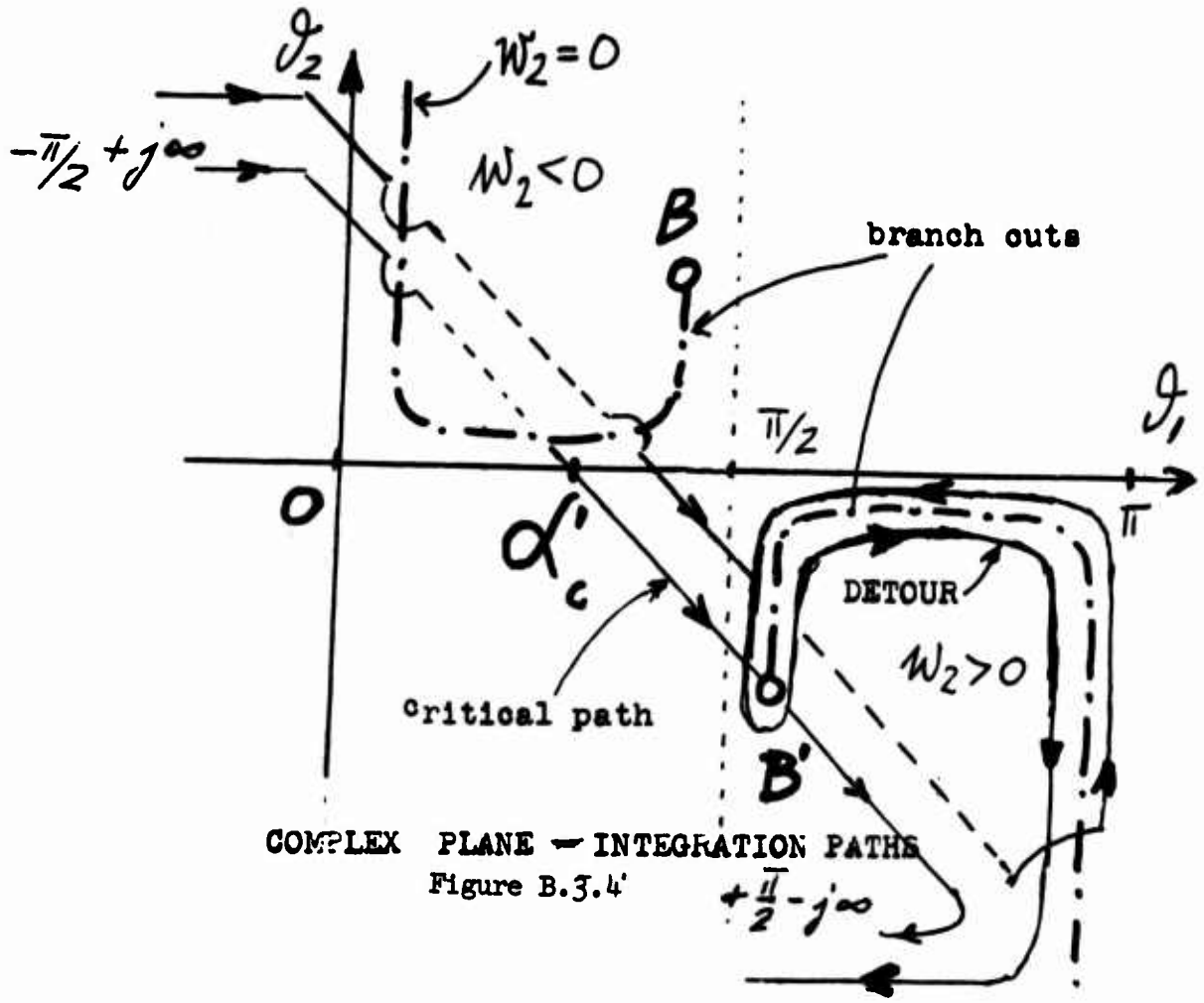

COMPLEX PLANE — INTEGRATION PATHS

Figure B.3.4

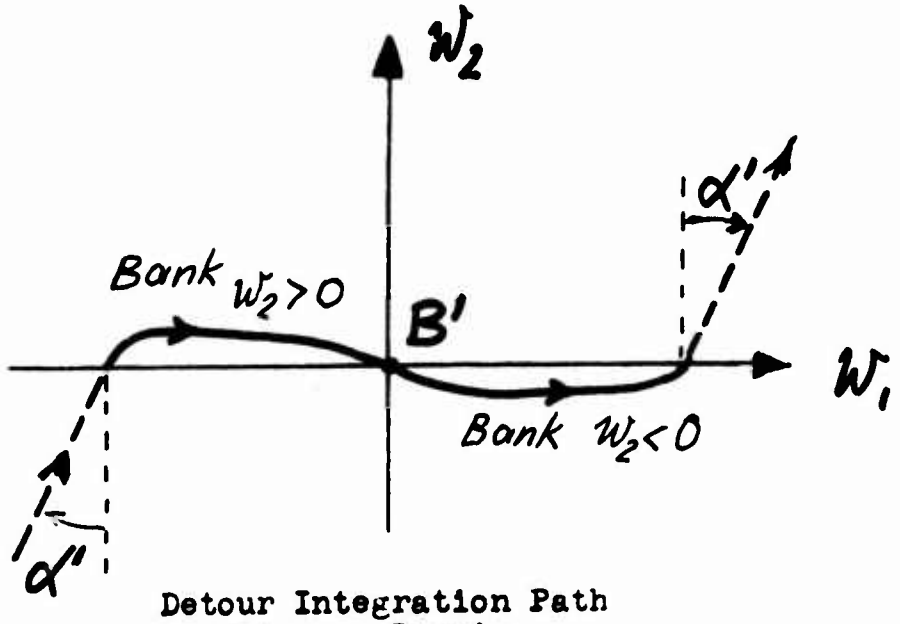

Detour Integration Path in the w Domain .

Figure B.3.5

Introducing further cylindrical coordinates:

$$R' \sin \alpha' = r$$
$$R' \cos(\alpha' - \vartheta) = (z+h)\cos\vartheta + r \sin\vartheta \qquad \text{B.3.40}$$

the branch cut detour contribution to the prototype integral J_x of Equation B.3.3 assumes the following format:

$$J_{B'} = \frac{I}{\sqrt{2\pi}} \cdot e^{-j\frac{\pi}{4}} \cdot \int_{w=-\infty}^{w=+\infty} \left(- \frac{w \cdot dw}{\sqrt{1-(n_g^2 - w^2)}} \right) \cdot$$

$$\cdot A(n_g w) \cdot \frac{e^{-jk_0 [r \cdot \sqrt{n_g^2 - w^2} + (z+h) \cdot \sqrt{1-(n_g^2 - w^2)}]}}{\sqrt{k_0 r \cdot \sqrt{n_g^2 - w^2}}} \qquad \text{B.3.41}$$

Similarly to the saddle point approximation for $\alpha \leq \alpha_c$ (Equation B.3.39) the integral for the branch cut detour $J_{x\,B'}$ is obtained by application of the saddle point approximation method to the w-domain. For this purpose we write the exponent term of e in Equation B.3.41 as follows:

$$j\,k_0\left[x\cdot\sqrt{n_g^2-w^2}+(z+h)\cdot\sqrt{1-(n_g^2-w^2)}\right]=$$

$$=jk_0R'\cdot\left[\sin\alpha'\cdot\sqrt{n_g^2-w^2}+\right.$$

$$\left.+\cos\alpha'\cdot\sqrt{1-n_g^2-w^2}\right]= \qquad \text{B.3.42}$$

$$=j\,s\,k_0R'$$

From

$$\frac{ds}{dw}=-j2w\cdot\left[\frac{\sin\alpha'}{2\sqrt{n_g^2-w^2}}-\frac{\cos\alpha'}{2\sqrt{1-n_g^2+w^2}}\right] \qquad \text{B.3.43}$$

and the resultant saddle point

$$w=0 \qquad \text{B.3.44}$$

the corresponding branch point B' of the ϑ domain is recognized as a saddle point.

Introduction of the expansions

$$\sqrt{n_g^2-w^2}=n_g\left(1-\frac{1}{2}\,\frac{w^2}{n_g^2}+\dots.\right) \qquad \text{B.3.45}$$

$$\sqrt{1-n_g^2+w^2}=\sqrt{1-n_g^2}\cdot\left(1+\frac{1}{2}\,\frac{w^2}{1-n_g^2}+\dots\right) \qquad \text{B.3.46}$$

and reintroduction of ϑ via Equation B.3.15

$$n_g=\sin\vartheta_{B'} \qquad \text{B.3.47}$$

gives

$$s = j\cos(\alpha' - \vartheta_{B'}) - jw^2 \frac{\sin(\alpha' - \vartheta_{B'})}{\sin 2\vartheta_{B'}} \qquad \text{B.3.48}$$

where we set:

$$\frac{\sin(\alpha' - \vartheta_{B'})}{\sin 2\vartheta_{B'}} = |c| \cdot e^{j\gamma} \qquad \text{B.3.48'}$$

The line of steepest descent is then given by:

$$\mathrm{Imag}\left\{ j \cdot \cos(\alpha' - \vartheta_{B'}) - jw^2 \cdot |c| \cdot e^{j\gamma} \right\} = \text{const.} \qquad \text{B.3.49}$$

with the const. determined by substitution of

$$w = 0 \quad \text{into} \qquad \text{B.3.49'}$$

$$\mathrm{Imag}\{s\} = (\text{const.})$$

which gives

$$-|w_1^2 - w_2^2| \cdot |c| \cdot \cos\gamma + |c| \cdot 2w_1 w_2 \cdot \sin\gamma = 0 \qquad \text{B.3.50}$$

This is brought into the format, using:

$$w = |w| \cdot e^{j\eta} = w_1 + jw_2 \qquad \text{B.3.51}$$

$$w^2 = |w| \cdot e^{j2\eta} = |w|^2 [\cos 2\eta + j \sin 2\eta] =$$
$$= w_1^2 - w_2^2 + 2j w_1 w_2$$

$$|w|^2 |c| \cdot \{ -\cos 2\eta \cdot \cos\gamma + \sin 2\eta \cdot \sin\gamma \} = 0 \qquad \text{B.3.52}$$

i.e.,

$$-\cos(2\eta + \gamma) = 0 \qquad \text{B.3.53}$$

which yields the angle

$$\eta = -\left(\frac{\pi}{4} + \frac{\gamma}{2}\right) \qquad \text{B.3.54}$$

at which the line of steepest descent crosses the saddle point w = 0 (i.e., the branch point B' of the $\mathcal{J}$ domain).

Thus analogous to Equations B.3.28 to B.3.33, the largest contribution to the integral comes from the vicinity of the saddle point, where the path is represented by:

$$w = \ell \cdot e^{-j\left(\frac{\pi}{4} + \frac{\gamma}{2}\right)} \qquad \text{B.3.55}$$

and

$$dw = d\ell \cdot e^{-j\left(\frac{\pi}{4} + \frac{\gamma}{2}\right)} \qquad \text{B.3.56}$$

Equation B.3.48 assumes then the format:

$$s = j\cos(\alpha' - \vartheta_0) - k\ell^2 \qquad \text{B.3.57}$$

With Equation B.3.57 substituted into the integral Equation B.3.41 one obtains the contribution from the path of steepest descent through the saddle point w = 0 as follows:

$$J_{B'} = \frac{d}{2} \cdot \sqrt{\frac{2}{\pi}} \cdot e^{-j\frac{\pi}{4}} \cdot$$

$$\cdot \int_{l=-\varepsilon}^{l=+\varepsilon} \left(-\frac{dw \cdot w}{\sqrt{1 - n_g^2 + w^2}} \right) \cdot \frac{A(n_g; w)}{\sqrt{k_0 R \cdot \sqrt{n_g^2 - w^2}}} \cdot \qquad \text{B.3.58}$$

$$\cdot e^{\left[j \cos(\alpha' - \vartheta_{B'}) - |\kappa| \cdot l^2 \right] \cdot k_0 R'}$$

Expansion of:

$$A(n_g; w) = A(n_g; 0) + w \left[\frac{d}{dw} A \right]_{w=0} + \cdots \qquad \text{B.3.59}$$

with

$$w = l \cdot e^{-j\left(\frac{\pi}{4} + \frac{\chi}{2}\right)}$$

associated with the following functions $A(n_g; w)$ from B.3.55, and associated with respectively π ; $\pi\pi$ of Equation B.2.1 to B.2.7 in terms of the w-variable (Equation B.3.38).

$$\Pi_x^{(0)} \; ; \quad A_x^{(0)} = \frac{\sqrt{1-n_g^2+w^2} - w}{\sqrt{1-n_g^2+w^2} + w} \qquad \text{B.3.60}$$

$$\Pi_z^{(0)} \; ; \quad A_z^{(0)} = 2 \cdot \sqrt{n_g^2-w^2} \cdot \sqrt{1-n_g^2+w^2} \cdot \qquad \text{B.3.61}$$

$$\cdot \frac{\sqrt{1-n_g^2+w^2} - w}{n_g^2 \cdot \sqrt{1-n_g^2+w^2} + w}$$

$$\Pi\!\Pi_z^{(0)} \; ; \quad B_z^{(0)} = \frac{n_g^2 \cdot \sqrt{1-n_g^2+w^2} - w}{n_g^2 \cdot \sqrt{1-n_g^2+w^2} + w} \qquad \text{B.3.62}$$

where in particular by application of de L'Hospital's rule the following expressions become valid:

$$\lim_{w \to 0} \frac{w}{\sqrt{1-n_g^2+w^2}} \cdot A_x^{(0)} \longrightarrow 0 \qquad \text{B.3.63}$$

Consequently, in connection with $T_x^{(01)}$ one must keep the total expansion (Equation B.3.59) under the integral sign, since the zero order term alone $A_x^{(01)}(n_y, 0)$ taken before the integral as slowly varying with w, yields a trivial zero contribution to

Thus with

$$\left(\frac{dA_x^{(01)}}{dw}\right)_{w=0} = -\frac{2}{\sqrt{1-n_y^2}} \qquad \text{B.3.64}$$

the integral for $T_x^{(01)}$; $J_{xB'}^{(01)}$ becomes

$$J_{xB'}^{(01)} = -\frac{1}{2}\cdot\sqrt{\frac{2}{\pi}}\cdot e^{-j\frac{\pi}{4}}\cdot e^{-j\gamma}\cdot\frac{e^{jk_0R'\cos(\alpha'-\vartheta_n')}}{\sqrt{k_0R'}}\cdot$$

$$\cdot\left[\frac{A_x^{(01)}(n_y;0)}{\sqrt{1-n_y^2}\cdot\sqrt{n_y}}\cdot\int_{l=-\varepsilon}^{l=+\varepsilon} dl\cdot l\cdot e^{-|\kappa|l^2k_0R'} + \right.$$

$$\left. + \frac{e^{-j\left(\frac{\pi}{4}+\frac{\gamma}{2}\right)}}{\sqrt{n_y}\cdot\sqrt{1-n_y^2}}\cdot\left[\frac{dA_x^{(01)}}{dw}\right]_{w=0}\cdot\int_{l=-\varepsilon}^{l=+\varepsilon} dl\cdot l^2\cdot e^{-k_0R'|\kappa|\cdot l^2}\right] \qquad \text{B.3.65}$$

As pointed out before, the zero order term involving

$$\frac{1}{2}\int_{l=-\varepsilon}^{l=+\varepsilon} dl^2 \cdot e^{-|c|\cdot k_0 R' l^2} \qquad \text{B.3.65'}$$

vanishes:

$$= 0$$

whereas the first order term becomes by change of the variable:

$$t^2 = k_0 R' |c| \cdot l^2 \qquad \text{B.3.66}$$

in:

$$\int_{l=-\varepsilon}^{l=+\varepsilon} dl \cdot l^2 \cdot e^{-k_0 R' |c| l^2} =$$

$$t = +\sqrt{k_0 R' |c|}$$

$$= \frac{1}{(k_0 R' |c|)^{3/2}} \cdot \int_{t=-\sqrt{k_0 R' |c|}} e^{-t^2} \cdot t^2 \cdot dt =$$

B.3.67

a Laplace integral which assumes the value:

$$= \longrightarrow \text{for } k_0 R' \gg 1 = \left[\frac{1}{2} \cdot \frac{\sqrt{\pi}}{(k_0 R' |c|)^{3/2}} \right]$$

Reintroducing $\vartheta_{B'}$; for w = 0 the corresponding

$$n_g = \sin\vartheta_{B'} \qquad \text{B.3.68}$$

one obtains for B.3.64 with B.3.65 and 66 the branch cut contribution to $\Pi_x^{(0)}$ with

$$J_{x_{B'}}^{(0)} = \frac{1+j}{4} \cdot \left(\frac{dA_x^{(0)}}{dw}\right)_{w=0} \cdot \frac{1}{\cos\vartheta_{B'} \sqrt{\sin\vartheta_{B'}}} \cdot \qquad \text{B.3.69}$$

$k_0 R' \gg 1$

$\alpha' \gg \alpha_c$

$$\cdot \left[\frac{2\sin\vartheta_{B'} \cdot \cos\vartheta_{B'}}{\sin(\alpha' - \vartheta_{B'})}\right]^{3/2} \cdot \frac{1}{\sqrt{\sin\alpha'}} \cdot$$

$$\cdot \frac{1}{(k_0 R')^2} \cdot \left[e^{j k_0 R' \cdot \cos(\alpha' - \vartheta_{B'})}\right]$$

where from B.3.64 B.3.69'

$$\left(\frac{dA_x^{(0)}}{dw}\right)_{w=0} = \frac{-2}{\sqrt{1-n_g^2}} = -\frac{2}{\cos\vartheta_{B'}}$$

For the branch cut contributions to $\Pi_z^{(0)}$ on the other hand, where (Different from Equation B.3.36)

$$\lim_{w \to 0} \frac{A_z^{(0)} \cdot w}{(n_g^2 - w^2)^{1/4} \cdot (1 - n_g^2 + w^2)^{1/2}} = \frac{4\sqrt{1-n_g^2}}{(n_g)^{3/2}} \neq 0 \qquad \text{B.3.70}$$

the resultant finite zero-order approximation is sufficient one gets:
(by otherwise fully analogous procedures)

$$J^{(0)}_{z_{B'}} = \frac{4}{k_0 R'} \cdot \frac{(\cos\vartheta_B)^{3/2}}{\sin\vartheta_{B'} \cdot \sqrt{\sin\alpha' \cdot \sin(\alpha' - \vartheta_{B'})}} \cdot e^{j\left[k_0 R' \cos(\alpha' - \vartheta_{B'}) - \frac{\pi}{2}\right]} \qquad \text{B.3.71}$$

Similarly, for the branch cut contributions to $III_z^{(0)}$ where

$$\lim_{w \to 0} \frac{\beta_z \cdot w}{\sqrt{1 - n_g^2 + w^2}} = \frac{n_g^2 - 2}{2n_g^2} \neq 0 \qquad \text{B.3.72}$$

one gets:

$$II^{(0)}_{z_{B'}} = \frac{1}{k_0 R'} \cdot \frac{2 - \sin^2\vartheta_{B'}}{2\sin^2\vartheta_{B'}} \cdot \sqrt{\frac{\cos\vartheta_{B'}}{\sin\alpha' \cdot \sin(\alpha' - \vartheta_{B'})}} \cdot e^{jk_0 R' \cos(\alpha' - \vartheta_{B'})} \qquad \text{B.3.73}$$

Further, in addition to the saddle point α_s' and the branch cut $\vartheta_{B'}$ contributions, the integrand functions $A_z'^{(0)}$ $A_z'^{(1)}$ $B_z'^{(1)}$ of respectively $\Pi_z'^{(0)}; \Pi_z'^{(1)}$; and $\Pi_z'^{(1)}$ contain poles. The resultant residue-integral terms* correspond to ground surface wave modes. At the frequencies which are of interest here (VHF, UHF) and at the heights of transmitters and receivers above ground as used in practice, these ground surface wave modes become insignificant, even for ideally flat ground surface conditions, and even more so under actual rough ground surface conditions.

Hence the ground surface wave mode contributions are neglected in the subsequent formulas for the Hertz- Vector functions as obtained by superposition of the respective primary and secondary -- saddle point and branch cut terms (Equations B.2.1, B.2.5, B.2.7, B.3.3, Figure B.3.2, Equation B.3.39, B.3.69, B.3.69', B.3.71, and B.3.73.

The resultant equations are given in the following section B.4 in conjunction with the derivation of the electrical field components as functions of ground conditions.

* $+\frac{n_g}{\sqrt{n_g^2+1}} = \sin\vartheta_{op}$ (Equation B.2.7)

$$\left[\Pi_z^{(0)}\right]_{\text{wave mode}}^{\text{surface}} \approx -2jk_0 n_g^2 \sqrt{\frac{2\pi}{\sin\vartheta_{op}}} \cdot \left(e^{-z\cdot\cos\vartheta_{op}}\right) \cdot \left(\cos\vartheta_{op}\right)^2 \cdot \left[\frac{e^{j\left[k_0 x\cdot\sin\vartheta_{op} + \frac{\pi}{4} - \omega t - \varphi(t) + \frac{\pi}{2}\right]}}{\sqrt{(k_0 x)}}\right]$$

*for example the pole yields ϑ_{op} at: $+\frac{n_g}{\sqrt{n_g^2+1}} = \sin\vartheta_{op}$

B.4 The Hertz-Vector Functions $\Pi_x^{(0)}$; $\Pi_z^{(0)}$ and $\Pi_z^{(0)}$; the resultant electrical fields in the air space

$$\Pi_x^{(0)} \doteq -\frac{1}{4\pi} \cdot \sqrt{\frac{\mu_0}{\varepsilon_0}} \cdot M_x \cdot e^{-j(\omega t + \psi)} \cdot$$

$k_0 R' \gg 1$

$$\cdot \left\{ \frac{e^{j k_0 R}}{k_0 R} + \frac{\cos\alpha' - \sqrt{n_g^2 - \sin^2\alpha'}}{\cos\alpha' + \sqrt{n_g^2 + \sin^2\alpha}} \cdot \frac{e^{j k R'}}{k_0 R'} \right.$$

B.4.1

$$\left. - \left[\frac{1+j}{\sqrt{2}} \cdot \frac{\sin\vartheta_{B'}}{(\cos\vartheta_{B'} \cdot \sin\alpha')^{1/2} \cdot [\sin(\alpha' - \vartheta_{B'})]^{3/2}} \cdot \right. \right.$$

for $\alpha \geq \alpha_c$

$$\left. \left. \cdot \frac{1}{(k_0 R')^2} \cdot e^{j k_0 R' \cos(\alpha' - \vartheta_{B'})} \right] \right\}$$

$$\Pi_z^{(0)} = -j \cdot \frac{M_x}{4\pi} \cdot \sqrt{\frac{\mu_0}{\varepsilon_0}} \cdot e^{-j[\omega t + \psi]} \cdot \cos\varphi \cdot$$

$$\cdot \left\{ (\sin 2\alpha') \cdot \frac{\cos\alpha' - \sqrt{n_g^2 - \sin^2\alpha'}}{n_g^2 \cos\alpha' + \sqrt{n_g^2 - \sin^2\alpha'}} \cdot \frac{e^{jk_0R'}}{k_0R'} + \right.$$

B.4.2

$$\left. + \left[\frac{4 \cdot (\cos\vartheta_{B'})^{3/2}}{\sin\vartheta_{B'} \cdot \sqrt{\sin\alpha' \cdot \sin(\alpha' - \vartheta_{B'})}} \cdot \frac{1}{k_0R'} \cdot \right. \right.$$

for $\alpha \geq \alpha_c$

$$\left. \left. \cdot e^{j[k_0R'\cos(\alpha' - \vartheta_{B'})]} \right] \right\}$$

Of significance is here the cos φ dependence of $\Pi_z^{(0)}$ relative to $\Pi\!\Pi_z^{(0)}$. The latter (Equation B.4.1) on the other hand involves in its third term $(k_0R')^{-2}$. Hence, for $k_0R' \gg 1$ this third term becomes small when $\alpha > \alpha_c$ (Figure B.3.4).

Simiarly for the vertical dipole element N_z one gets the Hertz-Vector function $\Pi\!\Pi_z^{(0)}$ as follows:

B.4.3

$$\Pi_z^{(0)} \doteq -\frac{j}{4\pi}\sqrt{\frac{\mu_0}{\varepsilon_0}}\cdot N_z \cdot e^{-j(\omega t+\varphi-\frac{\pi}{2})} \cdot$$

$$\cdot\left\{\frac{e^{-jk_0R}}{k_0R} + \frac{n_g^2\cos\alpha' - \sqrt{n_g^2-\sin^2\alpha'}}{n_g^2\cos\alpha' + \sqrt{n_g^2-\sin^2\alpha'}}\cdot\frac{e^{-jk_0R'}}{k_0R'} + \right.$$

$$+\left[\frac{2-\sin^2\vartheta_{B'}}{2\sin^2\vartheta_{B'}}\cdot\sqrt{\frac{\cos\vartheta_{B'}}{\sin\alpha'\cdot\sin(\alpha'-\vartheta_{B'})}}\cdot\right.$$

for $\alpha' \geq \alpha_c$

$$\left.\left.\cdot\frac{1}{k_0R'}\cdot e^{-jk_0R'\cos(\alpha'-\vartheta_{B'})}\right]\right\}$$

Equations B.4.1 to B.4.3 above, are valid in the far zone, i.e., for distances $k_0R' \gg 1$. Hence, in the subsequent determination of the electrical fields via (Equation A.1.6):

$$\bar{E} = \nabla(\nabla\cdot\bar{\Pi}) - \frac{1}{c^2}\cdot\ddot{\bar{\Pi}} \qquad \text{B.4.4}$$

we retain from the grad division terms those which are inversely proportional to R and drop the higher order $1/R^n$; $n>1$ contributions. Employing spherical coordinates R, ϑ, α and $\bar{n}\ \bar{m}\ \bar{o}$ unit base vectors $\bar{n}$, $\bar{m}$, $\bar{o}$ one gets:

(in general, in the unprimed and the primed image system)

$$(\nabla \cdot \bar{\Pi}) = \frac{\partial}{\partial x}\Pi_x + \frac{\partial}{\partial z}\Pi_z =$$

$$= \cos\varphi \cdot \sin\alpha \cdot \frac{\partial \Pi_x}{\partial R} + \cos\alpha \cdot \frac{\partial \Pi_z}{\partial R} \qquad \text{B.4.4'}$$

$$\nabla(\nabla \cdot \Pi) = \left[\bar{n}\frac{\partial}{\partial R} + \frac{\bar{m}}{R\sin\alpha}\cdot\frac{\partial}{\partial\varphi} + \frac{\bar{\theta}}{R}\cdot\frac{\partial}{\partial\alpha}\right] \cdot$$

$$\cdot\left[\frac{\partial \Pi_x}{\partial R}\cdot\cos\varphi\cdot\sin\alpha + \frac{\partial \Pi_z}{\partial R}\cdot\cos\alpha\right] =$$

$$= \bar{n}\left[\frac{\partial^2 \Pi_x}{\partial R^2}\cdot\cos\varphi\sin\alpha + \frac{\partial^2 \Pi_z}{\partial R^2}\cdot\cos\alpha\right] + \qquad \text{B.4.5}$$

$$+\bar{m}\cdot\left[\frac{1}{R}\frac{\partial}{\partial\varphi}\left(\frac{\partial \Pi_x}{\partial R}\cdot\cos\varphi\right) + \frac{1}{R}\frac{\cos\alpha}{\sin\alpha}\cdot\frac{\partial}{\partial\varphi}\cdot\frac{\partial \Pi_z}{\partial R}\right] +$$

$$+\bar{\theta}\left[\frac{\cos\varphi}{R}\cdot\frac{\partial}{\partial\alpha}\cdot\left(\frac{\partial \Pi_x}{\partial R}\cdot\sin\alpha\right) + \frac{1}{R}\cdot\frac{\partial}{\partial\alpha}\left(\frac{\partial \Pi_z}{\partial R}\cdot\cos\alpha\right)\right]$$

---

and further:

$$-\frac{1}{c^2}\frac{\partial^2}{\partial t^2}\bar{\Pi} \approx -\frac{1}{c^2}\frac{\partial^2}{\partial t^2}\cdot C^{-j[\omega t + \varphi + \gamma]} = \qquad \text{B.4.5'}$$

$$= k_0^2 \cdot C^{-j[\omega t + \varphi + \gamma]}$$

In consideration of the magnitude of these equations and resultant expressions for the electrical fields, it becomes necessary to split the Hertz-Vector functions into primary and secondary (reflected) terms as follows:

$$\Pi_x^{(0)} = \Pi_x^{(0)P} + \Pi_x^{(0)S_1} + \Pi_x^{(0)S_2} \qquad \text{B.4.6}$$

$$\Pi_z^{(0)} = \Pi_z^{(0)S_1} + \Pi_z^{(0)S_2} \qquad \text{B.4.7}$$

$$\overline{\overline{\Pi}}_z^{(0)} = \overline{\overline{\Pi}}_z^{(0)P} + \overline{\overline{\Pi}}_z^{(0)S_1} + \overline{\overline{\Pi}}_z^{(0)S_2} \qquad \text{B.4.8}$$

where the secondary terms involve the primed variables $\alpha' \; R'$ in Equations B.4.1 to B.4.3.

Further, by inspection of the grad. div. $\overline{\Pi}$ terms in Equation B.4.5 one finds the following 1/R terms:

For the primary fields:

$$\bar{n} \cdot \frac{\partial^2}{\partial R^2} \overline{\Pi}_{x,R}^{(0)P} = \bar{n} M_x \left(-k_0^2 \cdot \frac{e^{jk_0R}}{k_0 R} \cos\varphi \sin\alpha + \right. \qquad \text{B.4.9}$$

and simiarly from

Further:

$$\bar{n} \frac{\partial^2}{\partial R^2} \overline{\overline{\Pi}}_{z\,R}^{(0)P} = \bar{n} N_z \left(-k_0^2 \frac{e^{jk_0R}}{k_0 R} \cos\alpha + \ldots \right. \qquad \text{B.4.10}$$

In the secondary Herts-Vector functions (Equation B.4.2 for $\Pi_z^{(0)} = \Pi_z^{(0)s}$ and the second and third term of $\Pi_z^{(0)}$ in Equation B.4.3) one finds in conjunction with Equation B.4.5 the following type contributions to the radiation field:

Similar as before for the primary fields:

from

$$\bar{n}\cdot\frac{\partial^2\Pi_z^{(0)s}}{\partial R'^2}\cdot\cos\alpha' = +jk_0^2\frac{M_x}{4\pi}\sqrt{\frac{\mu_0}{\varepsilon_0}}\cdot e^{-j[\omega t+\psi]}\cdot\cos\varphi\cdot$$

$$(\cos\alpha')\cdot\Big\{(\sin 2\alpha')\cdot[\quad]\cdot\frac{e^{-jk_0R'}}{k_0R'}+$$

$$+\Big\{\quad\Big\}\cdot\frac{[\cos(\alpha'-\vartheta_{n'})]^2}{k_0R'}\cdot \qquad \text{B.4.11}$$

for $\alpha \geq \alpha_c$

$$\cdot\, e^{-j[k_0R'\cos(\alpha'-\vartheta_{n'})]}\Big\}$$

and from

$$\bar{n}\cdot\frac{\partial^2\Pi_z^{(0)s}}{\partial R'^2}\cdot\cos\alpha' = +j k_0^2\frac{N_z}{4\pi}\sqrt{\frac{\mu_0}{\varepsilon_0}}\cdot e^{-j[\omega t+\psi-\frac{\pi}{2}]}\cdot$$

$$\cdot(\cos\alpha')\cdot\Big\{[\quad]\frac{e^{-jk_0R'}}{k_0R'}+ \qquad \text{B.4.12}$$

$$+\Big\{-\sqrt{\quad}\Big\}\cdot\frac{[\cos(\alpha'-\vartheta_{n'})]^2}{k_0R'}\cdot e^{-j[k_0R'\cos(\alpha'-\vartheta_{n'})]}\Big\}$$

for $\alpha \geq \alpha_c$

and further in connection with the term in Equation B.4.5

$$\bar{\theta}\cdot\left[\frac{1}{R'}\cdot\frac{\partial}{\partial\alpha'}\cdot\left[\cos\alpha'\cdot\frac{\partial\Pi_z}{\partial R'}\right]\right] \qquad \text{B.4.13}$$

one obtains a $1/R'$ contribution to the radiation field from

$\Pi_z^{(0)S_2}$ Equation B.4.2, second term B.4.14

$$\bar{\theta}\cdot\left[\frac{1}{R'}\cdot\left[\quad\right]_{\text{for }\alpha'>\alpha_c}\cdot\cos\alpha'\cdot \qquad \text{B.4.15}$$

$$\cdot\frac{\partial}{\partial\alpha'}\left(jk_0\cos(\alpha'-\vartheta_{B'})\cdot e^{jk_0R'\cos(\alpha'-\vartheta_{B'})}\right)\Big]=$$

$$\rightarrow\bar{\theta}\left\{\left[\quad\right]_{\text{for }\alpha'\geq\alpha_c}\cdot k_0^2\cdot\frac{\sin 2(\alpha'-\vartheta_{B'})}{2}\cdot\right.$$

$$\left.\cdot e^{jk_0R'\cos(\alpha'-\vartheta_{B'})}+\ldots\right\}$$

and fully analogous from $\Pi_z^{(0)S_2}$ Equation B.4.3 the third term

$$\rightarrow\bar{\theta}\cdot\left\{\left[\quad\right]_{\text{for }\alpha'\geq\alpha_c}\cdot k_0^2\cdot\frac{\sin 2(\alpha'-\vartheta_{B'})}{2}\cdot\right. \qquad \text{B.4.16}$$

$$\left.\cdot e^{jk_0R'\cos(\alpha'-\vartheta_{B'})}+\ldots\right\}$$

The third, branch cut, term in Equation B.4.1, i.e: of Equation B.4.6 yields, $1/R'$ no type contribution via Equation B.4.5. $\Pi_x^{(0)S_2}$

Expressing the carthesian unit base vectors $\bar{I}$ and $\bar{k}$ in respectively the primary and image source centered spherical systems by unprimed $R\ \varphi\ \alpha$ and primed $R'\ \varphi'\ \alpha'$ coordinates and respective base vectors $\bar{n}$; $\bar{m}$; $\bar{o}$ and $\bar{n}'$; $\bar{m}'$; $\bar{o}'$ where:

$$\varphi = \varphi' \ ; \quad \bar{m} = \bar{m}'$$

$$\bar{i} = \bar{n} \cdot \cos\varphi \cdot \sin\alpha - \bar{m} \cdot \sin\varphi + \bar{o} \cdot \cos\varphi \cdot \cos\alpha \qquad \text{B.4.17}$$

$$\bar{k} = \bar{n} \cdot \cos\alpha - \bar{o} \cdot \sin\alpha \qquad \text{B.4.17'}$$

one obtains the following equations for the primary (direct) and secondary (ground reflected) electrical fields from the dipoles M_x and N_z:

$$(1) \quad \bar{E}_{M_x}(p') = -\frac{jk_0^2}{4\pi}\sqrt{\frac{\mu_0}{\varepsilon_0}} \cdot \frac{M_x \cdot e^{jk_0 R}}{k_0 R} \cdot e^{-j[\omega t + \psi]} \cdot$$

$$\begin{Bmatrix} 0 \\ -\bar{m} \cdot \sin\varphi \\ +\bar{o} \cdot \cos\varphi \cdot \cos\alpha \end{Bmatrix} \qquad \text{B.4.18}$$

for $k_0 R \gg 1$

and fully analogous to Equation B.4.18

$$ {}^{(0)}_{(x)}\underline{E}_{M_x}^{(S_1)} = -\frac{j k_0^2}{4\pi}\cdot\sqrt{\frac{\mu_0}{\varepsilon_0}}\cdot M_x\cdot\frac{e^{-j k_0 R'}}{k_0 R'}\cdot e^{-j[\omega t+\varphi]}\cdot\frac{[\cos\alpha'-\sqrt{n_g^2-\sin^2\alpha'}]}{[\cos\alpha'+\sqrt{n_g^2-\sin^2\alpha'}]}\cdot \qquad \text{B.4.18'} $$

$$ \left\{\begin{array}{c} 0 \\ -\bar{m}\cdot\sin\varphi \\ +\bar{\theta}'\cdot\cos\varphi\cdot\cos\alpha' \end{array}\right\} \quad \text{for: } k_0 R' \gg 1 $$

whereas:

$$ {}^{(0)}_{(x)}\underline{E}_{M_x}^{(S_2)} \longrightarrow 0 \qquad \text{B.4.18''} $$

for $k_0 R' \gg 1$

Further from $\Pi_z^{(0)}$ of M_x Equation B.4.2 and subsequent derivations, Equation B.4.5, B.4.7, B.4.11 and B.4.15 follows:

$$\overline{E}^{(0)(S_1)}_{(z)M_x} = -\frac{jk_0^2}{4\pi}\sqrt{\frac{\mu_0}{\varepsilon_0}}\cdot M_x \cdot e^{-j[\omega t+\varphi]}$$

B.4.19

$$\cdot\cos\varphi\cdot\sin 2\alpha'\cdot\frac{\cos\alpha'-\sqrt{n_z^2-\sin^2\alpha'}}{n_z^2\cos\alpha'+\sqrt{n_z^2-\sin^2\alpha'}}\cdot\frac{e^{jk_0R'}}{k_0R'}\cdot$$

$$\cdot\begin{Bmatrix}0\\0\\-\bar{U}'\cdot\sin\alpha'\end{Bmatrix}$$

for $k_0R' \gg 1$

and from the branch cut term of $\Pi_z^{(0)}$ i.e. $\Pi_z^{(0)S_2}$ follows in this case a 1/R type contribution to the electrical radiation field, which is given by:

$$ {}^{(0)}_{(z)}E^{(s_2)}_{M_x} \doteq -\frac{j k_0^2}{4\pi}\sqrt{\frac{\mu_0}{\varepsilon_0}}\cdot M_x \cdot e^{-j[\omega t - \psi]} \cdot $$

for $\alpha \gtrsim \alpha_c$

$$ \cdot \cos\varphi \cdot \frac{4\cdot(\cos\vartheta_{B'})^{3/2}}{\sin\vartheta_{B'}\cdot\sqrt{\sin\alpha'\cdot\sin(\alpha'-\vartheta_{B'})}} \cdot $$

$$ \cdot \frac{1}{k_0 R'} \cdot e^{j k_0 R' \cdot \cos(\alpha'-\vartheta_{B'})} $$

B.4.19

$$ \cdot \begin{Bmatrix} +\bar{n}'\left[-\cos^2(\alpha'-\vartheta_{B'}) + 1\right]\cdot\cos\alpha' \\ 0 \\ -\bar{\theta}'\left[\frac{1}{2}\sin 2(\alpha'-\vartheta_{B'}) + 1\right]\cdot\sin\alpha' \end{Bmatrix} $$

for $k_0 R \gg 1$

Similar to these electrical fields from M_x one gets the primary and secondary fields from N_z with Equation B.4.3 and the subsequent Equations B.4.8, B.4.10, B.4.12, and B.4.16 resultant from Equation B.4.5 and B.4.5'

$$(0)\vec{E}^{(p)}_{N_z} = -\frac{jk_0^2}{4\pi}\cdot\sqrt{\frac{\mu_0}{\varepsilon_0}}\cdot\frac{N_z\cdot e^{-jk_0R}}{k_0R}\cdot e^{-j\left[\omega t+\gamma-\frac{\pi}{2}\right]}\cdot$$

$$\cdot\begin{Bmatrix}0\\0\\-\bar{\sigma}'\sin\alpha\end{Bmatrix}$$

B.4.20

$$(0)\vec{E}^{(s_1)}_{N_z} = -\frac{jk_0^2}{4\pi}\cdot\sqrt{\frac{\mu_0}{\varepsilon_0}}\cdot N_z\cdot e^{-j\left[\omega t+\gamma-\frac{\pi}{2}\right]}\cdot$$

$$\cdot\frac{n_g^2\cdot\cos\alpha'-\sqrt{n_g^2-\sin^2\alpha'}}{n_g^2\cos\alpha'+\sqrt{n_g^2-\sin^2\alpha}}\cdot\frac{e^{-jk_0R'}}{k_0R'}\cdot$$

B.4.20'

$$\cdot\begin{Bmatrix}0\\0\\-\bar{\sigma}'\cdot\sin\alpha'\end{Bmatrix}$$

and

$$1^{o})\ \underline{E}^{(S_2)}_{N_z} \doteq -\frac{j k_0^2}{4\pi}\sqrt{\frac{\mu_0}{\varepsilon_0}}\cdot N_z \cdot e^{-j\left[\omega t+\psi-\frac{\pi}{2}\right]}\cdot$$

$$\text{for } \alpha \gg \alpha_c$$

$$\cdot\frac{2-\sin^2\vartheta_{B'}}{2\sin^2\vartheta_{B'}}\cdot\sqrt{\frac{\cos\vartheta_{B'}}{\sin\alpha'\cdot\sin(\alpha'-\vartheta_{B'})}}\cdot$$

$$\cdot\frac{1}{k_0 R'}\cdot e^{j k_0 R'\cdot\cos(\alpha'-\vartheta_{B'})}\cdot \qquad \text{B.4.20''}$$

$$\begin{Bmatrix} +\bar{n}'\cdot\left[\cos^2(\alpha'-\vartheta_{B'})+1\right]\cdot\cos\alpha' \\ 0 \\ -\bar{\theta}'\cdot\left[\frac{1}{2}\sin 2(\alpha'-\vartheta_{B'})+1\right]\cdot\sin\alpha' \end{Bmatrix}$$

$$\text{for } k_0 R' \gg 1$$

The complete solution for the polarization modulated electrical radiation field in the air half space above ground is obtained by superposition of the above primary and secondary field solutions (Equations B.4.18 to B.4.20').

$$ {}^{(0)}\bar{E}_{Pol\,Mod.\ total} = {}^{(0)}\bar{E}^{(p)}_{M_x} + {}^{(0)}\bar{E}^{(s_1)}_{M_x} + {}^{(0)}\bar{E}^{(s_1)}_{M_x} + {}^{(0)}\bar{E}^{(s_2)}_{M_x} + {}^{(0)}\bar{E}^{(p)}_{N_z} + {}^{(0)}\bar{E}^{(s_1)}_{N_z} + {}^{(0)}\bar{E}^{(s_2)}_{N_z} \qquad \text{B.4.21} $$

The electric field equations B.4.18 to B.4.21 are valid for the dielectric ground regime (i.e., $f > f_2$ e.g. the VHF - range). Of particular interest are these specializations of Equations B.4.18 to B.4.21 which conform to the practical conditions of the experimental system. These specializations are the topics of the subsequent sections.

B.5 REGULAR POLARIZATION MODULATION CASE -- INFLUENCE OF GROUND ON POLARIZATION MODULATED VHF RADIO SIGNAL TRANSMISSIONS.

Consider the geometrical specialization described by Figure B.5.1 and referred to as theoretical model, where transmitter and receiver antennas are at equal heights "h" above ground (z = 0)* such that

$$ \alpha = \frac{\pi}{2} \; ; \; R = r = R' \cdot \sin\alpha' = y \qquad \text{B.5.1} $$

$$ \varphi = \frac{\pi}{2} \; ; \; 2h = R' \cos\alpha' \qquad \text{B.5.1'} $$

*The local reflecting area labelled parkway in Figure B.5.1 refers to the Red Bank, N.J. No. 109 exit-entrance section of the Garden State Parkway which touches the ground projection of the line of sight, Fort Monmouth to Middletown (Telegraph Hill Park) transmission path of the experimental system.

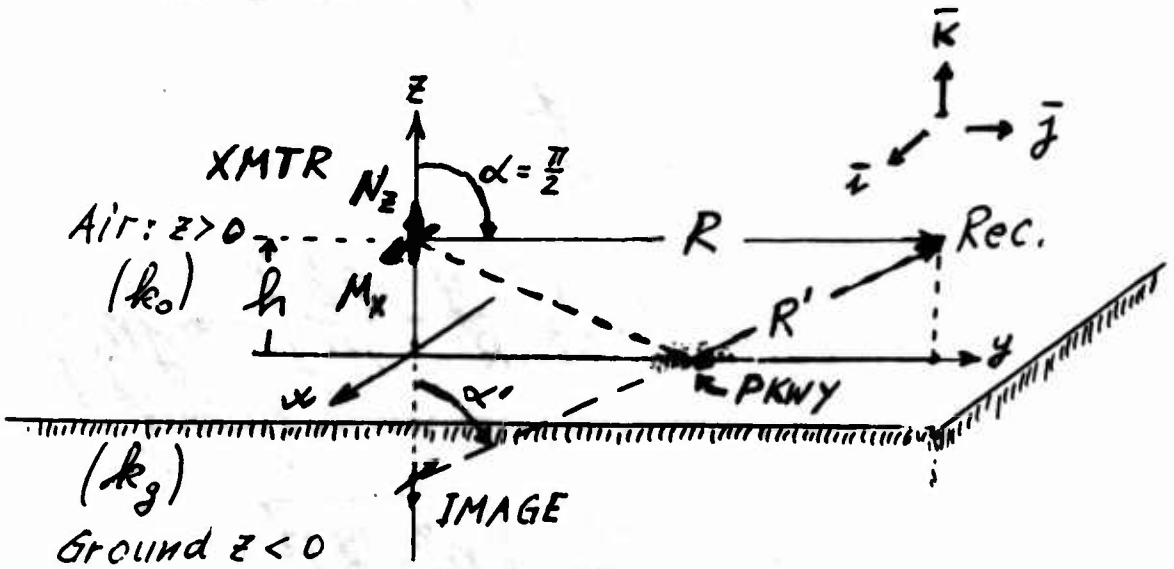

Figure B.5.1. Geometrical Specialization

By the above specialization of the geometrical parameters, the following relations become valid:

$$-\bar{\theta} = \bar{k}\,; \quad -\bar{m} = \bar{\imath}\,; \quad \bar{n} = \bar{\jmath} \qquad \text{B.5.2}$$

$$R' = y \cdot \sqrt{1+(2h/y)^2}\,; \quad R = y\,; \qquad \text{B.5.2'}$$

$$\bar{n}' = \bar{\jmath}\cdot\sin\alpha' + \bar{k}\cdot\cos\alpha' = \frac{1}{R'}\left[\bar{\jmath}\cdot y + \bar{k}\cdot 2h\right] \qquad \text{B.5.2''}$$

$$\bar{\theta}' = \bar{\jmath}\cdot\cos\alpha' - \bar{k}\cdot\sin\alpha' = \frac{1}{R'}\left[\bar{\jmath}\cdot 2h - \bar{k}\cdot y\right]$$

further, from Equation B.3.15

$$\sin\vartheta_{B'} = n_g\,; \quad \cos\vartheta_{B'} = \sqrt{1-n_g^2} \qquad \text{B.5.3}$$

and

$$j\cos[\alpha' - \vartheta_{B'}] = n_g\left[-\sqrt{1-\frac{1}{n_g^2}}\cdot\cos\alpha' + j\sin\alpha'\right] =$$

$$= n_g\cdot\left[-\frac{2h}{R'}\cdot\sqrt{1-\frac{1}{n_g^2}} + j\frac{y}{R'}\right] \qquad \text{B.5.4}$$

In practice where

$$|n_g|^2 \gg 1 \; ; \; y \gg 2h \; ; \; R' \gg 2h \qquad \text{B.5.5}$$

the following approximations become applicable:

$$j\cos(\alpha' - \vartheta_{0,1}) \rightarrow j n_g \cdot \frac{y}{R'} \qquad \text{B.5.6}$$

similarly

$$\sin(\alpha' - \vartheta_{0,1}) = n_g \cdot \left[j\sqrt{1 - \frac{1}{n_g^2}} \cdot \frac{y}{R'} - \frac{2h}{R'} \right] \rightarrow j n_g \frac{y}{R'} \qquad \text{B.5.7}$$

and the secondary (reflected) wave terms assume then the following approximate representations:

$$\frac{\cos\alpha' - \sqrt{n_g^2 - \sin^2\alpha'}}{\cos\alpha' + \sqrt{n_g^2 - \sin^2\alpha'}} = \frac{\frac{2h}{R'} - \sqrt{n_g^2 - \left(\frac{y}{R'}\right)^2}}{\frac{2h}{R'} + \sqrt{n_g^2 - \left(\frac{y}{R'}\right)^2}} \rightarrow (-1) \qquad \text{B.5.8}$$

$$\frac{e^{jk_0R'}}{k_0R'} \doteq \frac{1}{k_0 y} \cdot e^{jk_0 y \cdot \left[1 + \frac{2h}{y^2}\right]} =$$

$$= \frac{e^{jk_0 y}}{k_0 y} \cdot e^{jk_0 h\left(\frac{2h}{y}\right)} \rightarrow \frac{e^{jk_0 y}}{k_0 y} \cdot \left[1 + jk_0 h \cdot \frac{2h}{y}\right] \qquad \text{B.5.9}$$

$$\frac{n_g^2\cos\alpha' - \sqrt{n_g^2 - \sin^2\alpha'}}{n_g^2\cos\alpha' + \sqrt{n_g^2 - \sin^2\alpha}} = \frac{\frac{2h}{R'} - \frac{1}{n_g} \cdot \sqrt{1 - \left(\frac{y}{n_g R'}\right)^2}}{\frac{2h}{R'} + \frac{1}{n_g} \cdot \sqrt{1 - \left(\frac{y}{n_g R'}\right)^2}} =$$

$$= \begin{cases} \rightarrow (-1) \text{ for PKWY traffic} \rightarrow 0 \\ \dashrightarrow (+1) \text{ for PKWY traffic} \rightarrow \infty \text{ (i.e: } |n_g|_{local} \rightarrow \infty) \end{cases} \qquad \text{B.5.10}$$

and in conjunction with Equation B.5.7 one gets for Equation B.4.20'

$$\frac{2-\sin^2\vartheta_{B'}}{2\sin^2\vartheta_{B'}}\cdot\sqrt{\frac{\cos\vartheta_{B'}}{\sin\alpha'\cdot\sin(\alpha'-\vartheta_{B'})}}\doteq$$

$$\doteq\left[\frac{1}{n_g^2}-\frac{1}{2}\right]\cdot\frac{(1-n_g^2)^{1/4}}{\left(\frac{y}{R'}\right)^{1/2}\cdot\left(j n_g\frac{y}{R'}\right)^{1/2}}\doteq \qquad \text{B.5.11}$$

$$\doteq-\frac{1}{2}\cdot\frac{R'}{y}\cdot\sqrt{\frac{j n_g}{j n_g}\cdot\left(1-\frac{1}{n_g^2}\right)^{1/2}}\longrightarrow\left(-\frac{R'}{2y}\right)$$

The primed (image) base vector - sine and cos α' products approach

$$-\bar{\delta}'\cdot\sin\alpha'=-\left[\bar{j}\cdot\frac{2h}{R'}-\bar{K}\frac{y}{R'}\right]\cdot\frac{y}{R'}\doteq\bar{K}\cdot\left(\frac{y}{R'}\right)^2\longrightarrow\bar{K} \qquad \text{B.5.12}$$

and

$$\bar{n}'\cdot\cos\alpha'=\left[\bar{j}\frac{y}{R'}+\bar{K}\cdot\frac{2h}{R'}\right]\cdot\frac{2h}{R'}\doteq\bar{j}\cdot\frac{y}{R'}\cdot\frac{2h}{R'}\longrightarrow\bar{j}\frac{2h}{R'} \qquad \text{B.5.12'}$$

and the products: (Equation B.4.20')

$$\bar{n}'\left[\cos^2(\alpha'-\vartheta_{B'})\right]\cos\alpha'\doteq$$

$$\doteq\bar{j}\,\frac{y}{R'}\cdot\frac{2h}{R'}\cdot\left[\frac{y}{R'}+j\,\frac{2h}{R'}\right]^2\doteq\bar{j}\left(\frac{y}{R'}\right)^3\cdot\frac{2h}{R'}\cdot n_g^2\doteq \qquad \text{B.5.13}$$

$$\doteq\longrightarrow\frac{2h}{R'}\cdot n_g^2$$

and

$$-\bar{\delta}'\cdot\frac{1}{2}\sin 2(\alpha'-\vartheta_{B'})\sin\alpha'\doteq\bar{K}\cdot\left(\frac{y}{R'}\right)^2\cdot\cos(\alpha'-\vartheta_{B'})\cdot \qquad \text{B.5.13'}$$

$$\cdot\sin(\alpha'-\vartheta_{B'})\doteq\bar{K}\cdot\left(\frac{y}{R'}\right)^2\cdot j n_g^2\cdot\left(\frac{y}{R'}\right)^2\longrightarrow\bar{K}\cdot j n_g^2$$

Further taking note of the vanishing of all terms involving cos φ for $\varphi = \pi/2$ i.e., in particular vanishing of $\overline{E}^{(1)}_{M_z}$ and $\overline{E}^{(2)}_{M_z}$ (Equations B.4.19 and B.4.19'), one gets the following approximate contributions to the total electrical field at the receiver location x = 0; y = R; z = h (Figure B.5.1) for $k_0 R \gg 1$; $k_0 h > 0$.

(1) From Equations B.4.18 and B.4.18' with the specialisations Equation B.5.2 and related approximations of Equations B.5.8 and B.5.9:

$$\overline{E}^{(1)}_{M_x} \doteq -\frac{j k_0^2}{4\pi} \cdot \sqrt{\frac{\mu_0}{\varepsilon_0}} \cdot M_x \cdot e^{-j[\omega t + \psi]} \cdot \frac{e^{j k_0 y}}{k_0 y} \cdot \left\{ \bar{r} \cdot \left[-j k_0 h \cdot \left(\frac{2h}{y} \right) \right] \right\} \qquad \text{B.5.14}$$

(2) From Equation B.4.20 with the specialisations (B.5.2):

$$\overline{E}^{(2)}_{N_z} = -j \frac{k_0^2}{4\pi} \cdot \sqrt{\frac{\mu_0}{\varepsilon_0}} \cdot N_z \cdot e^{-j[\omega t + \psi - \frac{\pi}{2}]} \cdot \frac{e^{j k_0 y}}{k_0 y} \cdot \{\bar{F}\} \qquad \text{B.5.15}$$

(3) From Equation B.4.20' and with the specializations and related approximations Equations B.5.2, B.5.2", B.5.3 and B.5.5, B.5.9, B.5.10, B.5.12 and B.5.12'

$$(3)E_{N_z}^{(S_1)} \doteq -j\frac{k_0^2}{4\pi}\sqrt{\frac{\mu_0}{\varepsilon_0}}\cdot N_z \cdot e^{-j\left[\omega t+\psi-\frac{\pi}{2}\right]}\cdot$$

PRIMARY TRAFFIC (0) (3)

$$\cdot(\mp 1)\cdot\frac{e^{jk_0 y}}{k_0 y}\cdot\left(1+jk_0 h\cdot\frac{2h}{y}\right)\cdot \qquad \text{B.5.15'}$$

$$\cdot\begin{Bmatrix}0\\0\\\bar{K}\end{Bmatrix}$$

and similarly from Equation B.4.20", in conjunction with the approximations Equations B.5.4, B.5.11 and B.5.13:

$$(3)E_{N_z}^{(S_2)} \doteq -j\frac{k_0^2}{4\pi}\sqrt{\frac{\mu_0}{\varepsilon_0}}\cdot N_z \cdot e^{-j\left[\omega t+\psi-\frac{\pi}{2}\right]}\cdot$$

$$\cdot\left(-\frac{1}{2}\right)\cdot e^{-2n_2 k_0 h}\cdot\frac{e^{jk_0 n_2 y}}{k_0 y}\cdot \qquad \text{B.5.15"}$$

$$\cdot\begin{Bmatrix}\bar{I}\cdot\left(\frac{2h}{y}\right)\cdot\left[n_2^2+1\right]\\ \bar{K}\cdot\left[jn_2^2+1\right]\end{Bmatrix}$$

Super position of the field Equations B.5.14 to B.5.15" and neglecting terms involving $1/y_3$, yields the total electric field in the carthesian vector components of Figure B.5.1 at the receiver location x = 0, R = y, z = h for $0 < h \ll y$ and $k_o y \gg 1$.

In the subsequent Equation B.5.16 for this field $\bar{E}$ (0; y ; h), the upper (-) signs and the lower (+) signs refer to respectively zero and infinite (i.e., bumper to bumper) automobile traffic density in the Red Bank, N. J. area of the Garden State Parkway, about halfway between the Fort Monmouth and Middletown terminal stations. This reflecting Red Bank section of the Garden State Parkway (No. 109 exit and entrance) bulges towards north from an essentially northwest course, such that it touches there the ground projected direct signal transmission path (Figure B.5.1).

The effects from the automobile traffic density related local ground reflectivity and corresponding signal distortions show up in the $\pm\bar{g}$ and $\bar{k}$ components of the space wave. Part of E (0; y; h) (Equation B.5.16, next page):

For zero traffic density we have the terms:

$$\bar{E}_{total}(0;y;h) \approx 2\left(\frac{h}{y}\right)^2 \cdot \begin{Bmatrix} -\bar{\varepsilon} M_x \\ 0 \\ -\bar{k}\, j N_z \end{Bmatrix} + \dots$$

whereas for infinite bumper to bumper traffic density

and then constructive interference

$$E_{total}(0;y;h) \approx\approx +\bar{K} \cdot \frac{2N_z}{k_o y} + \dots$$

the "Total Electric Radiation Field" at $x=0$; $R=y$; $z=h$ (for $f>f_j$)

$$\overline{E}_{total}(0;y;h) \doteq \frac{k_0^2}{4\pi}\cdot\sqrt{\frac{\mu_0}{\varepsilon_0}}\cdot\left(\frac{1}{k_0 y}\right)\cdot\left[\left(e^{j[k_0 y-\omega t-\psi]}\right)\right.$$

B.5.16

$$\cdot\left\{\begin{array}{c}(-\bar{i})\cdot M_x\cdot(k_0 h)\cdot\left(\frac{2h}{y}\right)\\ 0\\ (+\bar{k})\cdot N_z\cdot\left[\mp j(k_0 h)\left(\frac{2h}{y}\right)+(1\mp 1)\right]\end{array}\right\}$$

$$\left.-\frac{1}{2}\left(e^{-2n_g k_0 h+j n_g k_0 y}\right)\cdot\left\{\begin{array}{c}(+\bar{j})\cdot N_z\left(\frac{2h}{y}\right)\cdot\left[n_g^2+1\right]\\ (+\bar{k})\cdot N_z\cdot\left[1+j n_g^2\right]\end{array}\right\}\right]$$

where $\left(\bar{+}\right)$ corresponds to PKh'y traffic density $\left\{\begin{array}{c}\to 0\\ \to\infty\end{array}\right\}$

C. SCATTER OF POLARIZATION MODULATED RADIO WAVES FROM METAL STRIP SHAPED BODIES

C.1 Application of Babinets Principle.

The mathematical discussion of the scatter problem is based on Babinets Principle. Whereby a narrow slow in an infinite large metal screen, and a thin long metal conductor are complementary with regard to diffraction of the incident EM wave field and the scattered, i.e., the transmitted and the reflected wave fields. The corresponding situation is illustrated below in Figure C.1.1.

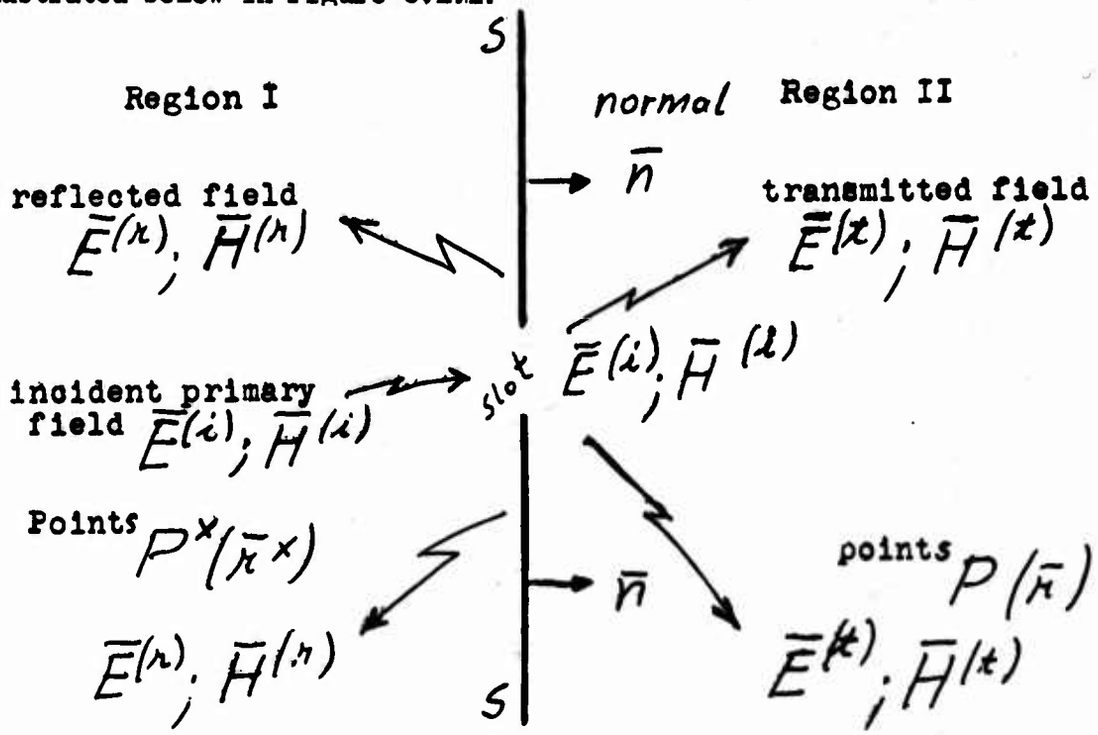

Fig.C.1.1 Field Vector Notation

Reflected and transmitted fields form the scatter field $\bar{E}^{(s)}$ and $\bar{H}(s)$. The total field in regions I and II is written as:

$$\bar{E} = \bar{E}^{(i)} + \bar{E}^{(s)}$$

$$\bar{H} = \bar{H}^{(i)} + \bar{H}^{(s)} \qquad \text{C.1.1}$$

where s = r in region I and s = t in region II. Point locations $P^x(\bar{r}^x)$ and $P(\bar{r})$ in region I and II respectively are referred to a common arbitrary origin. Distances from points P* and P are taken large compared with the wave length, such that Frauenhofer type diffraction is observed at these points.

The symmetry conditions imposed by the screen of infinite large electrical conductivity and the resultant boundary conditions yield for the electrical fields:

$$\left\{\bar{n}\times\bar{E}\right\}_I^{II} = \bar{n}\times\bar{E}^{(t)} - \bar{n}\times\bar{E}^{(r)} = 0 \qquad \text{C.1.2}$$

and

$$\left\{\bar{n}\times\bar{E}\right\}_I^{S} = \bar{n}\times\left(\bar{E}^{(i)} + E^{(r)}\right) - 0 = 0 \qquad \text{C.1.3}$$

Further, antisymmetry conditions with regard to the surface current density $\bar{J}$ as inducated by the incident field $\bar{H}^{(i)}$ in conjunction with the boundary conditions for $\bar{H}^{(n)}$ and $\bar{H}^{(t)}$ gives the following relations for the magnetic fields:

$$\left\{\bar{n}\times\bar{H}\right\}_I^{S} = \bar{n}\times\left(\bar{H}^{(i)} + \bar{H}^{(r)}\right) - 0 = \qquad \text{C.1.4}$$
$$= \bar{J} + \bar{n}\times\bar{H}^{(r)} = 0$$

and thus,

$$\bar{n}\times\bar{H}^{(i)} = J = -\bar{n}\times\bar{H}^{(r)} = +\bar{n}\times\bar{H}^{(t)} \qquad \text{C.1.5}$$

Equations C.1.4 and C.1.5 specify the scattered fields in terms of the surface current - secondary source on the screen surfaces. Consequently, at the mirror image points in regions I and II (relative to the screen) the following relations remain valid as they exist on the screen.

$$\bar{n}\times\bar{E}^{(r)}(\bar{r}^x) = \bar{n}\times\bar{E}^{(t)}(r) \qquad \text{C.1.6}$$

$$\bar{n}\cdot\bar{E}^{(r)}(\bar{r}^x) = -\bar{n}\cdot\bar{E}^{(t)}(r) \qquad \text{C.1.6'}$$

$$\bar{n}\times\bar{H}^{(r)}(\bar{r}^x) = -\bar{n}\times\bar{H}^{(t)}(r) \qquad \text{C.1.7}$$

$$\bar{n}\cdot\bar{H}^{(r)}(r^x) = \bar{n}\cdot\bar{H}^{(t)}(r) \qquad \text{C.1.7'}$$

C.2 Field Representation in Terms Vector Potential Function $\bar{A}$ and as a Green Integral over $\bar{J}$ and $\bar{J}'$ for Complementary Diffraction Systems

Employing the following relation between the Herta-Vector function Equation A.1.5 and the vector potential function A,

$$\dot{\bar{\Pi}} = -c^2 \bar{A} \qquad \text{C.2.1}$$

so that

$$\bar{B} = \mu_0 \bar{H} = \nabla \times \bar{A} \qquad \text{C.2.2}$$

one gets

$$\bar{A} = \frac{\mu_0}{4\pi} \iiint_{\text{Source Vol.}} \bar{\imath}(\bar{r}_s) \cdot \frac{e^{jk|\bar{r}-\bar{r}_s|}}{|\bar{r}-\bar{r}_s|} \cdot dVol_s \qquad \text{C.2.3}$$

where $\bar{\imath}(r_s)$, (in A/m^3)

shall correspond to a sinusoidally varying source current density

$$\bar{\imath}(\bar{r}_s, t) = \bar{\imath}(\bar{r}_s) \cdot e^{j\omega t} \qquad \text{C.2.4}$$

Let the source volume shrink to thin sheet δ thick, such that

$$\int_{-\delta/2}^{+\delta/2} \bar{\imath} \cdot dx \doteq (\bar{\imath}(\bar{r}_s)) \cdot \delta = \bar{J} \qquad \text{C.2.5}$$

remains finite as a surface current density (Amp/m). Then Equation C.2.3 reduces to a surface integral:

$$\bar{A} = \frac{\mu_0}{4\pi} \iint_S \bar{J}(\bar{r}_s) \cdot \frac{e^{jk|\bar{r}-\bar{r}_s|}}{|\bar{r}-\bar{r}_s|} \cdot da_s \qquad \text{C.2.6}$$

Here are $\bar{\pi}$ the field point and $\bar{\pi}_s$ the current source point and

$$G(\bar{\pi};\bar{\pi}_s) = \frac{e^{jk|\bar{\pi}-\bar{\pi}_s|}}{4\pi|\bar{\pi}-\bar{\pi}_s|} = \frac{e^{jkR}}{4\pi R} \qquad \text{C.2.7}$$

the Greens function Kernel via the vector-potential A of Equation C.2.6 and Equation C.2.2 one gets in our case

$$\mu_0 \bar{H}^{(s)} = \text{curl} \iint_S \bar{J} \cdot G(\bar{\pi};\bar{\pi}_s) \cdot d\alpha_s \qquad \text{C.2.8}$$

where $d\alpha_s$ is a surface element of the screen, and $G(\bar{\pi};\bar{\pi}_s)$ the Green function involving point locations $\bar{\pi}$ in region II and $\bar{\pi}_s$ on the screen. Substituting for $\bar{J}$ from Equation C.1.5 yields

$$\bar{H}^{(t)} = \frac{1}{4\pi} \nabla \times \iint_S (\bar{n} \times \bar{H}^{(t)}) \cdot \frac{e^{jk|\bar{\pi}-\bar{\pi}_s|}}{|\bar{\pi}-\bar{\pi}_s|} \cdot d\alpha_s = \qquad \text{C.2.9}$$

$$= \frac{1}{4\pi} \nabla \times \iint_S (\bar{n} \times \bar{H}^{(i)}) \cdot \frac{e^{jk|\bar{\pi}-\bar{\pi}_s|}}{|\bar{\pi}-\bar{\pi}_s|} \cdot d\alpha_s$$

where the integral is taken over current carrying part of the screen (i.e., exclusive the slot).

Application of Babinet's principle to Equation C.2.9 (i.e., transition to the complementary metal strip instead of the slot in the metal screen) involves interchange of H and E with E' and H' respectively for the complementary metal strip diffraction system.

$$\bar{H}^{(t)} \longrightarrow (\mp)\,\bar{E}' = (\mp)\left(\bar{E}^{(i)\prime} + \bar{E}^{(t)\prime}\right) \qquad \text{C.2.10}$$

$$\bar{E}^{(t)} \longrightarrow (\mp)\,\bar{H}' = (\mp)\left(\bar{H}^{(i)\prime} + \bar{H}^{(t)\prime}\right) \qquad \text{C.2.10'}$$

where the positive sign is chosen for the out going secondary radiation from the metal scatter strip. Thus on the basis of this correspondence, the incident field for the complementary system involves the change from

$$\bar{H}^{(i)} \longrightarrow -\bar{E}^{(i)\prime} \qquad \text{C.2.11}$$

Consequently, Equation C.2.9 becomes for the complementary diffraction system (thin metal strip):

$$\bar{E}'(\bar{r}) = +\nabla \times \frac{1}{4\pi} \iint_{S'} \left(\bar{n}' \times \bar{E}'(\bar{r}_{s'})\right) \cdot \frac{e^{jk\cdot|\bar{r}-\bar{r}_{s'}|}}{|\bar{r}-\bar{r}_{s'}|} \qquad \text{C.2.12}$$

The cross product term in the integrand of Equation C.2.12 can be considered as a ficitious mangetic surface current density $\bar{J}'$ (in volt/m). Analogous to the original slot screen diffraction system, this fictitious secondary magnetic surface current density is then induced by the primary incident electrical field $\bar{E}^{(i)'}$, and approximately given by

$$\bar{J}' = \bar{n}' \times \bar{E}^{(i)'}(\bar{r}_{s'}) \qquad \text{C.2.13}$$

The resultant forward scatter field from the strip corresponding to the field in region II, of the complementary slot system, Figure C.1.1, becomes therefore

$$\bar{E}^{(t)'} \doteq \frac{1}{4\pi} \nabla \times \iint_{S'} \bar{J}' \cdot \frac{e^{jk|\bar{r}-\bar{r}_{s'}|}}{|\bar{r}-\bar{r}_{s'}|} \cdot da_{s'} =$$

C.2.14

$$= \frac{1}{4\pi} \cdot \nabla \times \iint_{S'} [\bar{n}' \times \bar{E}^{(i)'}(\bar{r}_{s'}) \cdot \frac{e^{jk|\bar{r}-\bar{r}_{s'}|}}{|\bar{r}-\bar{r}_{s'}|} \cdot da_{s'}$$

In this format, the problem is recognized as the determination of the surface integral for a ficitious magnetic surface source current distribution equal to that of the tangential component of the incident electrical field. The back scatter field (i.e. the reflected field $\bar{E}^{(r)'}$ in region I) is found by symmetry considerations in conjunction with the original slot screen diffraction system.

Referring to Equations C.1.6 to C.1.7' and the transition Equations C.2.10 and C.2.10' the following relations are valid at the image points $\bar{r}^x$ of region I relative to $\bar{r}$ in region II for the complementary strip diffraction system:

$$\bar{E}^{(r)'}(\bar{r}^x) = +\bar{n}' (\bar{E}^{(t)'}(\bar{r}) \cdot \bar{n}') - \qquad \text{C.2.15}$$

$$- \bar{n}' \times (\bar{E}^{(t)'}(r) \times \bar{n}')$$

and vice versa

$$\bar{H}^{(r)'}(\bar{r}^x) = -\bar{n}' (\bar{H}^{(t)'}(\bar{r}) \cdot \bar{n}') + \qquad \text{C.2.16}$$

$$+ \bar{n}' \times (\bar{H}^{(t)'}(\bar{r}) \times \bar{n}')$$

In this format the problem is recognized as the determination of the surface source current distribution equal to that of the tangential component of the incident electrical.

C.3 SIDE SCATTER OF POLARIZATION MODULATED RADIO WAVE SIGNALS FROM STRIP SHAPED CONDUCTORS

(a) Statement of the problem:

A thin strip shaped conductor of length l and width b ($l \gg b$) is located to the side of and in the plane of the crossed dipole transmitter-antenna A. The distance ρ_s between this scatter strip and the antenna is large, such that the incident primary field at S corresponds to the antennas radiation field. Simiarly the observer's location shall be in the radiation field regions of both, the direct and the scatter waves from the transmitter and the scatter strip respectively. This situation is illustrated below in Figure C.3.1.

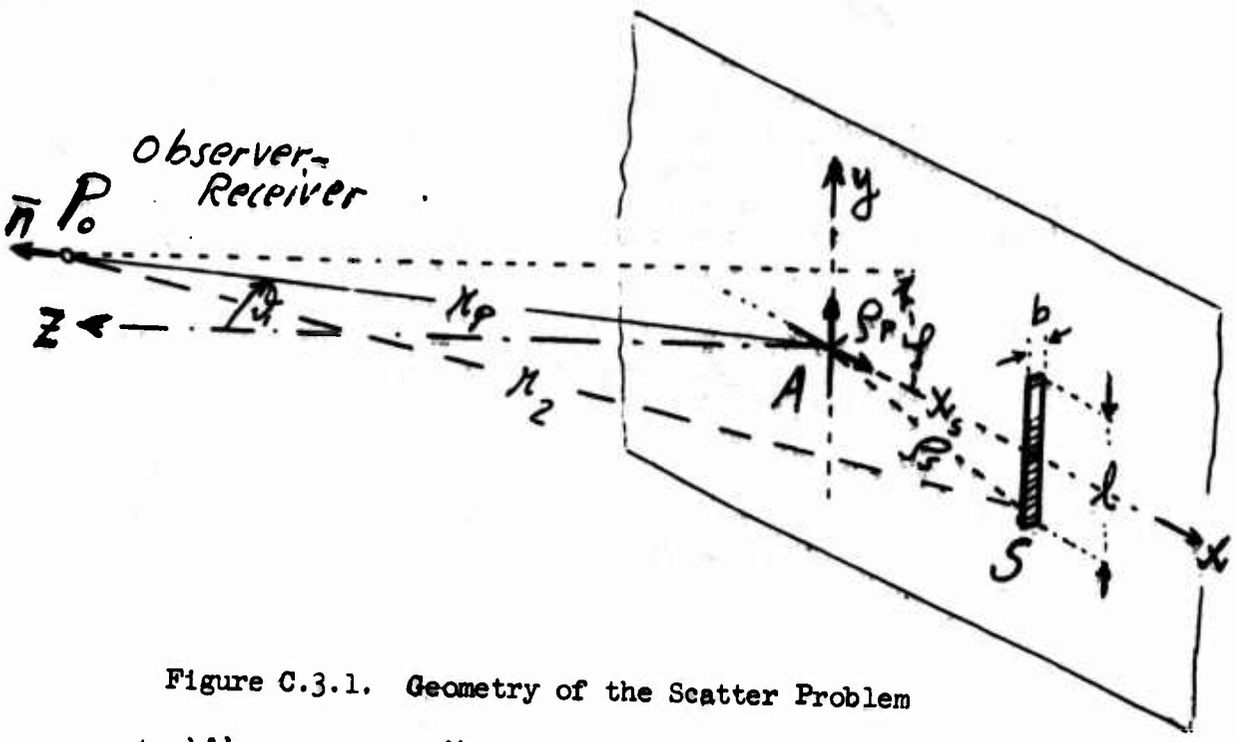

Figure C.3.1. Geometry of the Scatter Problem

For $|x_s| > \frac{2\ell^2}{\lambda_o}$ where $2\ell^2/\lambda_o$ is the approximate distance of transition from Fresnel type to Frauenhofer type diffraction. The effects on the antenna of scatter strip produced secondary field interactions can be neglected, and the field at the observer-receiver location P_o obtained by super position of the direct(primary) and the scatter field from respectively the crossed dipole transmitter antenna and the scatter strip.

(b) Formulation-Solution of the Problem for Regular Polarization Modulation

Applying Equation A.3.5 for the formulation of the radiation field $\bar{E}^{(i)}$ incident on the scatter strip (Figure C.3.1) the following specializations must be introduced

$$\omega_s = \omega_0 \; ; \; k_s = k_0$$
$$\varphi = \varphi_s \; ; \; r = r_s' = \rho_s \; ; \; (\vartheta_s = 90^\circ) \qquad \text{C.3.1}$$
$$\alpha = [\omega_0 t - k_0 \rho_s + \varphi_s + \psi_s]$$

Dropping the near field terms in Equation A.3.5, the tangentially incident field on S becomes:

$$E_{y_s}^{(i)} = E_\varphi \cos\varphi_s =$$
$$= \sqrt{\frac{\mu_0}{\varepsilon_0}} \cdot \frac{A \cdot k_0^2}{4\pi k_0 \rho_s} \cdot \left\{ \frac{\ddot{\psi}_s}{\omega_0^2} \cdot \cos\alpha_s \right. \qquad \text{C.3.2}$$
$$\left. - \left(1 + \frac{\dot{\psi}_s}{\omega_0}\right)^2 \cdot \sin\alpha_s \right\} \cdot \cos\varphi_s$$

where from Figure C.3.1:

$$\rho_s = \frac{x_s}{\cos\varphi_s} \qquad \text{C.3.3}$$
$$y_s = r_s \sin\varphi_s = x_s \cdot \tan\varphi_s$$

Considering Equation C.3.2 as the real part of a complex function, $E_{ys}^{(i)}$ in complex notation is expressed by:

$$E_{y_s}^{(i)} = \sqrt{\frac{\mu_0}{\varepsilon_0}} \cdot \frac{A \cdot k_0^2}{4\pi k_0 \rho_s} \cdot e^{j[k_0 \rho_s - \omega_0 t - \psi_s]} \cdot \qquad \text{C.3.4}$$
$$\cdot \left\{ \frac{\ddot{\psi}_s}{\omega_0^2} - j\left(1 + \frac{\dot{\psi}_s}{\omega_s}\right)^2 \right. \qquad \text{C.3.4}$$

In this complex format, $E_{ys}^{(i)}$ serves in accordance with Equation C.2.13 as source of the fictitious magnetic surface current density and the resultant scatter field.

For the in practice most important case of signal reception at points P_0 close to the z axes (Figure C.3.1) and interference from scatter radiation

emanating from S, the following approximate relations between the coordinates $r_P, \vartheta_P, \varphi_P$ of P_0 and $\rho_S ; (\vartheta_S = 90°) ; \varphi_S$ of S are applicable (See Figure C.3.2)

$$\xi^2 = \rho_P^2 + \rho_S^2 - 2\rho_P \cdot \rho_S \cdot \cos(\varphi_P - \varphi_S) \qquad \text{C.3.5}$$

i.e.

$$r_2^2 = z_P^2 + \xi^2 = z_P^2 + \rho_P^2 + \rho_S^2 - 2\rho_P \cdot \rho_S \cdot \cos(\varphi_P - \varphi_S) \qquad \text{C.3.6}$$

which gives

$$r_2 \doteq z_P \cdot \left[1 + \frac{1}{2} \cdot \frac{\rho_P^2 + \rho_S^2}{z_P^2} - \frac{\rho_P \cdot \rho_S}{z_P^2} \cdot \cos(\varphi_P - \varphi_S)\right] \qquad \text{C.3.7}$$

for $\rho_P \ll \rho_S \ll z_P$

$$\bar{E}^{(z)'} \doteq \nabla_p \times \frac{\bar{J}}{4\pi} \cdot \int_{y_s=-\frac{l}{2}}^{y_s=+\frac{l}{2}} (dy_s \cdot b) \cdot \sqrt{\frac{\mu_0}{\varepsilon_0}} \cdot \frac{A k_0^2}{4\pi k_0 \rho_s} \cdot$$

$$\cdot e^{j[k_0\rho_s - \omega_0 t - \psi_s]} \cdot \left\{ \frac{\ddot{\psi}_s}{\omega_0^2} - j\left(1 + \frac{\dot{\psi}_s}{\omega_0}\right)^2 \right\} \cdot \qquad \text{C.3.8}$$

$$\cdot \cos\varphi_s \cdot \frac{e^{jk_0 z_p}}{z_p} \cdot$$

$$\cdot e^{j\frac{k_0}{2}\cdot\frac{\rho_p^2+\rho_s^2}{z_p}} \cdot e^{-jk_0\cdot\frac{\rho_p\rho_s}{z_p}\cdot\cos(\varphi_p-\varphi_s)}$$

where

$$\rho_s^2 = x_s^2 + y_s^2 \quad ; \quad \sin\varphi_s = \frac{y_s}{\rho_s} \qquad \text{C.3.8'}$$

and $\bar{J}$ the unit vector in the +y direction of the $\bar{i}, \bar{j}, \bar{k}$ -x, y, z carthesian system.

For the practical conditions $-\frac{l}{2} \leq y_s \leq +\frac{l}{2}$ and $l < x_s$ one gets approximately:

$$\rho_s = x_s \cdot \sqrt{1 + y_s^2/x_s^2} \doteq x_s\left(1 + \frac{1}{2}\frac{y_s^2}{x_s^2}\right) \qquad \text{C.3.4}$$

and with $\varphi_s^2 = (\arctan y_s/x_s)^2 \ll 1$

$$\rho_s^2 = x_s^2(1+\tan^2\varphi_s) \doteq x_s^2(1+\varphi_s^2) \qquad \text{C.3.4'}$$

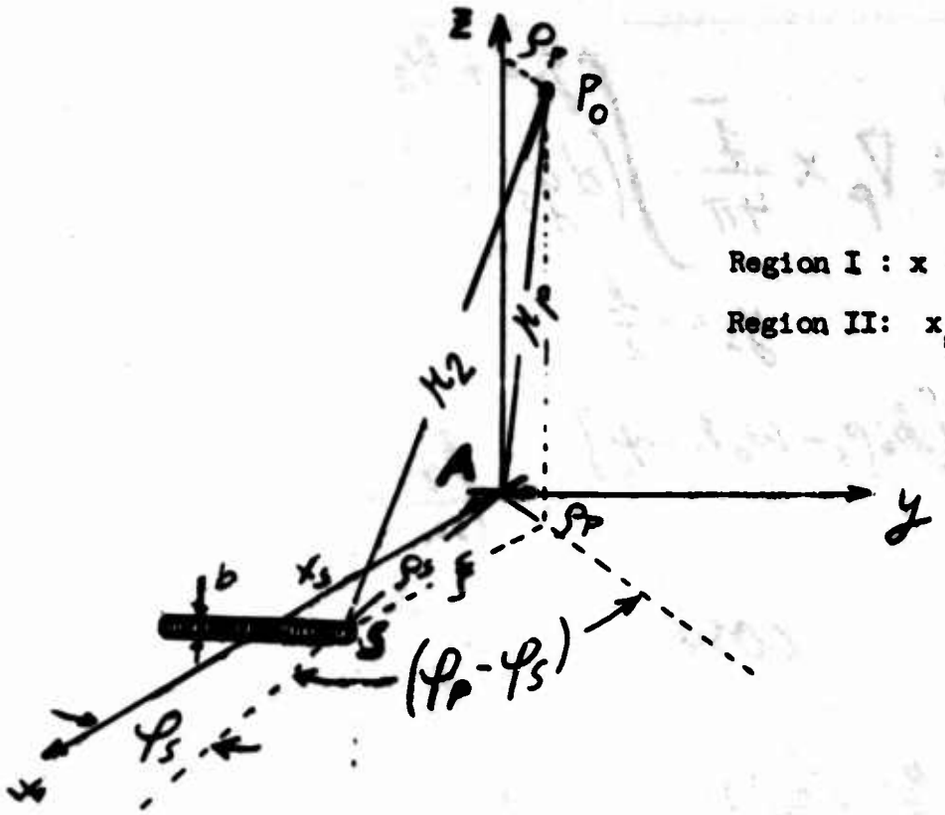

Figure C.3.2. Scatter Problem (Geometry)

Introduction of the approximation Equation C.3.6 into the Green's function Equation C.2.7 gives:

$$G(\bar{r}_P;\bar{r}_S) = \frac{1}{r_2}\cdot e^{-j k_0 r_2} \doteq \frac{e^{-j k_0 z_P}}{z_P}\cdot \qquad \text{C.3.10}$$
$$\cdot e^{-j\frac{k_0}{2}\cdot\frac{\rho_P^2+\rho_S^2}{z_P}}\cdot e^{+j k_0\frac{\rho_P\rho_S}{z_P}\cdot\cos(\varphi_P-\varphi_S)}$$

and Equation C.2.14 yields then the scatter field with:

$$\bar{E}(t)' \doteq \nabla_P \times \frac{\bar{A}}{4\pi}\cdot\int_{y_S=-l/2}^{y_S=+l/2}(dy_S\cdot b)\cdot\sqrt{\frac{\mu_0}{\varepsilon_0}}\cdot\frac{A k_0^2}{4\pi k_0\rho_S}\cdot G(\bar{r}_P;\bar{r}_S)\cdot \qquad \text{C.3.10'}$$
$$\cdot e^{-j[k_0\rho_S-\omega_0 t-\psi(t)]}\cdot\left\{\frac{\ddot{\psi}}{\omega_0^2}-j\left(1+\frac{\dot{\psi}}{\omega_S}\right)^2\right\}\cdot\cos\varphi_S$$

and $$\cos\varphi_s \doteq 1 - \frac{\varphi_s^2}{2}$$

$$\rho_s \doteq x_s \cdot (1 - \varphi_s^2/2) \qquad \text{C.3.10''}$$

Substitution of Equation C.3.10'' reduces Equation C.3.10' to approximately:

$$\bar{E}^{(x)\prime} \doteq \nabla_p \times \bar{J} \cdot \sqrt{\frac{\mu_0}{\varepsilon_0}} \cdot \frac{A k_0^2 \cdot b}{(4\pi)^2 \cdot k_0 z_p} \cdot e^{j[k_0 z_p - \omega_0 t - \psi_s]} \cdot e^{j k_0 x_s} \cdot e^{-j \frac{k_0}{2} \cdot \frac{\rho_p^2 + x_s^2}{z_p}} \cdot \qquad \text{C.3.11}$$

$$\cdot \int_{\varphi_s = -\frac{l}{2x_s}}^{\varphi_s = +\frac{l}{2x_s}} d\varphi_s \cdot \left\{ \left[e^{-j k_0 \cdot \frac{\rho_p x_s}{z_p} \cdot \cos(\varphi_p - \varphi_s)} \right] \cdot \left\{ \frac{\ddot{\psi}_s}{\omega_0^2} - j\left(1 + \frac{\dot{\psi}_s}{\omega_0}\right)^2 \right\} \right\}$$

where φ_s^2 has been neglected as small compared to one in the exponent of (e).

The integral expression in Equation C.3.11 involves:

$$J_0 = \int_{\varphi_s = -\frac{l}{2x_s}}^{\varphi_s = +\frac{l}{2x_s}} d\varphi_s \cdot e^{-j\alpha \cdot [\cos\varphi_p \cdot \cos\varphi_s + \sin\varphi_p \cdot \sin\varphi_s]} \doteq \qquad \text{C.3.11'}$$

$$\doteq \int_{\varphi_s = -\frac{l}{2x_s}}^{\varphi_s = +\frac{l}{2x_s}} d\varphi_s \cdot e^{-j\alpha[\cos\varphi_p \cdot (1 - \frac{\varphi_s^2}{2}) + \varphi_s \sin\varphi_p]} \doteq$$

(neglible rel. to 1)

$$\doteq e^{-j\alpha\cos\varphi_p} \cdot \frac{2 \cdot \sin(\alpha \frac{l}{2x_s} \cdot \sin\varphi_p)}{\alpha \cdot \sin\varphi_p}$$

and where we set:

$$k_0 x_s \cdot \frac{\rho_p}{z_p} = a \qquad \text{C.3.11''}$$

In terms of the integral-solution $\mathcal{F}_0$

Equation C.3.11;

$$\bar{E}^{(t)'} \doteq \nabla_p \times \bar{J} \cdot \sqrt{\frac{\mu_0}{\varepsilon_0}} \cdot \frac{A k_0^2 b}{(4\pi)^2 k_0 z_p} \cdot e^{j[k_0 z_p - \omega_0 t - \psi_s]}$$

$$\left(e^{j k_0 x_s}\right) \cdot \left(e^{j \frac{k_0}{2} \cdot \frac{\rho_p^2 + x_s^2}{z_p}}\right) \cdot \qquad \text{C.3.12}$$

$$\cdot \left\{\left[\frac{\ddot{x}_s}{\omega_s^2} - j\left(1 + \frac{\dot{x}_s}{\omega}\right)^2\right] \cdot \mathcal{F}_0\right.$$

Reintroduction of carthesian coordinates

$$x_p = \rho_p \cos \varphi_p \; ; \quad y_p = \rho_p \sin \varphi_p \qquad \text{C.3.12'}$$

yields then:

$$\bar{E}^{(t)'} \doteq \nabla_p \times \bar{J} \cdot \sqrt{\frac{\mu_0}{\varepsilon_0}} \cdot \frac{A \cdot k_0 b}{(4\pi)^2} \cdot$$

$$\cdot \left\{e^{j k_0 \left[z_p + x_s + \frac{1}{2z_p}\left(x_p^2 + y_p^2 + x_s^2\right) - \frac{1}{z_p}(x_p \cdot x_s)\right]}\right\} \cdot$$

$$2 \cdot \left\{\left[\frac{\ddot{x}_s}{\omega_0^2} - j\left(1 + \frac{\dot{x}_s}{\omega}\right)^2\right] \cdot \frac{\sin\left(k_0 l \cdot \frac{y_p}{2 z_p}\right)}{k_0 x_s y_p}\right\} \qquad \text{C.3.13}$$

The formation of the curl: $\nabla_p \times \ldots$

involves the operation:

$$\begin{Bmatrix} \bar{i}\frac{\partial}{\partial x_p} \\ \bar{j}\frac{\partial}{\partial y_p} \\ \bar{k}\frac{\partial}{\partial z_p} \end{Bmatrix} \times \begin{Bmatrix} 0 \\ \bar{j}A_y \\ 0 \end{Bmatrix} = \begin{Bmatrix} -\frac{\partial}{\partial z_p}A_y \\ 0 \\ +\frac{\partial}{\partial x_p}A_y \end{Bmatrix} = \begin{Bmatrix} E_x^{(+1)'} \\ 0 \\ E_z^{(+1)'} \end{Bmatrix} \qquad \text{C.3.14}$$

and requires the following differentials

$$\frac{\partial}{\partial z}\left[e^{j k_0 \cdot f(z_p; x_p)}\right] = j k_0 \frac{\partial f}{\partial z_p} \cdot e^{j k_0 \cdot f(z_p; x_p)} \qquad \text{C.3.14'}$$

where

$$f(z_p; x_p) = z_p + x_s + \frac{1}{2z_p}\left(x_p^2 + y_p^2 + x_s^2\right) - \frac{x_p x_s}{z_p}$$

and

$$\frac{\partial f}{\partial z_p} = 1 - \frac{y_p^2}{2z_p^2} - \frac{1}{2z_p^2}(x_p - x_s)^2 \qquad \text{C.3.14"}$$

and similarly

$$\frac{\partial f}{\partial x_p} = \frac{x_p - x_s}{z_p} \qquad \text{C.3.14'''}$$

further C.3.15

$$\frac{\partial}{\partial z_p}\left[\sin\left(k_0 l \cdot \frac{y_p}{2z_p}\right)\right] = -k_0 l \cdot \frac{y_p}{2z_p^2} \cdot \cos\left(k_0 l \frac{y_p}{2z_p}\right)$$

Collection of the respective differentials ,equs.C.3.14 to .15 in conjunction with equation C.3.13 gives the following field equations for $\vec{E}(t)'$ in region II , $x > x_s$

$$\xi_z^{(t)'} \doteq + \sqrt{\frac{\mu_0}{\varepsilon_0}} \cdot \frac{A k_0 b}{(4\pi)^2} \cdot e^{-j[\omega_0 t + \gamma_s]} \qquad \text{C.3.16}$$

$$\cdot j \frac{k_0 (x_p - x_s)}{z_p} \cdot \left[e^{j k_0 \left(z_p + x_s + \frac{x_p^2 + y_p^2 + x_s^2}{2 z_p} - \frac{x_p x_s}{z_p} \right)} \right]$$

$$\cdot 2 \cdot \left[\frac{\ddot{x}_s}{\omega_0^2} - j \left(1 + \frac{\dot{x}_s}{\omega_0} \right)^2 \right] \cdot \frac{\sin k_0 h \frac{y_p}{2 z_p}}{k_0 \cdot x_s \cdot y_p}$$

$$\xi_y^{(t)'} = 0 \qquad \text{C.3.16'}$$

$$\xi_x^{(t)'} = - \sqrt{\frac{\mu_0}{\varepsilon_0}} \cdot \frac{2A \cdot k_0 b}{(4\pi)^2} \cdot e^{-j[\omega_0 t + \gamma_s]} \qquad \text{C.3.16''}$$

$$\cdot \left[e^{j k_0 \cdot \left[z_p + x_s + \frac{x_p^2 + y_p^2 + x_s^2}{2 z_p} - \frac{x_p x_s}{z_p} \right]} \right] \cdot$$

$$\cdot \left[\frac{\ddot{x}_s}{\omega_0^2} - j \left(1 + \frac{\dot{x}_s}{\omega_0} \right)^2 \right] \cdot \left\{ j k_0 \left[1 - \frac{y_p^2}{2 z_p^2} - \frac{(x_p - x_s)^2}{2 z_p^2} \right] \cdot \right.$$

$$\left. \cdot \frac{\sin \left(k_0 l \cdot \frac{y_p}{2 z_p} \right)}{k_0 x_s \cdot y_p} - \frac{k_0 \cdot l \cdot \cos \left(k_0 l \frac{y_p}{2 z_p} \right)}{2 k_0 x_s z_p^2} \right\}$$

$\bar{E}(t)$'The reflected field in region I, $x < x_s$ Figure C.3.2 follows from by application of Equation C.2.15, where in our case the normal and tangential field components relative to the scatter strip surface correspond to the x and the y, z components respectively.

Further, since of interest are here the fields primary and scattered on or close to the z-axes (Figure C.3.1 and F gure C.3.2) where:

$$\rho_p \lll z_p \; ; \quad x_p \lll z_p ; \; y_p \lll z_p \qquad \text{C.3.17}$$

we let

$$\frac{x_p}{z_p} \to 0 \; ; \quad \frac{y_p}{z_p} \to 0 \qquad \text{C.3.18}$$

and via De L'Hospital's rule

$$\lim_{y_p \to 0} \left\{ \frac{\sin k_0 l \frac{y_p}{2 z_p}}{k_0 x_s y_p} \right\} \to \frac{1}{x_s} \cdot \frac{l}{2 z_p} \qquad \text{C.3.18'}$$

Introduction of these approximations into Equations C.3.17 and C.3.16 respectively, gives the following equations for the scatter field components on and close to the z-axes:

$$\left(\mathcal{E}_x^{(n)'} \right)_{\rho_p \to 0} \doteq - \sqrt{\frac{\mu_0}{\varepsilon_0}} \frac{A k_0^2 b \cdot l}{(4\pi)^2 \cdot x_s \cdot z_p} \cdot e^{j k_0 x_s \left(1 + \frac{x_s}{2 z_p}\right)} \cdot e^{j[k_0 z_p - \omega_0 t - \gamma_s]} \cdot \left[\left(1 + \frac{\dot{x}_s}{\omega_0}\right)^2 + j \frac{\ddot{x}_s}{\omega_0} \right] \cdot \left[\left(1 - \frac{x_s^2}{2 z_p^2}\right) + j \frac{1}{k_0 z_p} \right] \qquad \text{C.3.19}$$

$$\left(\mathcal{E}_z^{(n)'}\right) \doteq \sqrt{\frac{\mu_0}{\varepsilon_0}} \cdot \frac{A k_0^2 b \cdot l}{(4\pi)^2 \cdot z_p^2} \cdot \qquad \text{C.3.19'}$$

$$\rho_p \to 0$$

$$\cdot \left[\left(1+\frac{\dot{x}_s}{\omega_0}\right)^2 + j\frac{\ddot{x}_s}{\omega_0^2}\right] \cdot e^{jk_0 x_s\left(1+\frac{x_s}{2z_p}\right)} \cdot$$

$$\cdot e^{j\left[k_0 z_p - \omega_0 t - \gamma_s\right]}$$

Further, in practice where

$$\left(x_s/z_p\right)^2 \ll 1 \qquad \frac{1}{k_0 z_p} \ll 1 \qquad \text{C.3.20}$$

the back scatter field on or close to the s-axes (Fig.C.3.1) approaches :

$$\left(\mathcal{E}_x^{(n)'}\right) \to -\sqrt{\frac{\mu_0}{\varepsilon_0}} \cdot \frac{A \cdot k_0^2 b \cdot l}{(4\pi)^2 \cdot x_s \cdot z_p} \cdot \qquad \text{C.3.20'}$$

$$\rho_p \to 0$$

$$\cdot \left[\left(1+\frac{\dot{x}_s}{\omega_0}\right)^2 + j\frac{\ddot{x}_s}{\omega_0^2}\right] \cdot$$

$$\cdot e^{j\left[k_0 \cdot (z_p + x_s) - \omega_0 t - \gamma_s\right]}$$

$$\left(\mathcal{E}_y^{(n)'}\right) = 0 \qquad \text{C.3.20''}$$

$$\rho_p = 0$$

$$\left(\xi_z^{(n)'}\right)_{\rho_p \to 0} \to \sqrt{\frac{\mu_0}{\varepsilon_0}} \cdot \frac{A \cdot k_0^2 \cdot b \cdot l}{(4\pi)^2 \cdot z_p^2} \cdot \qquad \text{c.3.20'''}$$

$$\cdot \left[\left(1 + \frac{\ddot{x}_s}{\omega_0}\right)^2 + j \frac{\dddot{x}_s}{\omega_0^2}\right] \cdot$$

$$\cdot e^{j\left[k_0(z_p + x_s) - \omega_0 t - \gamma_s\right]}$$